Antiproliferative Constituents of Roots of

Podocarpus falcatus (Thunb.) R.Br. ex Mirb.

Ermias Mekuria Addo

A Thesis Submitted to

The Department of Pharmaceutical Chemistry and Pharmacognosy

Presented in Partial fulfillment of the Requirements of for the Degree of

Master of Science in Pharmacognosy

Addis Ababa University

Addis Ababa, Ethiopia

June, 2015

Addis Ababa University

School of Graduate Studies

This is to certify that the thesis prepared by Ermias Mekuria Addo, entitled: "Antiproliferative Constituents of Roots of *Podocarpus falcatus* (Thunb.) R.Br. ex Mirb" and submitted in partial fulfillment of the requirements for the Degree of Master of Science (Pharmacognosy) complies with the regulations of the University and meets the accepted standards with respect to originality and quality.

Signed by the Examining Committee:

External examiner_____	Signature_____	Date_____
Internal examiner_____	Signature_____	Date_____
Dr. Ariaya Hymete (AAU) (Advisor)	Signature_____	Date_____
Dr. Mariamawit Yonathan Yeshak (AAU) (Advisor)	Signature_____	Date_____
Dr. L. Harinantenaina Rakotondraibe (The Ohio State University, Columbus, Ohio, USA) (Advisor)	Signature_____	Date_____

Chair of Department or Graduate Program Coordinator

Abstract

Antiproliferative Constituents of Roots of *Podocarpus falcatus* (Thunb.) R.Br. ex Mirb.

Ermias Mekuria Addo

Addis Ababa Univeristy, 2015

Once thought of as the disease of the developed, cancer nowadays is becoming the problem of every nation across the globe claiming millions of lives every year. Incidence, and thus prevalence, is increasing every year due to adoption of lifestyle factors that are known to be major cancer risk factors. Making things worse is the development of MDR to the known effective anticancer drugs. Moreover, the currently available drugs are costly and are associated with severe side effects. Thus, discovering new anticancer drugs with new and safe modes of action is urgently needed. Natural products derived from medicinal plants are well-known contributors of clinically useful anticancer drugs; suffice to mention taxol, the *Vinca* alkaloids, podophyllotoxin and camptothecin and their derivatives. Relying on traditional medicines for most of their health needs, Ethiopians use various plants for prevention and treatment of cancer. For example, the roots of *Podocarpus falcatus* are used as "anticancer" remedies in some parts of Ethiopia, which formed the basis of the present study to isolate the "responsible" "bioactive" compounds.

Bioassay guided fractionation using the human colorectal adenocarcinoma (HT-29) cell line of the methanol extract of dried roots of *P. falcatus* (Podocarpaceae) led to the isolation of two new type C nagilactones, 16-hydroxy nagilactone F (**PF-1**) and 2*β*,16-dihydroxy nagilactone F (**PF-3**) and a new totarane-type bisditerpenoid 7*β*-hydroxy macrophyllic acid (**PF-2**), along with the seven known compounds: inumakinol D (**28**), mac-

rophyllic acid (**37**), nagilactone D (**41**), ponasterone A (**94**), 2β-hydroxy nagilactone F (**108**), nagilactone I (**109**), and 15-hydroxy-nagilactone D (**110**). The structures of the new compounds were determined by 1D and 2D-NMR, HRESIMS and by comparison with the reported spectroscopic data of their congeners. The orientation of the hydroxyl group at C-2 of **108** and **109** was revised to be β based on evidence from detailed analysis of 1D and 2D-NMR data and single crystal X-ray diffraction studies. Among the isolated compounds the nagilactones, including the new dilactones 16-hydroxy nagilactone F (**PF-1**) and 2β,16-dihydroxy nagilactone F (**PF-3**), were the most active (ED_{50} 0.3–5.13 µM range) against the HT-29 cell line, whereas the bisditerpenoids (**PF-2** and **37**) and the other known compounds **28** and **94** were inactive. The presence of bioactive nagilactones in *P. falcatus* supports its traditional use.

Acknowledgments

Before and above all, I would like to thank The Almighty God-Power, Praise and Dignity for You God. Thank You Saint Mary, I am living because of You.

My family!!! I have no words how to express what you did, and will do, for me. But in simple words let me say 'Thank You all'.

I would like to thank my advisors Dr. L. Harinantenaina Rakotondraibe, Dr. Hee-Byung Chai, Dr. Ariaya Hymete and Dr. Mariamawit Yonathan Yeshak, for all of ideas and supports they provided. My special gratitude goes to Dr. L. Harinantenaina Rakotondraibe, who provided me with ideas, materials and all kinds of support especially in the publishing of this work.

I also like to thank The Ohio State University College of Pharmacy for a Research Training Fellowship; Prof. Robert W. Brueggemeier and Prof. Karl A. Werbovetz who initiated the collaboration between AAU and The Ohio State University College of Pharmacy; Prof. Werner Tjarks and Prof. Jack C. Yalowich-interviewers; my lab mates in the Division of Medicinal Chemistry and Pharmacognosy, College of Pharmacy, The Ohio State University; to all faculty members of College of Pharmacy, OSU, Ohio, USA and Prof. David G. I. Kingston and Dr. Carla Slebodnick at Department of Chemistry and Virginia Tech Center for Drug Discovery Virginia Tech, Blacksburg, Virginia, USA for X-ray crystallography.

My appreciation also goes to Dr. Kaleab Asres, Dr. Daniel Bisrat, Shemsu Umer, Solomon Tadessese, H/meskel Meshesha; Mr. Melaku Wondafrash, senior botanist at The National Herbarium, for plant material identification and authentication; Addis Ababa University for the study leave, material and monetary support; to all faculty members of School of Pharmacy, AAU; Ethiopian Biodiversity Institute for granting permission for plant material export. Last, but not least, I don't exactly know how to thank my friends-thank you for all things! Nice knowing you all!

Manuscript prepared

Published

Ermias Mekuria Addo, Hee-Byung Chai, Ariaya Hymete, Mariamawit Yonathan Yeshak, Carla Slebodnick, David G. I. Kingston and L. Harinantenaina Rakotondraibe (2015). Antiproliferative Constituents of the Roots of Ethiopian *Podocarpus falcatus* and Structure Revision of 2α-Hydroxynagilactone F and Nagilactone I. *Journal of Natural Products* **78**: 827−835.

Contents

List of Figures xi

List of Tables xvi

List of Acronyms xvii

1. Introduction 1

1.1. Cancer 1

1.1.1. Definition, pathogenesis and causes: An overview 1

1.1.2. Epidemiology 3

1.1.3. Prevention and treatment modalities: An overview 4

1.2. Natural products 7

1.2.1. The role of medicinal plants in cancer 7

1.2.2. Ethiopian medicinal plants in cancer 9

1.3. The family Podocarpaceae 11

1.4. The genus *Podocarpus* 12

1.4.1. Description and distribution 12

1.4.2. Chemistry 12

1.4.2.1. Terpenoinds 12

1.4.2.1.1. Diterpenes and derivatives 13

1.4.2.1.2. Nagilactones 15

1.4.2.2. Flavonoids 18

1.4.2.3. Phytoecdysteroids 20

1.4.2.4. Miscellaneous compounds 21

1.4.3. Ethnobotanical and pharmacological uses 22

1.5. *Podocarpus falcatus* 23

1.5.1. Description and distribution 23

1.5.2. Chemistry, ethnobotanical uses and ethnopharmacological reports 24

1.6. Statement of the problem 25

2. Objectives 27

2.1. General objective 27

2.2. Specific objectives 27

3. Materials and methods 28

3.1. Materials 28

3.1.1. Chemicals 28

3.1.2. Instruments 28

3.1.3. Plant material collection 29

3.2. Methods 29

3.2.1. Extraction, bioassay-guided fractionation and isolation 29

3.2.2. Cell culture and cytotoxicity assay 30

3.2.3. X-ray crystallography of compounds **41**, **108** and **109**. 31

4. Results and discussion 33

4.1. Antiproliferative activity of extracts and fractions 33

4.2. General overview of fractionation and isolation..... 39

4.3. Structure revision of compounds **108** and **109** 40

4.4. Structure elucidation of the new compounds **PF-1**, **PF-2** and **PF-3** 44

4.5. Cytotoxicity of the isolated compounds from the roots of *P. falcatus* 55

5. Conclusion 58

6. Recommendations.....59

References.....60

Appendices.....90

Appendix I: Summary of physical and spectral data of isolated compounds..... 90

Appendix II: ^{1}H and ^{13}C NMR, ^{1}H-^{1}H COSY, HSQC, HMBC, 2D-NOESY, UV, IR and HRESIMS of 16-hydroxynagilactone F (**PF-1**)..... 93

Appendix III: ^{1}H and ^{13}C NMR, ^{1}H-^{1}H COSY, HSQC, HMBC, 2D-NOESY, UV, IR and HRESIMS of 2β,16-dihydroxynagilactone F (**PF-3**)..... 97

Appendix IV: ^{1}H and ^{13}C NMR, ^{1}H-^{1}H COSY, HSQC, HMBC, 2D-NOESY, UV, IR and HRESIMS of 7β-hydroxymacrophyllic acid (**PF-2**)..... 102

Appendix V: ^{1}H and ^{13}C NMR, ^{1}H-^{1}H COSY, HSQC, HMBC, 2D-NOESY, UV, IR and HRESIMS of inumakiol D (**28**) 109

Appendix VI: ^{1}H and ^{13}C NMR, ^{1}H-^{1}H COSY, HSQC, HMBC, 2D-NOESY, UV, IR and HRESIMS of macrophyllic acid (**37**)..... 110

Appendix VII: ^{1}H and ^{13}C NMR, ^{1}H-^{1}H COSY, HSQC, HMBC, 2D-NOESY, UV, IR and HRESIMS of nagilactone D (**41**) 111

Appendix VIII: ^{1}H and ^{13}C NMR, ^{1}H-^{1}H COSY, HSQC, HMBC, 2D-NOESY, UV, IR and HRESIMS of ponasterone A (**94**) 112

Appendix IX: ^{1}H and ^{13}C NMR, ^{1}H-^{1}H COSY, HSQC, HMBC, 2D-NOESY, UV, IR and HRESIMS of 2β-hydroxynagilactone F (**108**) 113

Appendix X: ^{1}H and ^{13}C NMR, ^{1}H-^{1}H COSY, HSQC, HMBC, 2D-NOESY, UV, IR and HRESIMS of nagilactone I (**109**) 115

Appendix XI: ^{1}H and ^{13}C NMR, ^{1}H-^{1}H COSY, HSQC, HMBC, 2D-NOESY, UV, IR and HRESIMS of 15-hydroxynagilactone D (**110**) 118

Appendix XII: X-ray crystallographic data of compounds **41**, **108** and **109**..... 122

List of Figures

Figure 1. Nagilactone, totarane and abtietane diterpene nucleus..... 15

Figure 2. Types of nagilactones..... 16

Figure 3. Picture of *Podocarpus falcatus* 24

Figure 4. Flow chart showing bioassay-guided fractionation of the roots of *P. falcatus* using the HT-29 cell line..... 36

Figure 5. HPLC chromatogram of fraction F3-4 (Solvent system: MeOH:H_2O gradient; Flow rate: 2 mL/min; Detection wavelength: 254 nm)..... 37

Figure 6. HPLC chromatogram of fraction F3-5 (Solvent system: MeOH:H_2O gradient; Flow rate: 2 mL/min; Detection wavelength: 254 nm)..... 37

Figure 7. HPLC chromatogram of fraction F3-5-I (Solvent system: MeOH:H_2O gradient; Flow rate: 2 mL/min; Detection wavelength: 280 nm)..... 38

Figure 8. HPLC chromatogram of fraction F3-1 (Solvent system: MeOH:H_2O gradient; Flow rate: 2 mL/min; Detection wavelength: 254 nm)..... 38

Figure 9. HPLC chromatogram of fraction F3-9 (Solvent system: MeOH:H_2O gradient; Flow rate: 2 mL/min; Detection wavelength: 280 nm)..... 39

Figure 10. Stable conformation of the 2α- and 2β-hydroxynagilactone F after MM2 energy minimization 43

Figure 11. X-ray ORTEP drawing of the crystal structures of **41**, **108** and **109** 43

Figure 12. Chemical structure of 16-hydroxynagilactone F (**PF-1**) 47

Figure 13. Key HMBC and ^{1}H-^{1}H COSY correlations of the new compounds **PF-1**, **PF-2** and **PF-3**..... 48

Figure 14. Chemical structure of 2*β*,16-dihydroxynagilactone F (**PF-3**) 50

Figure 15. Key NOESY correlations of compounds **PF-1**, **PF-2**, **PF-3**, **108** and **109**..... 51

Figure 16. Chemical structure of 7*β*-hydroxymacrophyllic acid (**PF-2**) 53

Figure 17. Structure-activity requirement of nagilactones 56

Figure 18. Plausible mechanism of action of nagilactones..... 57

Figure 19. ^{1}H NMR spectrum of 16-hydroxynagilactone F (**PF-1**) (CD_3OD, 400 MHz) 93

Figure 20. ^{13}C NMR spectrum of 16-hydroxynagilactone F (**PF-1**) (CD_3OD, 100 MHz)93

Figure 21. ^{1}H-^{1}H COSY spectrum of 16-hydroxynagilactone F (**PF-1**) (CD_3OD, 400 MHz)..... 94

Figure 22. HSQC spectrum of 16-hydroxynagilactone F (**PF-1**) (CD_3OD, 400 MHz).... 94

Figure 23. HMBC spectrum of 16-hydroxynagilactone F (**PF-1**) (CD_3OD, 400 MHz)... 95

Figure 24. 2D-NOESY spectrum of 16-hydroxynagilactone F (**PF-1**) (CD_3OD, 400 MHz) 95

Figure 25. UV spectrum of 16-hydroxynagilactone F (**PF-1**) 96

Figure 26. IR spectrum of 16-hydroxynagilactone F (**PF-1**) (KBr) 96

Figure 27. HRESIMS of 16-hydroxynagilactone F (**PF-1**) 97

Figure 28. ^{1}H NMR spectrum of 2*β*,16-dihydroxynagilactone F (**PF-3**) (CD_3OD, 400 MHz)..... 97

Figure 29. ^{13}C NMR spectrum of 2*β*,16-dihydroxynagilactone F (**PF-3**) (CD_3OD, 100 MHz) 98

Figure 30. ^{1}H-^{1}H COSY spectrum of 2*β*,16-dihydroxynagilactone F (**PF-3**) (CD_3OD, 400 MHz) 98

Figure 31. HSQC spectrum of 2*β*,16-dihydroxynagilactone F (**PF-3**) (CD_3OD, 400 MHz) 99

Figure 32. HMBC spectrum of 2*β*,16-dihydroxynagilactone F (**PF-3**) (CD_3OD, 400 MHz) 99

Figure 33. 2D-NOESY spectrum of 2*β*,16-dihydroxynagilactone F (**PF-3**) (CD_3OD, 400 MHz) 100

Figure 34. UV spectrum of 2*β*,16-dihydroxynagilactone F (**PF-3**) 100

Figure 35. IR spectrum of 2*β*,16-dihydroxynagilactone F (**PF-3**) (KBr) 101

Figure 36. HRESIMS of 2*β*,16-dihydroxynagilactone F (**PF-3**) 101

Figure 37. ^{1}H NMR spectrum of 7*β*-hydroxymacrophyllic acid (**PF-2**) (A. Pyridine-d_5, B. DMSO-d_6, 400 MHz) 102

Figure 38. ^{13}C NMR spectrum of 7*β*-hydroxymacrophyllic acid (**PF-2**) (A. Pyridine-d_5, B. DMSO-d_6, 100 MHz) 103

Figure 39. ^{1}H-^{1}H COSY spectrum of 7*β*-hydroxymacrophyllic acid (**PF-2**) (Pyridine-d_5, 400 MHz) 104

Figure 40. HSQC spectrum of 7*β*-hydroxymacrophyllic acid (**PF-2**) (A. Pyridine-d_5, B. DMSO-d_6, 400 MHz) 105

Figure 41. HMBC spectrum of 7β-hydroxymacrophyllic acid (**PF-2**) (A. Pyridine-d_5, B. DMSO-d_6, 400 MHz) 106

Figure 42. 2D-NOESY spectrum of 7β-hydroxymacrophyllic acid (**PF-2**) (A. Pyridine-d_5, B. DMSO-d_6, 400 MHz) 107

Figure 43. UV spectrum of 7β-hydroxymacrophyllic acid (**PF-2**) 107

Figure 44. IR spectrum of 7β-hydroxymacrophyllic acid (**PF-2**) (KBr) 108

Figure 45. HRESIMS of 7β-hydroxymacrophyllic acid (**PF-2**) 108

Figure 46. ^{1}H NMR spectrum of inumakiol D (**28**) (CD_3OD, 400 MHz) 109

Figure 47. ^{13}C NMR spectrum of inumakiol D (**28**) (CD_3OD, 100 MHz)..... 109

Figure 48. ^{1}H NMR spectrum of macrophyllic acid (**37**) ($CDCl_3$, 400 MHz)..... 110

Figure 49. ^{13}C NMR spectrum of macrophyllic acid (**37**) ($CDCl_3$, 100 MHz)..... 110

Figure 50. ^{1}H NMR spectrum of nagilactone D (**41**) ($CDCl_3$, 400 MHz) 111

Figure 51. ^{13}C NMR spectrum of nagilactone D (**41**) ($CDCl_3$, 100 MHz) 111

Figure 52. ^{1}H NMR spectrum of ponasterone A (**94**) (CD_3OD, 400 MHz) 112

Figure 53. ^{13}C NMR spectrum of ponasterone A (**94**) (CD_3OD, 100 MHz) 112

Figure 54. ^{1}H NMR spectrum of 2β-hydroxynagilactone F (**108**) (CD_3OD, 400 MHz) 113

Figure 55. ^{13}C NMR spectrum of 2β-hydroxynagilactone F (**108**) (CD_3OD, 100 MHz) 113

Figure 56. HMBC spectrum of 2β-hydroxynagilactone F (**108**) (CD_3OD, 400 MHz)... 114

Figure 57. 2D-NOESY spectrum of 2β-hydroxynagilactone F (**108**) (CD_3OD, 400 MHz) 114

Figure 58. ^{1}H NMR spectrum of nagilactone I (**109**) (A. $CDCl_3$, B. Pyridine-d_5, 400 MHz) 115

Figure 59. ^{13}C NMR spectrum of nagilactone I (**109**) (A. $CDCl_3$, B. Pyridine-d_5, 100 MHz) 116

Figure 60. 2D-NOESY spectrum of nagilactone I (**109**) (A. $CDCl_3$, B. Pyridine-d_5, 400 MHz) 117

Figure 61. ^{1}H NMR spectrum of 15-hydroxynagilactone D (**110**) ($CDCl_3$, 400 MHz).. 118

Figure 62. ^{13}C NMR spectrum of 15-hydroxynagilactone D (**110**) ($CDCl_3$, 100 MHz) 118

Figure 63. HSQC spectrum of 15-hydroxynagilactone D (**110**) ($CDCl_3$, 400 MHz) 119

Figure 64. HMBC spectrum of 15-hydroxynagilactone D (**110**) ($CDCl_3$, 400 MHz) 119

Figure 65. 2D-NOESY spectrum of 15-hydroxynagilactone D (**110**) ($CDCl_3$, 400 MHz) 120

Figure 66. UV spectrum of 15-hydroxynagilactone D (**110**)..... 120

Figure 67. IR spectrum of 15-hydroxynagilactone D (**110**) (KBr)..... 121

Figure 68. HRESIMS of 15-hydroxynagilactone D (**110**)..... 121

List of Tables

Table 1. List of chemotherapy drugs classified based on their biochemical properties 6

Table 2. ^{1}H NMR (400 MHz) data for compounds **108** and **109**..... 41

Table 3. ^{13}C NMR (100 MHz) data for compounds **108** and **109**..... 42

Table 4. ^{1}H NMR (400 MHz) data for compounds **PF-1**, **PF-2**, **PF-3** and **110**..... 46

Table 5. ^{13}C NMR (100 MHz) data for compounds **PF-1**, **PF-2**, **PF-3** and **110**..... 49

Table 6. ^{1}H NMR (400 MHz) data for compounds **28**, **37** and **41**..... 54

Table 7. ^{13}C NMR (100 MHz) data for compounds **28**, **37** and **41**..... 55

Table 8. Cytotoxicity of the isolated compounds from the roots of *P. falcatus* 56

Table 9. Crystal data and structure refinement for nagilactone D (**41**) 124

Table 10. Bond lengths [Å] and angles [°] for nagilactone D (**41**)..... 125

Table 11. Hydrogen bonds for nagilactone D (**41**) [Å and °] 127

Table 12. Crystal data and structure refinement for 2β-hydroxynagilactone F (**108**) 128

Table 13. Bond lengths [Å] and angles [°] for 2β-hydroxynagilactone F (**108**)..... 128

Table 14. Hydrogen bonds for 2β-hydroxynagilactone F (**108**) [Å and °]. 130

Table 15. Crystal data and structure refinement nagilactone I (**109**)..... 131

Table 16. Bond lengths [Å] and angles [°] for nagilactone I (**109**) 132

Table 17. Hydrogen bonds for nagilactone I (**109**) [Å and °]..... 133

List of Acronyms

CC	*C*olumn *C*hromatography
COSY	*Co*rrelation *S*pectroscop*y*
DCM	*D*ichloro*m*ethane
DNA	*D*eoxyribo*n*ucleic *A*cid
ED_{50}	*E*ffective *d*ose to kill *50 %* of tumor cells
HER2	*H*uman *E*pidermal *G*rowth *F*actor *R*eceptor *2*
HMBC	*H*eteronuclear *M*ultiple *B*ond *C*orrelation
HPLC	*H*igh-*p*erformance *L*iquid *C*hromatography
HRESIMS	*H*igh-*r*esolution *E*lectrospray *I*onization *M*ass *S*pectrometry
HSQC	*H*eteronuclear *S*ingle *Q*uantum *C*oherence *S*pectroscopy
IR	*I*nfra*r*ed
MDR	*M*ulti*d*rug-*r*esistance
NMR	*N*uclear *M*agnetic *R*esonance *S*pectroscopy
NOESY	*N*uclear *O*verhauser *E*ffect *S*pectroscopy
PUFAs	*P*oly*u*nsaturated *F*atty *A*cids
Q-TOF	*Q*uadrupole-*t*ime-*o*f-*f*light
ROS	*R*eactive *O*xygen *S*pecies

RP-18	*R*everse-*p*hase C_{18} column
TLC	*T*hin-*l*ayer *C*hromatography
UV	*U*ltra*v*iolet

1. Introduction

1.1. Cancer

1.1.1. Definition, pathogenesis and causes: An overview

Cancer, which encompasses more than 200 unique diseases, is a deregulated multiplication of cells with the consequence of an abnormal increase of the cell number in particular organs (Schwab, 2012; Abernethy *et al.*, 2014). Typically aberrant gene function and altered patterns of gene expression results in alteration of crucial intracellular signaling pathways associated with the regulation of cell survival, proliferation, differentiation and death mechanisms, ending up in uncontrolled cell division and dissemination to other organs–which is the major cause of cancer death (Yokota, 2000; Jones and Baylin, 2007; de Souza *et al.*, 2011). Thus, the hallmarks of cancer can be identified as self-sufficiency in growth signals, insensitivity to growth-inhibitory (antigrowth) signals, evasion of programmed cell death (apoptosis), limitless replicative potential, sustained angiogenesis, and tissue invasion and metastasis (Hanahan and Weinberg, 2000; 2011). In short, exposure to carcinogens, failure of DNA repair and progressive genetic instability lead to accumulation of mutations that drive cancer development, growth and metastasis (Dancey *et al.*, 2012).

Progressing through initiation, promotion and progression to metastasis, cancer mainly results from an imbalance in the function of oncogenes and tumor suppressor genes that involve the gain-of-function mutation, amplification, and/or overexpression of key oncogenes together with the loss-of-function mutation, deletion, and/or epigenetic silencing of key tumor suppressors (Luo *et al.*, 2009). Proposed by Otto Warburg some 50 years ago, it is thought that chronic hypoxia and/or reactive oxygen species (ROS) accumulation

leading to reprogramming of energy metabolism as the major initiator of cancer (Zhang *et al.*, 2015). Studies indicate chronic inflammation as a major linker of hypoxia, ROS and cancer (Federico *et al.*, 2007; Borrello *et al.*, 2008; Kundu and Surh, 2008; Reuter *et al.*, 2010; Kundu and Surh, 2012; Candido and Hagemann, 2013).

Perhaps the major cause of death, accounting for more than 90% cancer-associated mortality, from cancer results from the final stages of cancer progression-metastasis-that impairs the function of vital organs (Aguirre-Ghiso, 2007; Jiang and Ablin, 2011; Sosa *et al.*, 2014). Metastasis is the spread, by a process called metastatic cascade, of malignant tumour cells from the primary tumour site to distant organs (through the lymphatic system or the blood), in which they grow expansively to develop deadly secondary tumours (Kitamura *et al.*, 2015). In brief, the metastatic cascade starts with the evasion of anti-tumour immune surveillance by tumor cells at the primary site and then intravasation into blood and/or lymphatic vessels, which allows them to circulate and spread. At the metastatic site these circulating tumour cells extravasate, become established and proliferate to form the deadly metastatic tumour (Kitamura *et al.*, 2015).

The major causes of cancer can be conveniently categorized as internal factors (such as inherited mutations, hormones, and immune conditions) and environmental/acquired factors (such as tobacco, diet, radiation, and infectious organisms) (Anand *et al.*, 2008). While the former accounts for only 5–10% of all cancer cases, the major risk factor, accounting for 90–95%, roots from environmental and lifestyle factors that include cigarette smoking, diet (fried foods, red meat), alcohol, sun exposure, environmental pollutants, infections (viruses and other microorganisms), stress, obesity and physical inactivity (Belpomme *et al.*, 2007; Anand *et al.*, 2008; Khan *et al.*, 2010; Sung *et al.*, 2011). The

evidence indicates that of all cancer–related deaths, almost 25–30% are due to tobacco, as many as 30–35% are linked to diet, about 15–20% are due to infections and the remaining percentage are due to other factors like radiation, stress, physical activity, environmental pollutants etc (Anand *et al.*, 2008).

1.1.2. Epidemiology

With the adoption of lifestyle behaviors that are known to increase cancer risk, such as smoking, poor diet and physical inactivity, coupled with growth and aging of the population, the burden from cancer death is expected to grow worldwide, particularly in less developed countries, in which about 82% of the world's population resides (Kanavos, 2006; Torre *et al.*, 2015). According to a report by International Agency for Research on Cancer (IARC), a specialized agency of the World Health Organization, 14.1 million new cases have been recorded in 2012 and this raised the number of people living with cancer to 32.6 million at that time and the number of deaths were 8.2 million (Ferlay *et al.*, 2015). There is a slight increase compared to 2008 data: 12.7 million new cancer cases and 7.6 million cancer deaths (Ferlay *et al.*, 2010). In the 2012 data, 57% (8 million) of new cancer cases, 65% (5.3 million) of the cancer deaths and 48% (15.6 million) of the 5-year prevalent cancer cases occurred in the less developed regions (Ferlay *et al.*, 2013). Moreover, the number of new cases is expected to rise to 22 million within the next two decades if the current pharmaceutical arsenal to treat cancer has not improved (WHO, 2015).

Ethiopia, as one of less developed nations and coupled with lifestyle changes, is experiencing the increasing burden from cancer. There is also a lack of comprehensive cancer registration and population-based measurement of cancer burden. According to

Woldeamanuel *et al.* (2013), in Ethiopia most of the diagnosis occur at late stage, at which most patients have incurable disease and need mainly palliative care. Though, some hospital records show that there are more than 200,000 cancer cases per year, an estimated 60,000–125,000 per year patients visit the Oncology Unit, the only cancer referral center in the country located at Black Lion Hospital in Addis Ababa. Only about 500 patients (less than 1 %) per year could get treatment services where treatment costs exceed 80,000 ETB ($6,667), which most patients cannot afford (ECA, 2007).

1.1.3. Prevention and treatment modalities: An overview

The 'gold standard' for cancer prevention is to interrupt the cancer-initiating process before pre-cancers form (Umar *et al.*, 2012). Lifestyle modifications–that include better dietary choices, increasing physical activity, maintaining a healthy weight, stopping (or not starting) the use of tobacco, moderating alcohol intake and other lifestyle factors–offer an important strategy for cancer prevention (Mosby *et al.*, 2012; Umar *et al.*, 2012). Since this is not always the case, prevention of cancer–with the intention of intercepting those processes involved in progression to the invasive stage–remains the most promising strategy for reducing both its incidence and the mortality due to this disease and hence ultimately cancer-free survival (Umar *et al.*, 2012). The rationale for this approach is that once the disease is in the metastatic state, treatment is mainly palliative aimed at improving the quality of life the patients (Gennari *et al.*, 2011). To this end various prevention and treatment modalities has been devised.

Depending on the specific pathological and molecular characteristics of the cancer, its location, extent of disease and the health status of the patient, there are different types of treatment, which may be used alone or in combination, either simultaneously or sequen-

tially: surgery, radiotherapy and chemotherapy (Luqmani, 2005) with other relatively new additional options that use biological molecules, targeted therapies and immune-mediated therapies (Chabner and Roberts, 2005; Baxevanis *et al.*, 2009; Vanneman and Dranoff, 2012; Miller *et al.*, 2013). Surgery is most frequently the first line of therapy, and for 'early' cancers, it may be curative. Radiotherapy is most often used in a localized setting and in conjunction with surgical procedures (Luqmani, 2005).

The term 'chemotherapy' refers to the use of drugs to kill or inhibit the growth of cancer cells which can be used for either palliative or curative, as adjuvant or neodjuvant to surgery or primary radiotherapy (Bhosle and Hall, 2006; 2009). Chemotherapy drugs (Table 1) exert their effects by interfering with the processes involved in cell division (Fernando and Jones, 2015). Their therapeutic use stems from their ability to cause a greater proportion of cell kill in cancer cells as opposed to normal cells (Caley and Jones, 2012). Unfortunately, they can also be 'cytotoxic' to normal dividing cells, particularly those with a high turnover, such as the bone marrow and mucous membranes; which are the major cause of sever toxicities associated with chemotherapeutic drugs (Fernando and Jones, 2015).

Table 1. List of chemotherapy drugs classified based on their biochemical properties

Drug class	Mechanism of action	Examples
Alkylating agents	Impair cell function by forming covalent bonds on important molecules in proteins, DNA and RNA. Classified by their chemical structure and mechanism of covalent bonding	Platinums (Cisplatin, Carboplatin, Oxaliplatin) Nitrogen mustards (chlorambucil, melphalan) Oxazophosphorines (cyclophosphamide, ifosfamide)
Anti-metabolites	Structural analogues of naturally occurring metabolities involved in DNA and RNA synthesis. They either substitute for a metabolite that is normally incorporaated in to DNA or RNA or compete for the catalytic site of a key enzyme	Pyrimidine analogues (gemcitabine, 5-fluorouracil, capecitabine) Anti-folates (methotrexate, raltitrexed)
Anti-tumour antibiotics	Intercalate DNA at specific sequences, creating free radicals which cause strand breakage. Anthracyclines, products of the fungus *Streptomyces*, also have mechanism of action of topoisomerase I and II, required for the uncoiling of DNA required for DNA synthesis	Anthracyclines (doxorubicin, epirubicin, bleomycin, mitoxantrone)
Topoisomerase inhibitors	Topoisomerases are enzymes that control the 3D structure of DNA. Topoisoerase I and Topoisomerase II are enzymes responsible for the uncoiling of DNA during replication	Topoisomerase I inhibitors (irinotecan, topotecan) Topoisomerase II inhibitors (etoposide)
Tubulin-binding drugs	They bind to tubulin, and prevent the formation of the microtubule, which is important during mitosis, but also for cell shape, intracellular transport and axonal function Taxoids prevents the disassembly of the microtubules, thereby inhibit normal function	Vinca alkaloids (vincristine, vinorelbine), Taxanes (paclitaxel, docetaxel)

1.2. Natural products

1.2.1. The role of medicinal plants in cancer

Throughout the ages, humans have relied on nature for their basic needs–for the production of foodstuffs, shelters, clothing, means of transportation, fertilizers, flavors and fragrances and, not least, medicines (Newman *et al.*, 2000). The use of natural products (NPs) with therapeutic properties is as ancient as human civilization and for a long time natural products from plants, mineral and animals were the source of virtually all medicinal preparations and drugs (Newman, 2008; Qurishi *et al.*, 2011; Harvey *et al.*, 2015) and still play a vital role in the drug discovery process (Newman, 2008; Ji *et al.*, 2009; Carter, 2011; Morrison and Hergenrother, 2014; Patridge *et al.*, 2015). Many of the clinically used drugs derived from natural products originated from microbial species, particularly in the anti-infective area, but plant-derived drugs have also made significant contributions, and it is certain that mankind would be immeasurably the poorer without such natural plant–derived drugs as morphine, the vinca alkaloids, quinine, artemisinin, taxoids, podophyllotoxin and camptothecin and their derivatives (Kingston, 2011). Marine–based drugs are also making an increasing contribution, with cytarabine, trabectidin, eribulin and vedotin as examples of a marine-derived anticancer drugs (Simmons *et al.*, 2005; Newman and Cragg, 2014; Kita and Kigoshi, 2015).

Analysis of all approved therapeutic agents between 1981 and 2010 indicated that about 40 % of drugs are either NPs or NP-derivatives. More interestingly, the percentage contribution of NPs in the anticancer therapeutic area is more pronounced: Without considering the contribution from the high molecular weight materials (biologicals and vaccines), approximately 75% anticancers were either from NPs or naturally inspired agents

(Newman and Cragg, 2012). Thus, natural products tend to present more structurally diverse ‘‘drug-like’’ and ‘‘biologically friendly’’ molecular qualities than pure synthetic compounds at random and are an important source of novel lead structures for the synthetic and combinatorial chemistry aspects of anticancer drug discovery (Pan *et al.*, 2010a).

Plants have a long history of use as adjuvant (Ho and Cheung, 2014), prevention (Desai *et al.*, 2008; Singh *et al.*, 2012; Ji *et al.*, 2014) and treatment (Cragg and Newman, 2003; Amin *et al.*, 2009; Wang *et al.*, 2012; Perez *et al.*, 2014b) of cancer. Their use led to the discovery of many novel chemotherapeutic types showing a range of cytotoxic activities (Qurishi *et al.*, 2011). There are now four major structural classes of plant-derived compounds used in western medicine as single chemical entity compounds, namely, the *Vinca* alkaloids (vinblastine (**1**), vincristine (**2**), vinorelbine (**3**)), the epipodophyllotoxin lignans (podophyllotoxin (**4**), etoposide (**5**), teniposide (**6**)), the taxane diterpenoids (paclitaxel (**7**), docetaxel (**8**)), and the camptothecin quinoline alkaloid derivatives (camptothecin (**9**), topotecan (**10**), irinotecan (**11**)) (Pan *et al.*, 2010a). The respective plants from which the parent compounds isolated are *Catharanthus roseus* G. Don (Kingston, 2009), *Podophyllum peltuturn* L. (Gordaliza *et al.*, 2004; Guerram *et al.*, 2012), *Taxus brevifolia* L. (Kingston, 2007; Wani and Horwitz, 2014), and *Camptotheca acuminata* Decne (Lorence and Nessler, 2004). These compounds have been found to act on two important biochemical targets, tubulin and topoisomerase (Pan *et al.*, 2012). Besides these, there are numerous plant derived compounds that are active against various forms of cancer that are in clinical trial and these act in a variety of ways (Ouyang *et al.*, 2014).

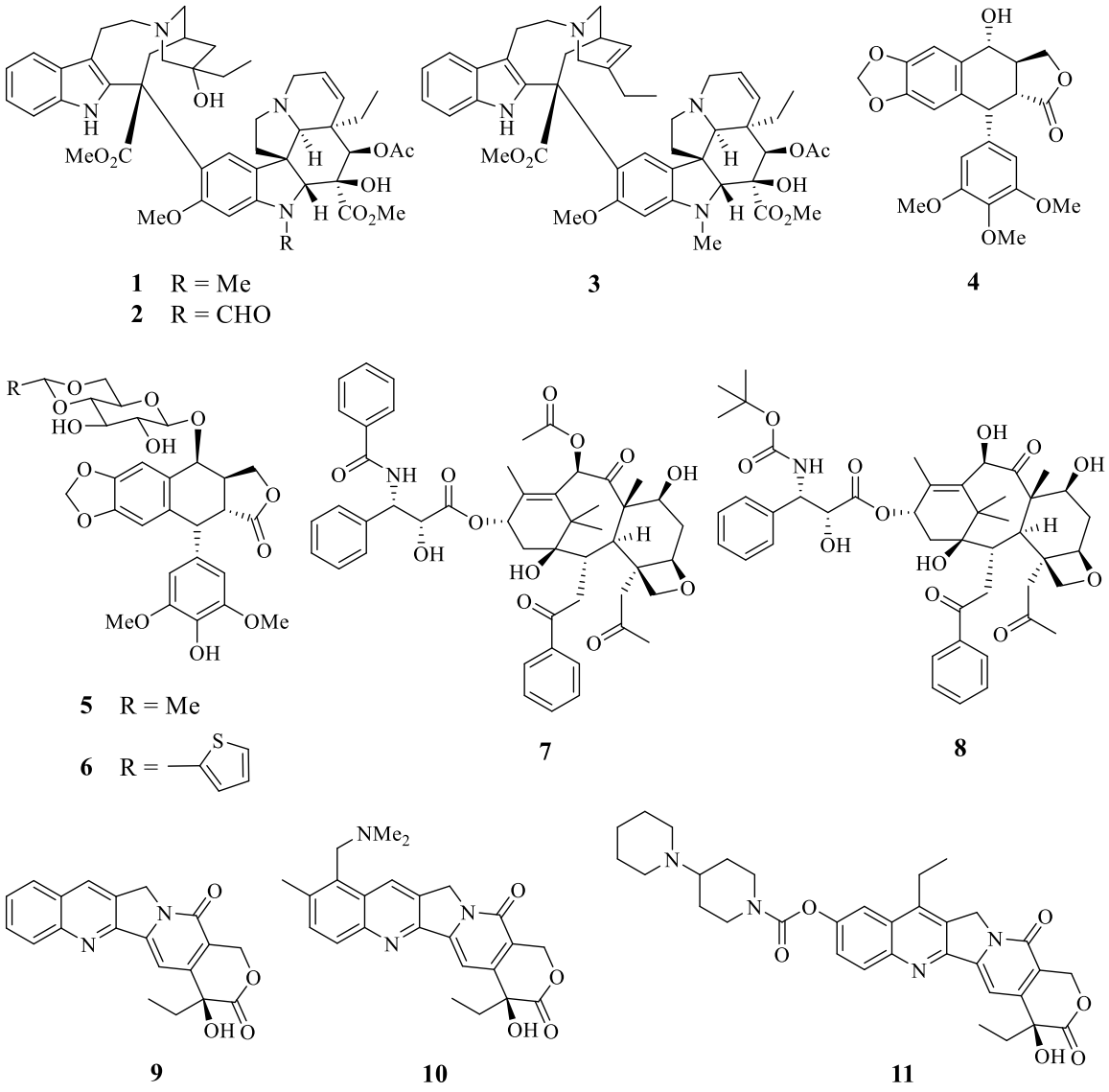

1.2.2. Ethiopian medicinal plants in cancer

Plants have traditionally been used as a source of medicine in Ethiopia since long time ago to control various ailments afflicting humans and their livestock (Wondimu *et al.*, 2007; Giday *et al.*, 2010). In fact, more than 80% of the people are dependent on plants for their health service (Wondimu *et al.*, 2007).

Even though, clear comprehensive cancer prevalence and incidence and definitive diagnostic criteria are absent, many ethnobotanical reports indicate the use of Ethiopian medicinal plants as "anticancer" remedy. These include *Tapinanthus globiferus* (A. Rich.) Tieghem, *Plumbago zeylanica* L., *Gloriosa superba* L. (Yineger *et al.*, 2008), *Clematis bracteata* (Roxb.) Kurz, *Kalanchoe petitiana* A. Rich, *Ranunculus multifidus* Forssk, *Zehneria scabra* (Linn. f.) Sond (Bussmann *et al.*, 2011), *Gladiolus candidus* (Rendle) Goldblatt, *Dorstenia barnimiana* Schwienf, *Podocarpus falcatus* (Thunb.) Mirb (Teklehaymanot, 2009) *Cucumis prophetarum* L., *Maytenus senegalensis* (Lam.) Excell and *Rubia discolor* Turcz (Graham *et al.*, 2000).

More interesting is the isolation of the potent tubulin inhibitor cytotoxic agent maytansine (**12**) (Kupchan *et al.*, 1972) and its analogues (Kupchan *et al.*, 1977; Kupchan and Smith, 1977) from the Ethiopian shrub *Maytenus serrata* and other *Maytenus* spp (Celastraceae). Even though maytansine was about 200– to 1000–fold cytotoxic than anticancer drugs in clinical use that affect tubulin polymerization, such as the *Vinca* alkaloids or taxol, it lacked a therapeutic window due to high systemic toxicity (Tassone *et al.*, 2004). However, due to the advent of antibody-drug conjugate (ADC) drug targeted delivery system (Flygare *et al.*, 2013; Chari *et al.*, 2014; Perez *et al.*, 2014a), a derivative of maytansine, DM1 (**13**) (N^2-deacetyl-N^2-(3-mercapto-1-oxopropyl)- maytansine) was linked with the cytostatic monoclonal antibody trastuzumab (Herceptin) that specifically targets the human epidermal growth factor receptor 2 (HER2) in breast cancer to produce trastuzumab emtansine (T-DM1; **14**) (LoRusso *et al.*, 2011; Amiri-Kordestani *et al.*, 2014).

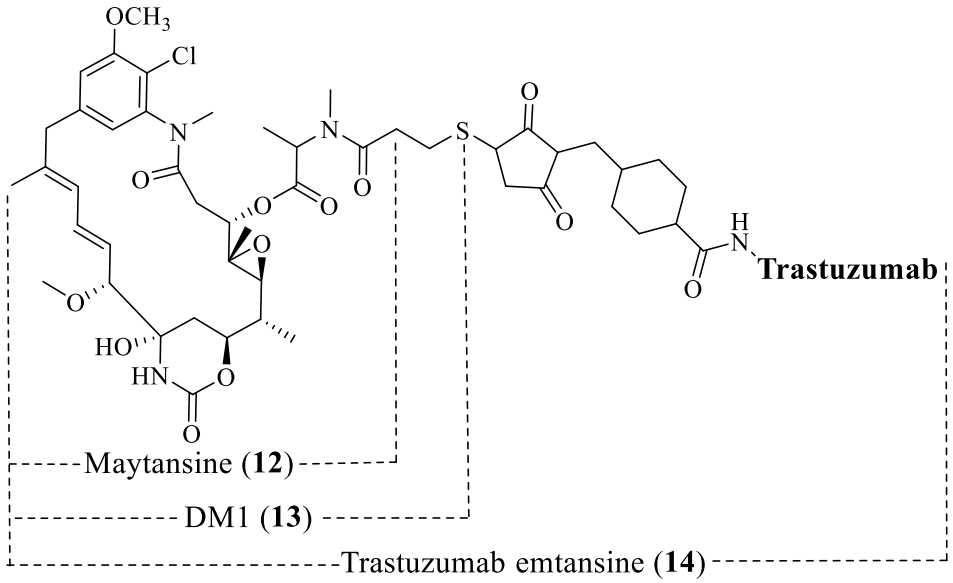

T-DM1, sold under the trade name Kadcyla, is now used for treatment of women with advanced, HER2-positive breast cancer who progress under treatment with trastuzumab and a taxane or develop disease progression after completion of this treatment (Verma *et al.*, 2012; Cho and Roukos, 2013; Barok *et al.*, 2014).

1.3. The family Podocarpaceae

The family Podocarpaceae is composed of evergreen trees or shrubs with resin ducts (Demissew and Friis, 2009). The Podocarpaceae is the most diverse family of conifers, both morphologically and ecologically (Kelch, 1998). The trees and shrubs are sometimes cultivated as ornamentals in suitably warm climates. In terms of number of species, Podocarpaceae is the second largest family of conifers after Pinaceae (Little *et al.*, 2013; Mill, 2014). Even though debates still exist as to the clear idea of the number of the genus that this family comprises (Demissew and Friis, 2009), three principal genera are recognized: *Phyllocladus*, *Podocarpus* and *Dacrydium* (Lowry, 1972), the latter two being the largest and the most diverse (Barkera *et al.*, 2004).

1.4. The genus *Podocarpus*

1.4.1. Description and distribution

The genus *Podocarpus* (Podocarpaceae) is composed of more than 100 species of evergreen coniferous trees or shrubs that are distributed widely throughout tropical, subtropical areas and the South Temperate Zone (Han *et al.*, 2014). Many of its species are important timber trees, and many are threatened with extinction for this or a variety of other reasons such as habitat loss, particularly deforestation or climate change (Mill, 2014).

1.4.2. Chemistry

The genus *Podocarpus* is one of the most extensively studied with respect to chemical composition and as a result many compounds have been characterized including lignans, terpenoids, flavonoids and steroids (Ito and Kodama, 1976).

1.4.2.1. Terpenoinds

The genus *Podocarpus* is well known to natural product chemists as a rich source of terpenoids (Hembree *et al.*, 1979). The most well characterized terpenoids are the diterpenoids, notably totarol (**15**) and its derivatives and a group of highly oxidized norditerpene dilactones generally known as nagilactones or podolactones (Figure 1 and 2) (Ito and Kodama, 1976). The latter are considered to be taxonomic markers for this genus (Abdillahi *et al.*, 2010), though less common sesquiterpenes including podoandin (**16**) (Kubo *et al.*, 1992b) and 15-hydroxyphaseic acid (**17**) (Faiella *et al.*, 2012) have been also isolated from podocarps.

1.4.2.1.1. Diterpenes and derivatives

The most common diterpenoids isolated from *Podocarpus* sp. are the phenolic diterpenes (**15**) and ferruginol (**18**), which are based on totarane and abietane diterpne skeleton, respectively (Figure 1) and their derivatives (Cox *et al.*, 2007). Also, diterpenes belonging to labdane (Kuo *et al.*, 2008), rosettane (Clarke *et al.*, 1997; Chin *et al.*, 2001), kaurene (Aplin *et al.*, 1963), isopimarane and phyllocladane (Campello *et al.*, 1975) class have been isolated from various *Podocarpus* species.

Ferruginol (**18**) is a simple representative of the abietane class that has been first isolated from the resin of *P. ferruginea* (Brandt and Neubauer, 1939) with subsequent isolation from many *Podocarpus* species such as *P. fleuryi* (Zhang *et al.*, 2013) and also from other unrelated genus such as *Vitex rotundifolia* L. f. (Verbenaceae) (Ono *et al.*, 1999) and *Salvia eriophora* (Lamiaceae) (Ulubelen *et al.*, 2002). Besides ferruginol, members of *Podocarpus* are well known to contain other abietane type diterpenoids such as carnosol (**19**) (Cambie *et al.*, 1984), podoimbricatin B (**20**) (Han *et al.*, 2014) and fleuryinols A–C (**21-23**) (Zhang *et al.*, 2013).

Totarol (**15**) is a diterpenoid with migrated abietane carbon skeleton (called totarane skeleton; Figure 1) that has been initially isolated from heartwoods of *P. totara* and then from various *Podocarpus* spp. (Bendall and Cambie, 1995). Totaradiol (**24**), totaral (**25**), 19-hydroxytotarol (**26**) (Cambie *et al.*, 1984; Ying and Kubo, 1991; Reynolds *et al.*, 2006), inumakiols C–H (**27-32**) (Sato *et al.*, 2008), cycloinumakiol (**33**), inumakal (**34**) and inumakoic acid (**35**) (Devkota *et al.*, 2011) are few of congeners of totarol from various *Podocarpus* species. Totarol (**15**) is also considered to be the precursor of the C_{40} totarane-dimeric compounds podototarin (**36**) (Cambie and Mander, 1962) and macrophyl-

lic acid (**37**) (Bocks *et al.*, 1963) originally isolated from the heartwoods of *P. totara* and *P. macrophylhs* D. Don, respectively. These are considered to be taxonomic markers of the family Podocarpaceae (Ito and Kodama, 1976).

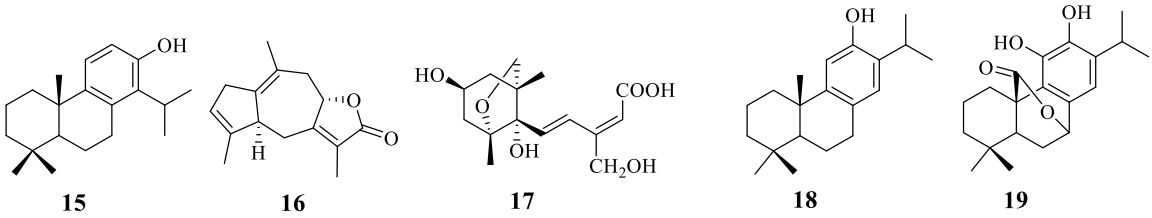

15 **16** **17** **18** **19**

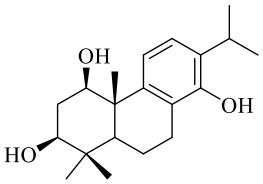

20

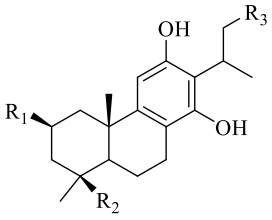

	R_1	R_2	R_3
21	H	CH_2OH	OH
22	OH	CH_3	H
23	OH	CH_3	OH

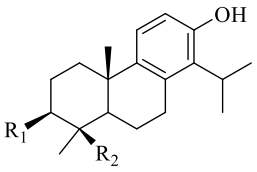

	R_1	R_2
24	OH	CH_3
25	H	CHO
26	H	CH_2OH

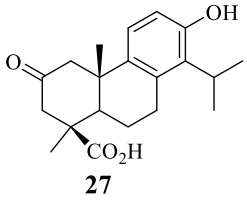

27

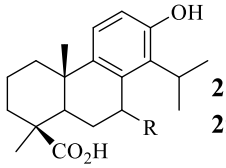

28 R= OH
29 R = OCH_3

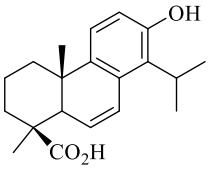

30

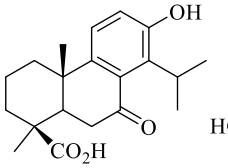

31

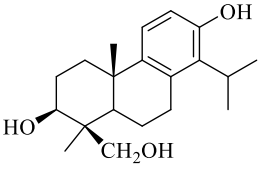

32

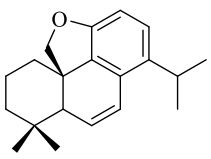

33

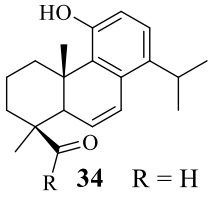

34 R = H
35 R = OH

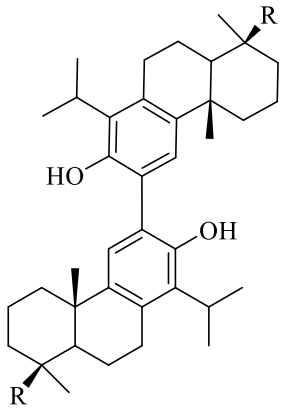

36 R = CH_3
37 R = CO_2H

1.4.2.1.2. Nagilactones

The family of nor- and bisnor- diterpenoid dilactones known as nagilactones (podolactones) consists of more than 70 members, exhibiting a wide range of biological activities (Hanessian *et al.*, 2009). The structural features common to the whole group is that they have 1) the degraded ring C of totarane carbon skeleton to unsaturated δ-lactone, as such the numbering of the podolactone skeleton follows that of totarane skeleton (Figure 1) 2) a γ-lactone between C-19 carbon and the β-oriented hydroxyl group at C_6, 3) two tertiary methyl groups, α-methyl at C4 and β-methyl at C-10 and 4) extensively oxidized carbocyclic rings A ond B with hydroxyl, epoxy and/or olefinic groups. So that all of these dilactones have 19 carbons at largest and up to 9 oxygen atoms in the molecule (Ito and Kodama, 1976).

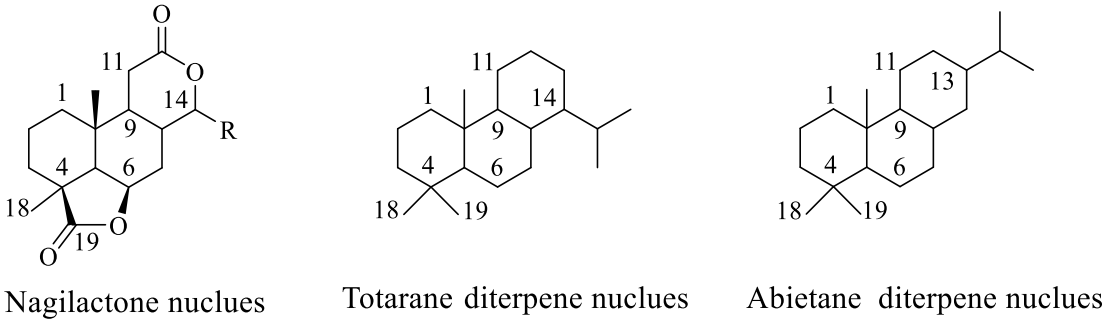

Figure 1. Nagilactone, totarane and abtietane diterpene nucleus

The three rings of nagilactones are designated as A, B and C similar to those found in abietane, totarane, podocarpane diterpenes (Figure 2). Based on the unsaturation patterns of B and C rings, nagilactones are classified into three major groups: type A, which are those with α-pyrone [8(14),9(11)-dienolide], type B with 7α,8α-epoxy-9(11)-enolide and type C with 7(8),9(11)-dienolide (Hayashi and Matsumoto, 1982; Barrero *et al.*, 2003).

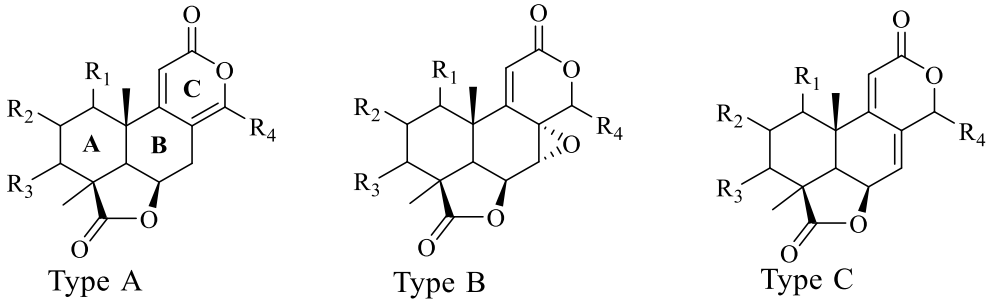

Figure 2. Types of nagilactones

Type A nagilactones

Typical UV features for this class is the presence of λ_{max} 300-305 nm while their IR is well characterized by absorptions for γ-lactone (at 1760–1780 cm^{-1}) and δ-lactone (1685–1740 cm^{-1}) in addition to a weak band due to C=C conjugated with C=O (1620–1640 cm^{-1}) (Ito and Kodama, 1976). Examples of this group include nagilactones A–D (**38-41**) (Hayashi *et al.*, 1968), inumakilactone E (**42**) (Hayashi *et al.*, 1972a), hallactone A (**43**) (Russell *et al.*, 1973) and the chlorine containing dilactone rakanmakilactone G (**44**) (Park *et al.*, 2004a).

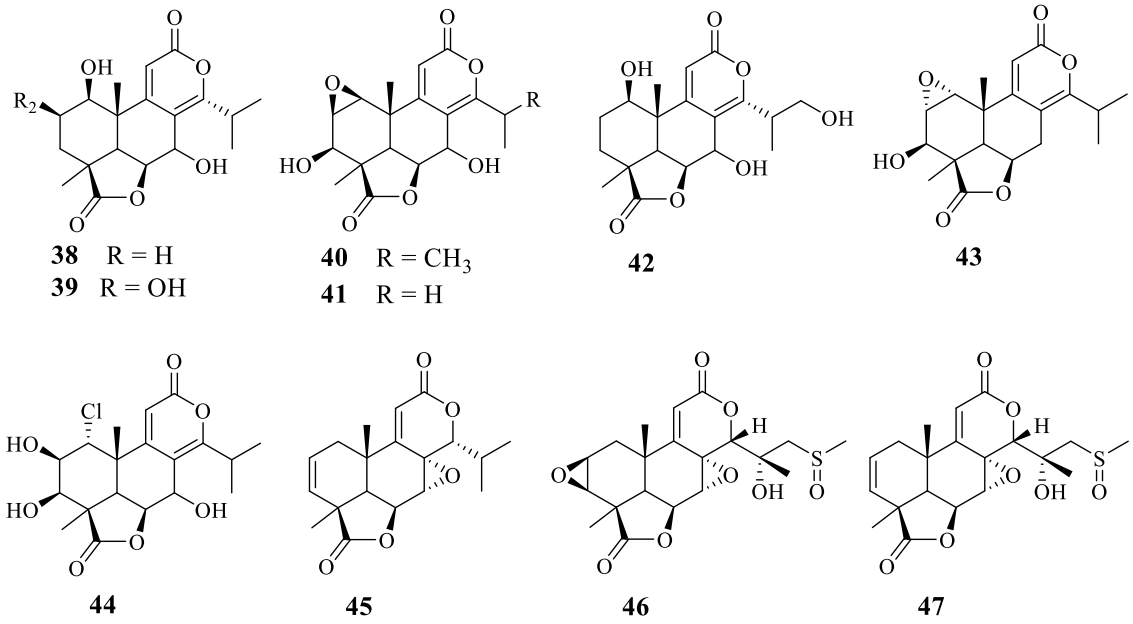

Type B nagilactones

This class of nagilactones are characterized by UV λ_{max} of 217-221 nm due to the conjugated δ-lactone which is also responsible for IR absorption at 1705-1733 cm^{-1}. A weak absorption due to C=C conjugated with C=O shows signal at 1640-1650 cm^{-1} while IR absorption due to γ-lactone is quite similar to type A dilactones (Ito and Kodama, 1976). A representative of this class is the antileukomic podolide (**45**) from twigs and leaves of *P. gracilior* Pilg (Kupchan *et al.,* 1975) with the additional examples as the sulfur containing derivatives podolactone C (**46**) and D (**47**) from bark of the *P. neriifolius* (Galbraith et al., 1971), rakanmakilactones A–F (**48-53**) from leaves of *P. macrophyllus* var. *maki* . (Park *et al.*, 2004b) and makilactones N–R (**54-58**) form the dried root of *P. macrophyllus* D. Don (Sato *et al.*, 2009a).

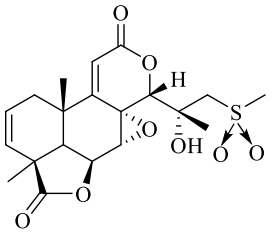

48

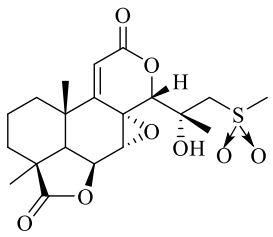

49

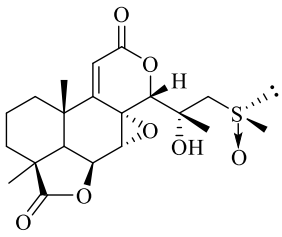

50

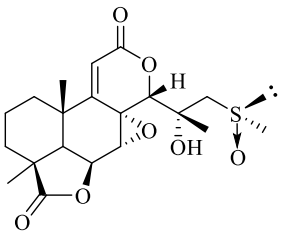

51

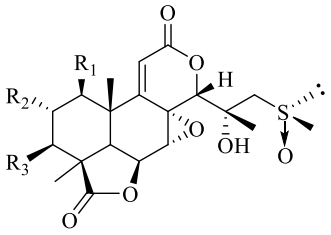

	R_1	R_2	R_3
52	H	Cl	OH
53	OH	H	H

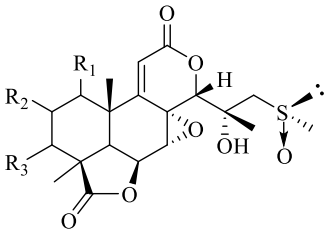

54 R_1 =R_2 = H, R_3 =β-OH
55 R_1–R_2 = β-epoxy, R_3 =β-OH
56 R_1–R_2 = β-epoxy, R_3 =α-OH
57 R_1 = β-OH, R_2 = R_3 = H
58 R_1 = H, R_2–R_3 =β-epoxy

Type C nagilactones

Though limited in number, this group contains the most cytotoxic norditerpenoids with 7:8,9:11-dienolide moiety (Hayashi *et al.*, 1979; Hayashi and Matsumoto, 1982). The conjugated dienolide gives a characteristic UV absorption at λ_{max} 257-263 nm, whereas IR typically shows signals at 1700-1720 cm^{-1} (δ-lactone) and 1608-1643 cm^{-1} (C=C conjugated with C=O) besides the signal for γ-lactone similar to the other two groups (Ito and Kodama, 1976). Nagilactone F (**59**) (Hayashi *et al.*, 1972b), ponalactone A (**60**) (Ito *et al.*, 1971), nubilactone A (**61**) (Silva *et al.*, 1973) and makilactones A–D (**62-65**) (Sato *et al.*, 2009b) are few examples that belong to this group.

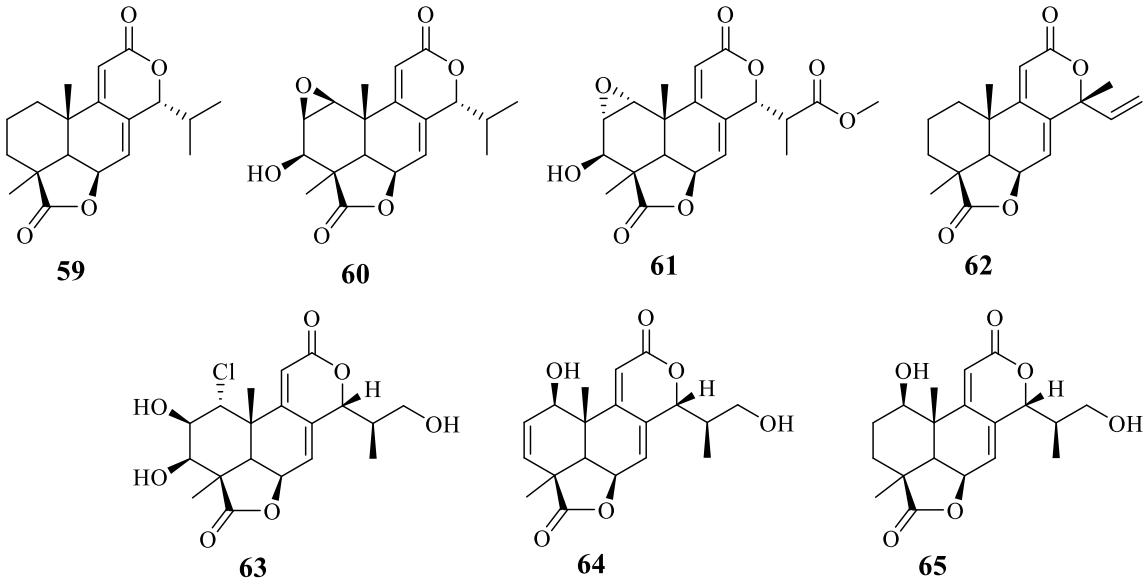

1.4.2.2. Flavonoids

Nubigenol (**66**) is a chalcone isolated from the extract from the leaves and stems the Chilean *P. nubigena* (Bhakuni *et al.*, 1973), whereas kaempferol (**67**), quercetin (**68**), aromadendrin (**69**) and taxifolin (**70**) have been isolated from various *Podocarpus* sp. (Briggs and Cain, 1959; Briggs *et al.*, 1959a). Many anthocyanins and their glycosides, such as pelargonidin (**71**) and peonidin (**72**) (Lowry, 1972), cyanidin-3-neohesperidoside

(**73**) (Crowden, 1974), delphinidin-3-neohesperidoside (**74**) and cyanidin-3-rutinoside (**75**) (Andersen, 1989), cyanidin-3-glucoside (**76**) (Crowden and Grubb, 1971) and delphinidin-3,5-diglucoside (**77**) (Lowry, 1968) have been isolated from various podocarps. Isoflavonoids have also been characterized as exemplified by biochanin A (**78**), daidzein (**79**), genistein (**80**), irisolidone (**81**) and podospicatin (**82**) (Briggs and Cain, 1959; Briggs and Cebalo, 1959; Carman *et al.*, 1985).

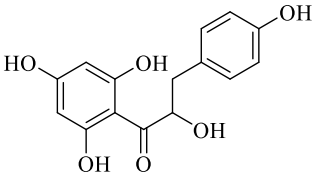

66

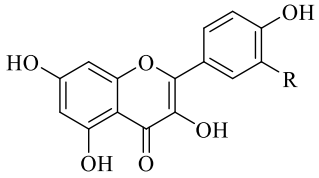

67 R = H
68 R = OH

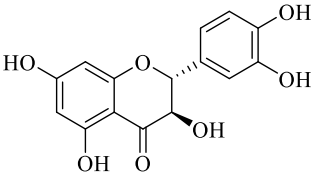

69 R = H
70 R = OH

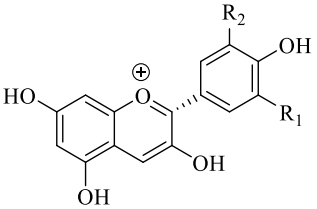

	R_1	R_2
71	H	H
72	H	OCH_3

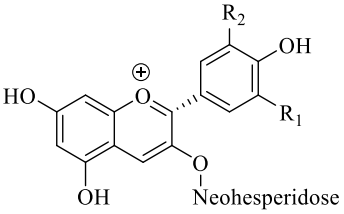

	R_1	R_2
73	H	OH
74	OH	OH

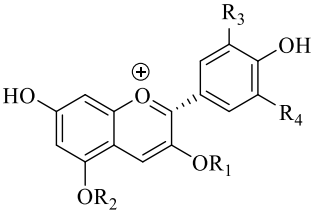

	R_1	R_2	R_3	R_4
75	Rutinose	H	H	OH
76	Glu	H	H	OH
77	Glu	Glu	OH	OH

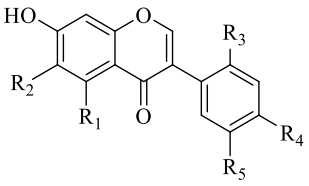

	R_1	R_2	R_3	R_4	R_5
78	OH	H	H	OCH_3	H
79	H	H	H	OH	H
80	OH	H	H	OH	H
81	H	OCH_3	H	OCH_3	H
82	OH	OCH_3	OH	H	OCH_3

As a member of the Gymnospermae, the family Podocarpaceae is characterized by occurrence of bioflavonoids (Krauze-Baranowska *et al.*, 2004). More specifically, *Podocarpus* species contain a simple pattern of derivatives based on amentoflavone (**83**) and hinokiflavone (**84**) (Roy *et al.*, 1987), which are C-3′/C-8″ and C-4′/O/C-6′ dimers of apigenin

(**85**) (Krauze-Baranowska *et al.*, 2004). Podocarpusflavanone (**86**) (Roy *et al.*, 1987), isoginkgetin (**87**), podocarpusflavone A (**88**) and B (**89**) (Haider *et al.*, 1974), bilobetin (**90**), sequoiaflavone (**91**) (Hameed *et al.*, 1973), neocryptomerin (**92**) (Miura *et al.*, 1968) and heveaflavone (**93**) (Yeh *et al.*, 2012) are just very few examples of bioflavonoids isolated from *Podocarpus* sp.

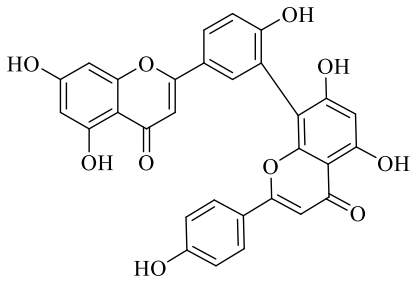

83

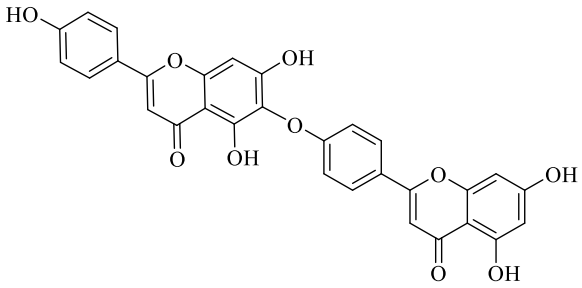

84

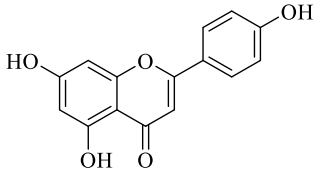

85

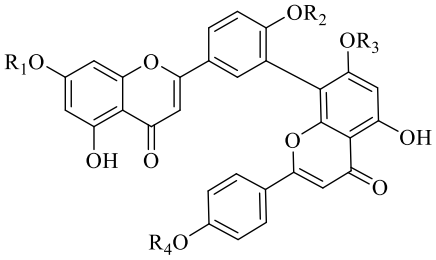

	R_1	R_2	R_3	R_4
86	CH_3	H	CH_3	CH_3
87	H	CH_3	H	CH_3
88	H	H	H	CH_3
89	CH_3	H	H	CH_3
90	H	CH_3	H	H
91	CH_3	H	H	H
92	CH_3	H	CH_3	CH_3

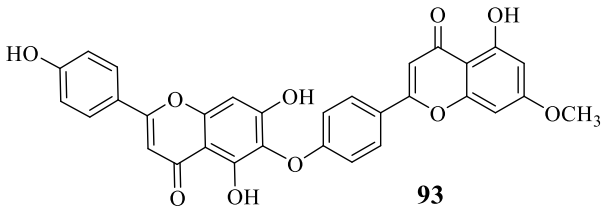

93

1.4.2.3. Phytoecdysteroids

The genus is well known as the first source of phytoecdysteroids (Nakanishi *et al.*, 1966), these are C_{27}–C_{29} analogues of the arthropod steroid hormones ecdysteroids which regulate moulting, metamorphosis, reproduction, embryogenesis and diapauses (Dinan, 2009). Almost all possess common key features: cholest-7-en-6-one carbon skeleton, β oriented

CH_3-10 and CH_3-13, *trans* B/C- and C/D-ring junctions and usually *cis* A/B configuration (Dinan, 2001).

The number of phytoecdysteroids isolated exceeds 463 (Laekeman and Vlietinck, 2013) and more than 20 species of *Podocarpus* are known to contain phytoecdysteroids (Mamadalieva, 2013). Ponasterone A (**94**) (Nakanishi *et al.*, 1966; Kubo *et al.*, 1984), crustecdysone (**95**) (Galbraith and Horn, 1969), ponasterone B (**96**) and C (**97**) (Nakanishi *et al.*, 1968) and makisterones A–D (**98-101**) (Imai *et al.*, 1968a; Imai *et al.*, 1968b) are just few representative examples.

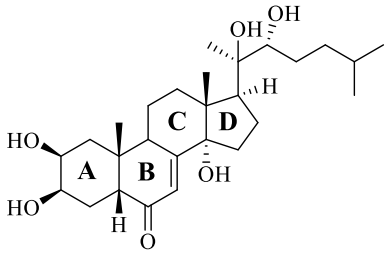

94

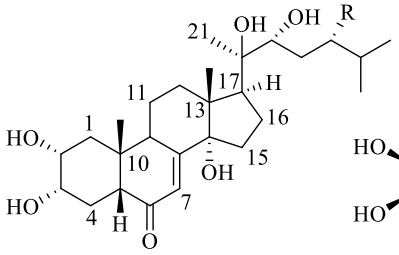

95 R = H
96 R = OH

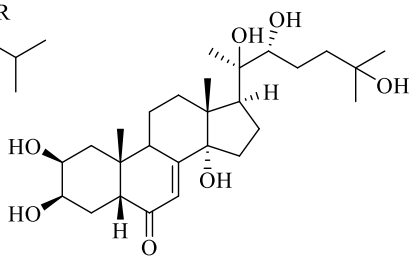

97

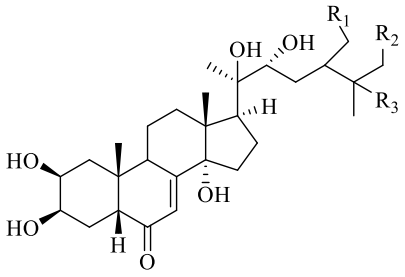

	R_1	R_2	R_3
98	H	H	OH
99	H	OH	H
100	CH_3	H	OH

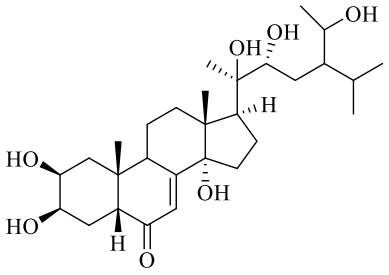

101

1.4.2.4. Miscellaneous compounds

Even though less common lignans such as thujaplicatin methyl ether (**102**) (Matlin *et al.*, 1984) and secoisolariciresinol (**103**) (Briggs *et al.*, 1959b), cyclopeptides such as nagitide A (**104**) and B (**105**) (Zhang *et al.*, 2012) and fatty acids such as sciadonic acid (20:3Δ5,11,14) (**106**) and juniperonic acid (20:4Δ5,11,14,17) (**107**) (Wolff *et al.*, 1999;

Hammann *et al.*, 2015) have been isolated from the genus *Podocarpus* besides those mentioned above.

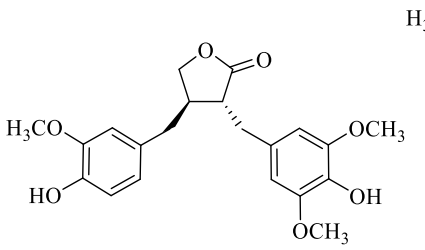

102

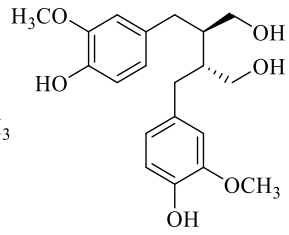

103

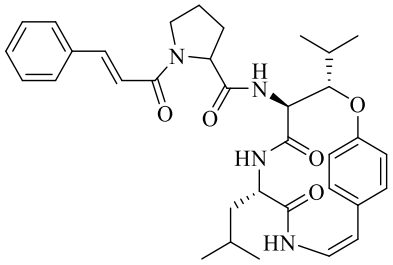

104

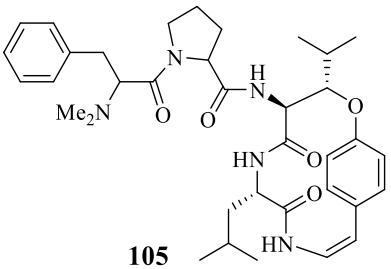

105

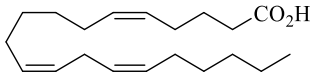

106

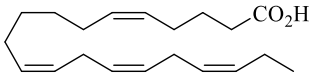

107

1.4.3. Ethnobotanical and pharmacological uses

The genus *Podocarpus* has got many applications ranging from commercial timber production to cultural use, e.g. as a love charm by the Zulu in South Africa and in treating all types of ailments in various parts of the world in the traditional system of medicine (Abdillahi *et al.*, 2010). For the natural product chemist, the genus is known to provide chemically, biologically and pharmacologically interesting compounds such as **15** and **18** and their derivatives, nagilactones, phytoecdysteroids and biflavonoids (Hayashi *et al.*, 1980). Specially, the nagilactones exhibit a broad spectrum of biological activity as anti-tumor agents against human and murine cancer lines2 and oncogenic transcription factors (Hayashi and Sakan, 1975; Kupchan *et al.*, 1975; Hayashi *et al.*, 1977b; 1977a; Hayashi *et al.*, 1979; Hembree *et al.*, 1979; Cassady *et al.*, 1984; Shrestha *et al.*, 2001; Park *et al.*, 2004a; Park *et al.*, 2004b; Kuo *et al.*, 2008; Sato *et al.*, 2009a; Sato *et al.*, 2009b), plant

growth regulators (Galbraith *et al.*, 1972; Hayashi *et al.*, 1972a; Hayashi *et al.*, 1972b; Sasse *et al.*, 1981; Kubo *et al.*, 1991b), insecticides (Russell *et al.*, 1973; Kubo *et al.*, 1984; Zhang *et al.*, 1992), antifeedants (Hayashia *et al.*, 1992; Macias *et al.*, 2000) and antifungal (Kubo *et al.*, 1991a).

The dominant diterpenoids **15** and **18** and their derivatives are also shown to possess a range of activities including antibacterial (Kubo *et al.*, 1992a; Micol *et al.*, 2001; Sato *et al.*, 2008), cytotoxicity to tumor cells (Reynolds *et al.*, 2006; de Jesus *et al.*, 2008; Zhang *et al.*, 2013; Han *et al.*, 2014), inhibition of lipid peroxidation, gastroprotective and ulcer healing effect (Rodriguez *et al.*, 2006). Interestingly, totarol is shown to be active against methicillin resistant *Staphylococcus aureus* (MRSA) (Kubo *et al.*, 1992a; Muroi and Kubo, 1994).

1.5. *Podocarpus falcatus*

1.5.1. Description and distribution

Locally known as *zigiba* and commercially as Podo or East African Yellow Wood (Pankhurst, 2000), *P. falcatus* (Thunb.) R.Br. ex Mirb. (synonym: *Afrocarpus falcatus* (Thunb.) C. N. Page) is an evergreen, dioecious, medium- to large-sized tree up to 60 m tall widely distributed in Ethiopia, Kenya, Tanzania, Mozambique, South Africa, and Madagascar (Figure 3) (Mabberley, 1997; Aerts, 2008). It is an indigenous tree species that grows at 1500–2500 m altitude above sea level in areas with mean annual rainfall of 1200–1800 mm (Feleke *et al.*, 2012; Tadele and Fetene, 2013). *P. falcatus* is known as a year round seeding tree whose seedlings and saplings are neither browsed by cattle and wildlife nor severely attacked by insects (Strobl *et al.*, 2011). *P. falcatus* is one of the potentially oldest tree species so far known from eastern Africa (Krepkowski *et al.*, 2012).

It is a multipurpose species with a wider range of socio-economic and environmental importance (Teketay, 2011).

Figure 3. Picture of *Podocarpus falcatus*

1.5.2. Chemistry, ethnobotanical uses and ethnopharmacological reports

The timber of *P. falcatus* is used for construction and household utensils. In addition, in some areas of Ethiopia local communities collect the fruit of *P. falcatus* growing in their areas to produce edible oil (Feleke *et al.*, 2012). Moreover, the oils are said to have medicinal properties in curing gonorrhoea and the powder from the bark is used for curing headaches (Pankhurst, 2000). Other ethnobotanical reports also indicate the use of various parts of *P. falcatus* for treatment of human and livestock diseases: roots for evil spirit and bone fracture (Lulekal *et al.*, 2014) and febrile illness (Mesfin *et al.*, 2009), leaves for hair loss and rabies and fruits for ringworm (Yineger *et al.*, 2008). Besides those and other medicinal, commercial and ecological importance, ethnobotanical reports from some parts of Ethiopia indicate that preparations from the roots of this plant are used as “anti-

cancer" remedies (Lulekal *et al.*, 2008; Teklehaymanot, 2009). This formed the basis for this research to isolate the "responsible" compounds for its traditional use as "anticancer" remedy.

A methanolic extract from the leaves and young stems of *P. falcatus* was shown to possess antioxidant, COX and tyrosinase inhibitory activities (Abdillahi *et al.*, 2011), while an ethanolic extract from the same parts was shown to be cytotoxic against HepG2 cells (Abdillahi *et al.*, 2012). The wood of *P. falcatus* has been shown to contain **15** and **37** (Cambie *et al.*, 1984). More recently, from the seed oil of *P. falctus*, Hammann *et al.* (2015) isolated the unusual polyunsaturated fatty acids (PUFAs) **106** and **107** along with other common PUFAs.

1.6. Statement of the problem

With rare exception, today's therapies for most forms of human cancer remain incompletely effective and transitory, despite knowledge of driving oncogenes and crucial oncogenic signaling pathways amenable to pharmacological intervention with targeted therapies (Hanahan and Coussens, 2012). Various factors contribute: While surgery is usually effective in early-stage disease (Fernando and Jones, 2015), radiotherapy (Marín *et al.*, 2015) and chemotherapy (Torrisi *et al.*, 2011; Livshits *et al.*, 2014) are shown to produce severe non–selective toxicities to normal cells–nausea and vomiting, myelosupression with leucopenia, thrombocytopenia, anaemia, mucous membrane ulceration and alopecia–among others (Garg, 2011; Caley and Jones, 2012; Fernando and Jones, 2015).

The emergence of drug resistance, the most common of which is multidrug resistance (MDR), to chemotherapeutic agents is another factor that limits the efficacy of chemo-

therapy and leads to failure of the treatment clinically, more specifically in over 90 % of patients with metastatic stage (Kibria *et al.*, 2014). Reduced delivery of cytotoxic agents to the cell, increased drug efflux, mutations of the drug target, DNA damage repair, increased drug metabolism and detoxification, activation of alternative signaling pathways and evasion of cell death are some of the mechanisms in MDR (Holohan *et al.*, 2013; Rebucci and Michiels, 2013; Fernando and Jones, 2015).

Accompanied with the ever increasing cancer incidence and prevalence, the above factors necessitate the search for new drugs with new mode of action and better safety profile. Highly reputed with their role in the drug discovery process (Taylor *et al.*, 2001; Balunas and Kinghorn, 2005; Gurib-Fakim, 2006; Itokawa *et al.*, 2008; Saklani and Kutty, 2008), medicinal plants from traditional medical system are proven to be an important source of anticancer drugs (Cragg and Newman, 2005; Brower, 2008; Poojari *et al.*, 2012), even in providing compounds active against MDR cancers (Chen *et al.*, 2010; Klepsch *et al.*, 2010; Li *et al.*, 2010; Nabekura, 2010; Wu *et al.*, 2011). Thus, the general aim of this research was *in vitro* evaluation and isolation of antiproliferative compounds from the roots of the Ethiopian traditional "anticancer" remedy, *P. falcatus*.

2. Objectives

2.1. General objective

To isolate antiproliferative compounds from the roots of the Ethiopian traditional "anticancer" remedy *Podocarpus falcatus* (Thunb.) R.Br. ex Mirb. (Podocarpaceae) using the human colorectal adenocarcinoma (HT-29) cell line through bioassay-guided fractionation and isolation.

2.2. Specific objectives

- To carry out cytotoxicity testing in a bioassay-guided manner, using sulforhodamine B colorimetric assay.
- To isolate and purify active compound(s) using HPLC
- To elucidate the structure of isolated compound(s) using various spectroscopic methods.

3. Materials and methods

3.1. Materials

3.1.1. Chemicals

Methanol, water, dichloromethane, ethyl acetate, hexanes for extraction, partition and fractionation on open column chromatography (CC) were either purchased from Sigma-Aldrich (Sigma-Aldrich Co., MO, USA) or Thermo Fisher Scientific (Thermo Fisher Scientific Inc., Waltham, MA, USA) and all were of analytical grade. HPLC grade methanol and water were purchased from either Sigma-Aldrich or Thermo Fisher Scientific. Sephadex LH-20 (GE, Uppsala, Sweden) and silica gel (SilicaFlash®P60, 230–400 mesh; SiliCycle Inc., Quebec, Canada) were used for open CC. Analytical TLC was performed using pre-coated silica gel 60 F_{254} plates (aluminium backed, 200 µm, Merck KGaA, Darmstadt, Germany) and a freshly prepared solution of Modified Godin's reagent was used for chemical detection on TLC plates. The deuterated NMR solvents, $CDCl_3$, CD_3OD, DMSO-d_6 and pyridine-d_5, were either purchased from Sigma-Aldrich or Cambridge Isotope Laboratories, Inc (Tewksbury, MA, USA)

3.1.2. Instruments

Water from the extract was removed using Operon freeze dryer (Operon Co. Ltd., South Korea). Organic solvents and water from fractions and compounds were removed using Heidolph rotary evaporators (Heidolph Instruments GmbH & Co.KG, Germany). Optical rotations were measured on a PerkinElmer model 343 polarimeter (PerkinElmer, Waltham, MA, USA). UV spectra were recorded on a Hitachi U2910 UV spectrophotometer (Hitachi High-Technologies Corporation, Tokyo, Japan). IR spectra were recorded on a Nicolet 6700 FT-IR spectrometer (Thermo Fisher Scientific Inc., Waltham, MA, USA).

^{1}H and ^{13}C, HSQC, HMBC, NOESY and COSY NMR spectra were recorded at room temperature on a Bruker AVIII400 instrument (Bruker, Billerica, MA, USA). HRESIMS were measured on a Q-TOF mass spectrometer (Waters Corp., Milford, MA, USA) in the positive-ion mode with NaI being used for mass calibration. HPLC was performed with a Hitachi Primaide HPLC (Hitachi High-Technologies Corporation, Tokyo, Japan) equipped with Primaide 1430 Diode Array Detector, Primaide 1210 Autosampler and Primaide 1110 pump with degasser and a semi-preparative C_{18} column (Dynamax C_{18} HPLC Column 10 × 250 mm).

3.1.3. Plant material collection

Roots of *P. falctus* were collected from the Berga forest, Addis Alem (55 km west of Addis Ababa), Oromia Region, Ethiopia, in March 2014. Identification of the plant material was done by Mr. Melaku Wondafrash, Senior Botanist at the National Herbarium, Addis Ababa University, Addis Ababa, Ethiopia. Voucher specimens (EMA004) were deposited at the National Herbarium, Addis Ababa University, Addis Ababa, Ethiopia.

3.2. Methods

3.2.1. Extraction, bioassay-guided fractionation and isolation

The air-dried roots of *P. falcatus* (270 g) were extracted with 90% MeOH (3 × 0.6 L) by maceration at room temperature for nine consecutive days with solvent renewal every 72 hrs.

The bioassay-guided fractionation and isolation was monitored by using the human colon cancer cells (HT-29) in which extracts and fractions, and isolated compounds were con-

sidered active if they have a dose that kills 50% (ED_{50}) of the tumors at less than 20 µg/ mL and 10 µM, respectively (Pan *et al.*, 2010b).

3.2.2. Cell culture and cytotoxicity assay

Cytotoxic potential of the extract, fractions and isolated compounds against HT-29 was determined using an established protocol (Pan *et al.*, 2010b) using paclitaxel as positive control. The detailed procedure is described below.

Human colon cancer cells (HT-29) were obtained from American Type Collection (ATCC catalog no. HTB-38). Cells were cultured in MEME medium (Hyclone, Logan, UT) supplemented with streptomycin (100 µg/mL), penicillin (100 units/ mL), amphotericin B (Fungizone, 0.25 µg/mL), and 10% fetal bovine serum (FBS) and incubated in a humidified incubator with an atmosphere of 95% air and 5% CO_2 at 37 °C. Cells were trypsinized and split for subculture when they reached near-confluent state (five days or later). Upon reaching about 60-70% confluence, the medium was changed and the cells were used for test procedures one day later.

The harvested cells, after appropriate dilutions, were seeded in 96- well (9500 cells/190 µL) plates using complete medium and treated with the test compounds (10 µL/well in triplicate) at various concentrations. Test samples were initially dissolved in DMSO and then diluted 10-fold with H_2O. Serial dilutions were performed using 10% DMSO as the solvent. For the control groups, 10 µL of 10% DMSO was also added to each well. The plates were incubated for three days at 37 °C in 5% CO_2. On the third day, the cells were fixed to the plates by the addition of 100 µL of cold 20% trichloroacetic acid and incubated at 4 °C for 30 min. The plates were washed three times with tap water and dried

overnight. The fixed cells were dyed with sulforhodamine B (SRB, an anionic protein stain) solution at 0.4% (w/v) in 1% acetic acid and incubated at room temperature for 30 min. The plates were washed three times with 1% acetic acid and allowed to air-dry. The bound SRB stain was then solubilized with 10 mM unbuffered Tris base (pH 10, 200 µL/well). The plates were placed on a shaker for 5 min, and the absorbance was read at 515 nm using a Bio-Tek µQuant microplate reader. The ED_{50} values of test samples with serial dilutions were calculated using nonliner regression analysis (Table Curve2Dv4; AISN Software, Inc., Mapleton, OR).

The use of HT-29 tumor cell line was just to monitor the activity of the extract, fractions and isolated compounds; it should not be interpreted in a way that the cell line was used because the plant is used traditionally for colon cancer. In fact, none of the reports indicate use for specific type of cancer. Moreover, this is a well-established protocol developed by the College of Pharmacy at The Ohio State University to evaluate the activity of extracts, fractions and synthetic and natural compounds.

3.2.3. X-ray crystallography of compounds 41, 108 and 109.

Crystals of compounds **41**, **108** and **109** were obtained from MeOH upon slow evaporation. Briefly, a methanolic solution of each compound was placed in separate small vials, then the lid was closed partially and the solutions were left (2–4 weeks) until a single crystal suitable-usually free of cracks when observed under microscope-for X-ray diffraction was formed. The crystals were then sent for structural analysis to Department of Chemistry and Virginia Tech Center for Drug Discovery, Virginia Tech, Blacksburg, Virginia, United States. The details of the structural analyses are described in Appendix XIII, which, along with CIF files, have also been deposited in the Cambridge Crystallo-

graphic Data Centre (CCDC Nos. 1038571, 1038573 and 1038572 for compounds **41**, **108** and **109**, respectively). A summary of the crystal data of each compound is also given in Appendix XII.

4. Results and discussion

4.1. Antiproliferative activity of extracts and fractions

Traditionally the roots of the plant are either used topically (crush and paint) or orally (powdered dry root mixed with water and then taken orally)-since the role of water is as a vehicle, 90% MeOH was used so as to extract "almost all of the constituents" that might contribute to the activity. Therefore, extraction of the air-dried roots of *P. falcatus* (270 g) with 90% MeOH yielded a brownish, gummy solid (13 g; 4.8%), which showed cytotoxicity against HT-29 with an ED_{50} value of 10 μg/mL. Liquid-liquid partition with hexanes, EtOAc and H_2O yielded the corresponding hexanes (1.21 g, ED_{50} = 11 μg/mL), EtOAc (2.15 g, ED_{50} = 3 μg/mL) and H_2O (9.44 g, ED_{50} >20 μg/mL) fractions. The most active EtOAc fraction (ED_{50} = 3 μg/mL) was partitioned with dichloromethane (DCM, 5 × 500 mL) and H_2O (400 mL) to afford 1.01 g of DCM (ED_{50} = 2 μg/mL) and 1.06 g (ED_{50} > 20 μg/mL) of H_2O fractions. Using DCM/MeOH (1:1) as eluent, the cytotoxic DCM fraction was subjected to Sephadex LH-20 CC (4.5 × 62 cm; flow rate = 2.5 mL/min) to afford 111 fractions. Fractions with similar TLC (stationary phase: silica gel; solvent system: $CHCl_3$: EtOAc: MeOH (7:2:1); TLC dimension: 5.5 × 6 cm; detection methods: physical-day light and UV (256 and 366 nm) and chemical-modified Godin's reagent) profiles were combined to yield seven pooled fractions (F1−F7), with F3 being the most active (ED_{50} = 0.7 μg/mL) (Figure 4).

The fraction F3 was subjected to silica gel CC (3.2 cm × 39 cm; flow rate = 3.5 mL/min; solvent system: $CHCl_3$: EtOAc: MeOH (7:2:1)) which, based on their similarity in TLC (stationary phase: silica gel; solvent system: $CHCl_3$: EtOAc: MeOH (7:2:1); TLC dimension: 5.5 × 6 cm; detection methods: physical-day light and UV (256 and 366 nm) and

chemical-modified Godin's reagent) to afford 14 pooled fractions (F3-1 through F3-14). Cytotoxicity evaluation of these fractions revealed that F3-4 and F3-5 were the most active, with equal ED_{50} values of 0.4 μg/ mL (Figure 4). These fractions were subjected to semipreparative RP-18 HPLC (Dynamax C_{18} HPLC column 10 × 250 mm; flow rate: 2 mL/min) using a gradient mixture of H_2O/MeOH from 50:50 to 0:100 for 41 min with a program of 50:50 to 40:60 for 10 min, 40:60 to 30:70 for 5 min, 30:70 to 20:80 for 10 min, 20:80 to 15:85 for 5 min, 15:85 to 0:100 for 1 min, 0:100 for 10 min. Fraction F3-4 (46.3 mg) yielded compounds, 2*β*-hydroxynagilactone F (**108**) (*Revised structure see Section 4.3*; 11.2 mg; t_R = 15.30 min), **PF-1** (1.3 mg; t_R = 16.12 min) and **PF-2** (11.7 mg; t_R = 27.00 min) (Figure 5), while F3-5 (83.0 mg) yielded compounds **108** (3 mg; t_R = 15.30 min) and **PF-2** (4.13 mg; t_R = 27.00 min) and an impure fraction (F3-5-I; 41.47 mg; t_R = 10.07 min) (Figure 6), which was resubjected to semipreparative RP-18 HPLC (gradient mixture of H_2O/MeOH from 90:10 to 0:100 for 37 min with program of 90:10 to 60:40 for 20 min, 60:40 to 50:50 for 5 min, 50:50 to 19:81 for 4 min, 19:81 to 0:100 for 1 min and 0:100 for 7 min) to yield compounds nagilactone D **(41)** (11.47 mg; t_R = 30.35 min) and nagilactone I **(109)** (*Revised structure see Section 4.3*; 12.89 mg; t_R = 31.43 min) (Figure 7).

From Figure 4, it can be seen that the dose to kill 50% of tumor cells (ED_{50}) increases somehow from the most active fraction F3-4 (ED_{50} = 0.4 μg/ mL) to F3-2 (ED_{50} = 6.4 μg/ mL) then decreases in F3-1 (ED_{50} = 2.4 μg/ mL). Likewise, activity decreases from the most active fraction F3-5 (ED_{50} = 0.4 μg/ mL) to F3-8 (ED_{50} = 6.5 μg/ mL) then increases in F3-9 (ED_{50} = 2.4 μg/ mL). This was a bit interesting and isolation was done on this fractions to isolate the "active" compounds that caused such changes. Thus, preparative

RP-18 HPLC (Dynamax C_{18} HPLC column 10 × 250 mm; flow rate: 2 mL/min) using a gradient of H_2O/ MeOH (from 20:80 to 0:100) for 22 min with program of 20:80 to 10:90 for 10 min, 10:90 to 0:100 for 5 min and 0:100 for 7 min of F3-1 (30.2 mg) yielded compound macrophyllic acid **(37)** (3.7 mg; t_R = 22.53 min) (Figure 8), whereas RP-18 HPLC (Dynamax C_{18} HPLC column 10 × 250 mm; flow rate: 2 mL/min) purification of F3-9 yielded compounds 15-hydroxynagilactone D (**110)** (0.9 mg; t_R = 8.19 min), **PF-3** (1.58 mg; t_R = 10.81 min), and ponasterone A **(94)** (6.08 mg; t_R = 25.49 min) (Figure 9) using a gradient of H_2O/ MeOH (from 60:40 to 0:100) for 32 min with program of 60:40 to 50:50 for 10 min, 50:50 to 10:90 for 14 min, 10:90 to 0:100 for 1 min and 0:100 for 7 min. Compound inumakiol D **(24),** (1 mg) was obtained as a precipitate from one of the inactive fractions after column chromatography.

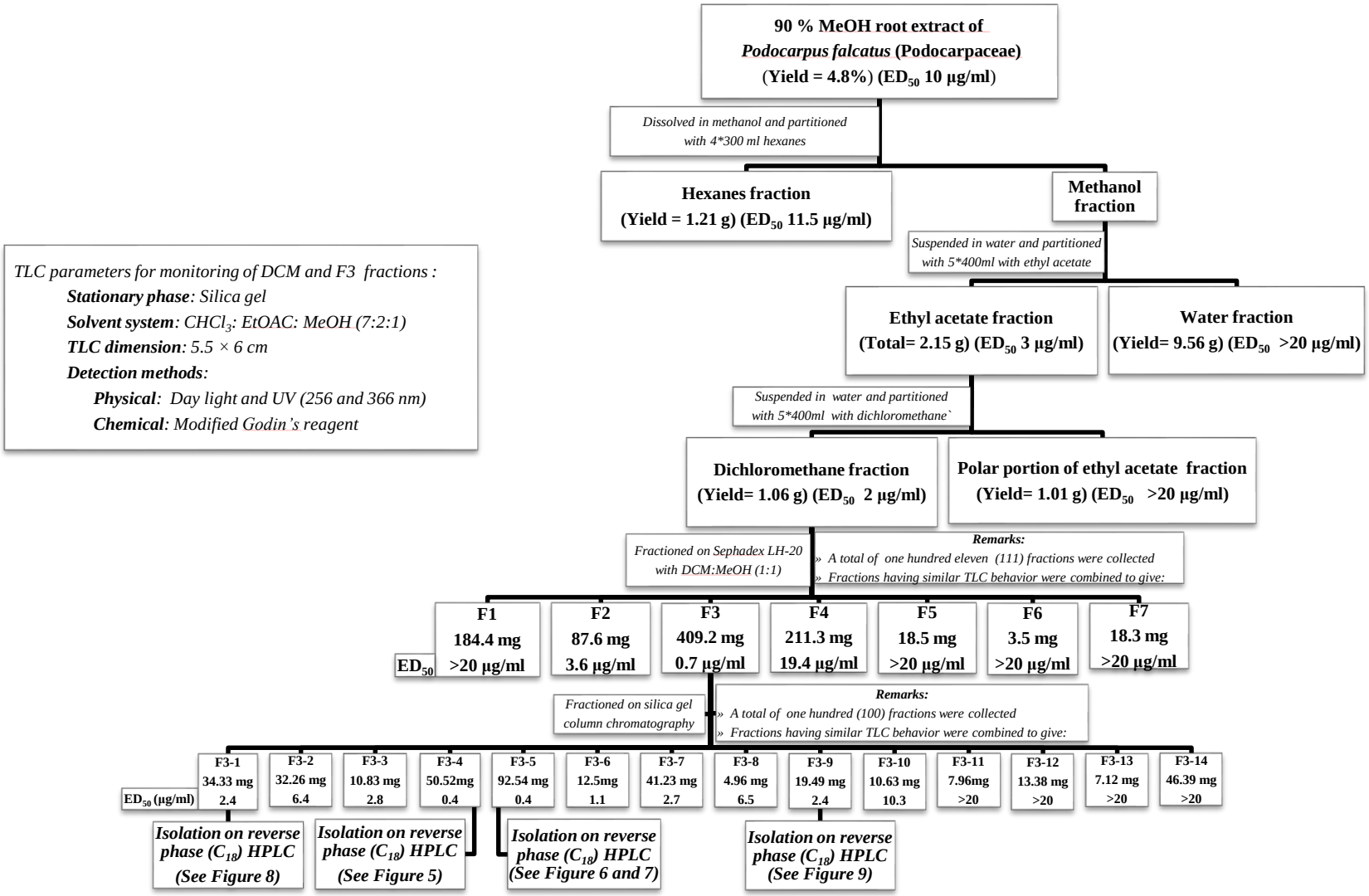

Figure 4. Flow chart showing bioassay-guided fractionation of the roots of *P. falcatus* using the HT-29 cell line

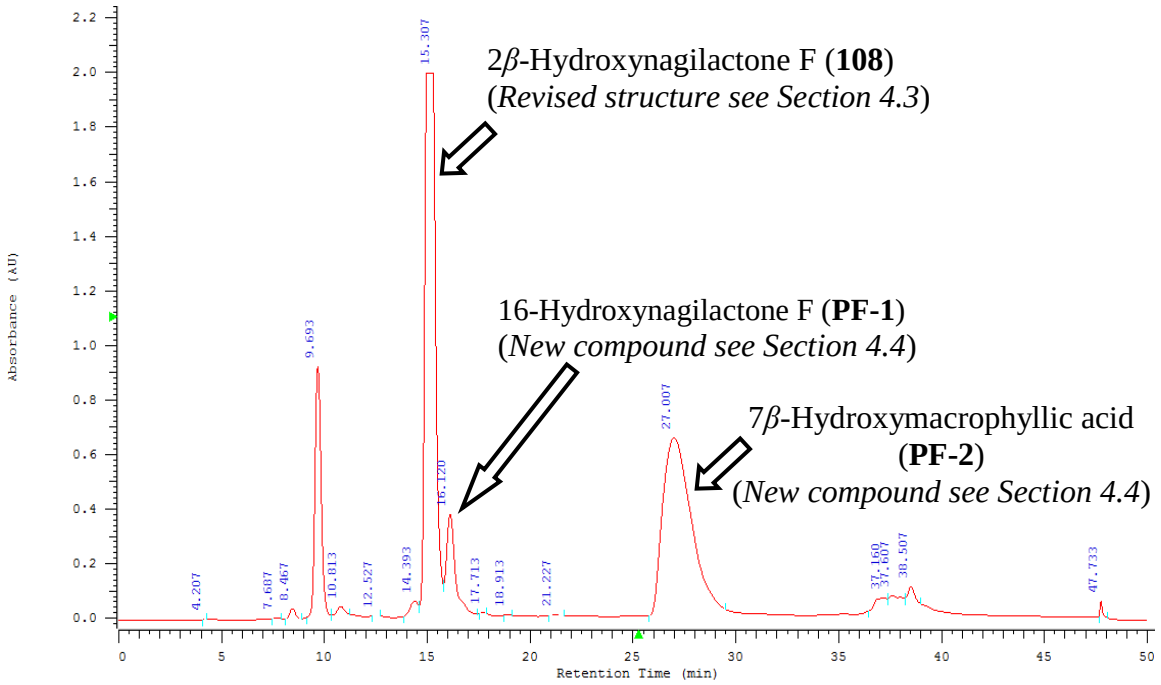

Figure 5. HPLC chromatogram of fraction F3-4 (Solvent system: MeOH:H_2O gradient; Flow rate: 2 mL/min; Detection wavelength: 254 nm)

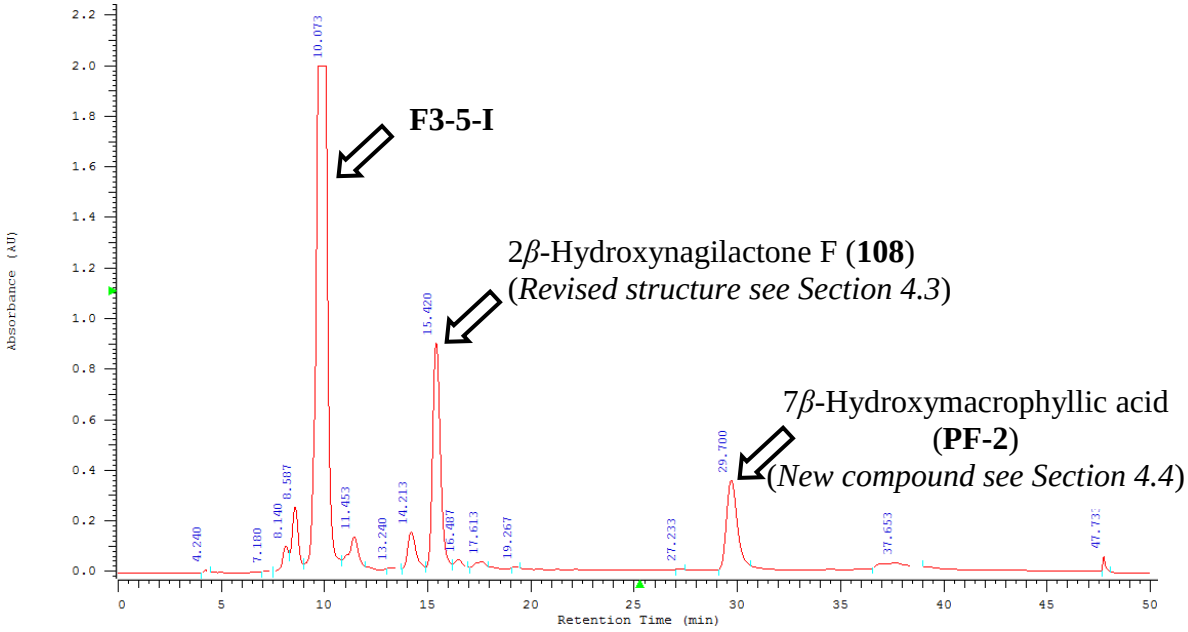

Figure 6. HPLC chromatogram of fraction F3-5 (Solvent system: MeOH:H_2O gradient; Flow rate: 2 mL/min; Detection wavelength: 254 nm)

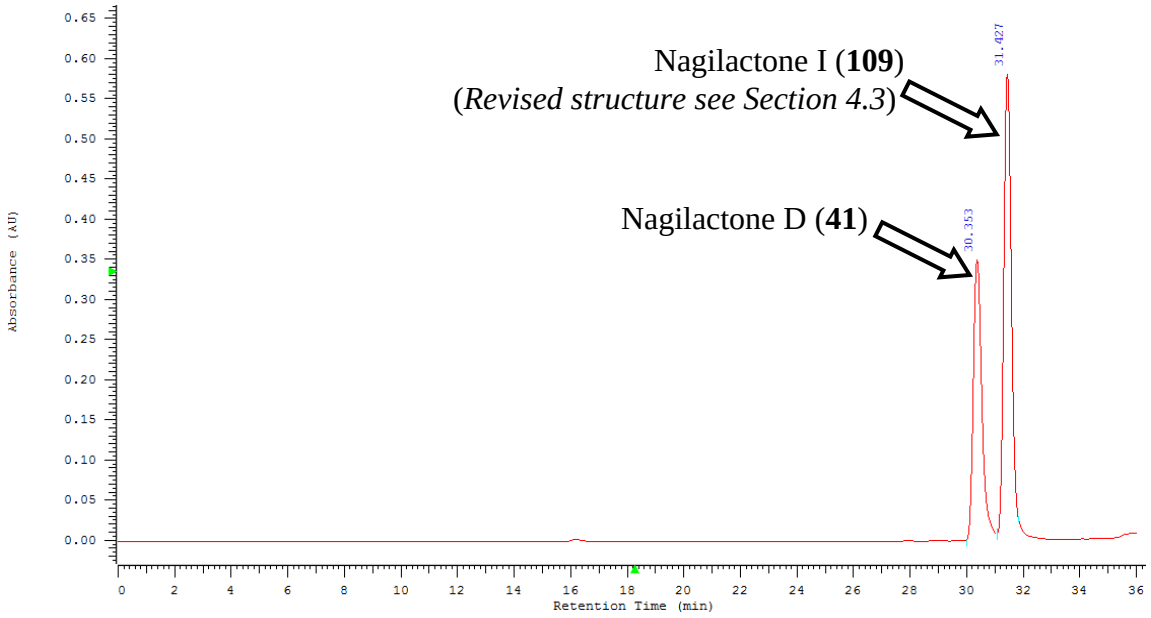

Figure 7. HPLC chromatogram of fraction F3-5-I (Solvent system: MeOH:H_2O gradient; Flow rate: 2 mL/min; Detection wavelength: 280 nm)

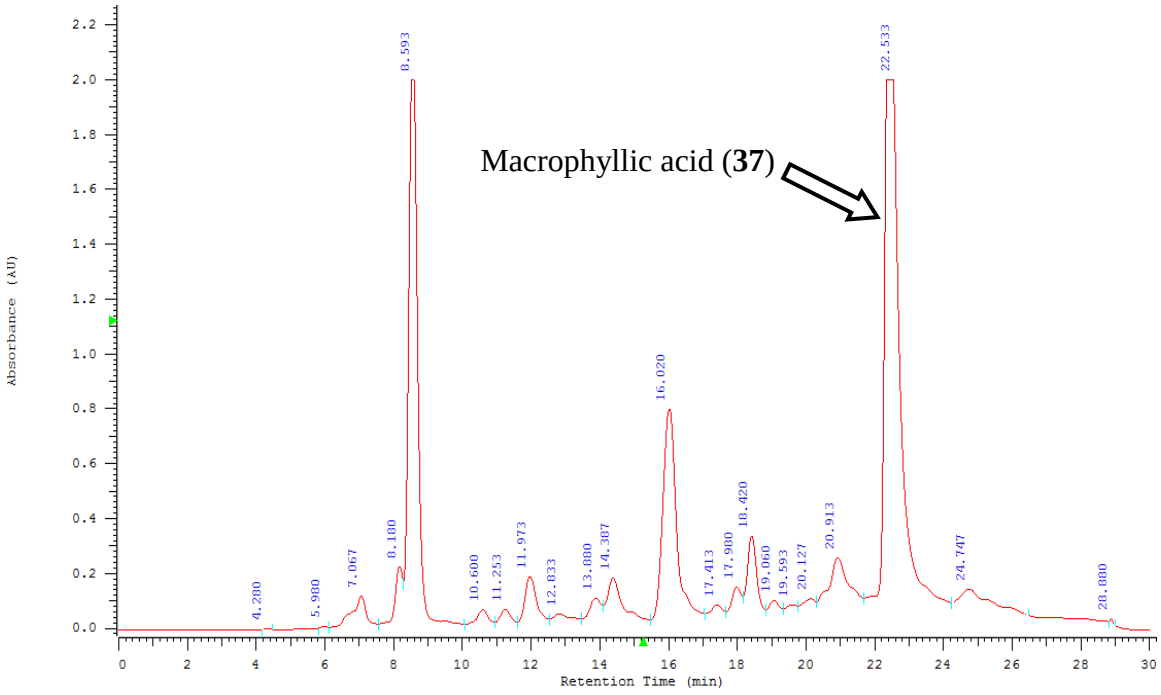

Figure 8. HPLC chromatogram of fraction F3-1 (Solvent system: MeOH:H_2O gradient; Flow rate: 2 mL/min; Detection wavelength: 254 nm)

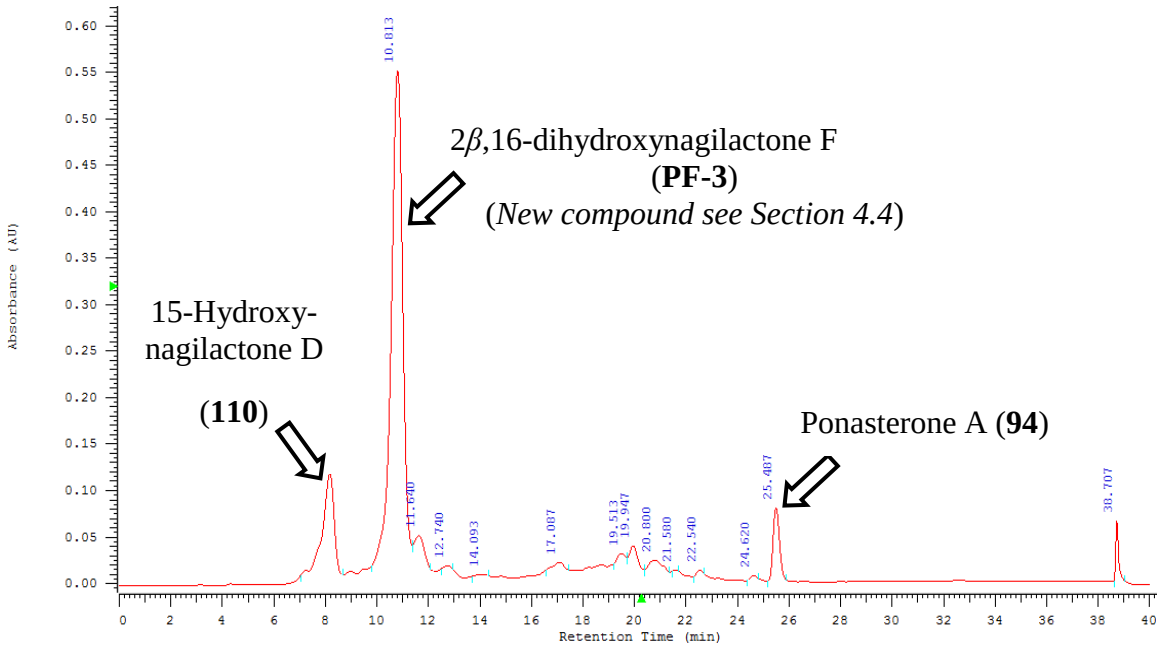

Figure 9. HPLC chromatogram of fraction F3-9 (Solvent system: MeOH:H_2O gradient; Flow rate: 2 mL/min; Detection wavelength: 280 nm)

4.2. General overview of fractionation and isolation

The antiproliferative methanolic extract (ED_{50} =10 µg/mL) of air-dried roots of *P. falcatus* was fractionated with hexanes, EtOAc and H_2O. Bioassay on HT-29 showed that the EtOAc fraction was the most active (ED_{50} of 3 µg/mL). Subsequent liquid-liquid partition and fractionations on Sephadex LH-20 and silica gel column chromatography resulted in two fractions with improved activities of ED_{50} 0.4 µg/mL (Figure 4). Reversed phase C_{18} HPLC (Figure 5) of each active fractions resulted in the isolation of the two new type C nagilactones, 16-hydroxynagilactone F (**PF-1**) and 2*β*,16-dihydroxynagilactone F (**PF-3**) and a bisditerpenoid 7*β*-hydroxymacrophyllic acid (**PF-2**) (*See Section 4.4 for structural elucidation*) along with seven known compounds identified as: inumakiol D (**25**), macrophyllic acid (**37**), nagilactone D (**41**), ponasterone A (**94**), 2*β*-hydroxynagilactone F (**108;** *Revised structure see Section 4.3*), nagilactone I (**109**; *Revised structure see Section 4.3*)

and 15-hydroxynagilactone D (**110**). The structure of **110** has been reported without ^{13}C NMR data (Hayashi *et al.,* 1977a) and in the present report we included the full NMR data of 15-hydroxynagilactone D (**106**) (Tables 4 and 5). The structures of compounds **104** and **105** were revised based detailed analysis of 1D and 2D NMR data and single-crystal X-ray diffraction studies; hence discussion of the structural elucidation of the isolated compounds starts with the structure revision of **108** and **109**.

4.3. Structure revision of compounds 108 and 109

Compounds **108** and **109** are known compounds; however, their C-2 hydroxy group was reported to be α-oriented (Ying *et al.,* 1990; Bloor and Molloy, 1991; Kubo *et al.,* 1991a). The ^{1}H and ^{13}C NMR, IR and UV spectroscopic data as well as the optical rotations of the newly isolated compounds **108** and **109** are similar with reported data (Tables 2 and 3; Appendix I). Minimization of the energy of the two structures of **108** with 2α and 2β hydroxy groups using the MM2 program in the ChemBioDrawUltra software (version 14.0.0.117, CambridgeSoft Corporation) showed that both compounds have a boat conformation of the ring A. This observation was different from the reported data suggesting a chair conformation of the parent compounds. Moreover, it is noteworthy that comparison of our NMR data of **108** with the data of reported compounds led to the conclusion that the assignments of the ^{13}C NMR chemical shifts of C-18 and C-20 methyl groups of compound **108** in ref (Kubo *et al.,* 1991a) should be interchanged.

Table 2. ^{1}H NMR (400 MHz) data for compounds 108 and 109

Reference		Kubo *et al.*, 1991	Bloor *et al.*, 1991	Present data	Ying *et al.*, 1990	Present data	
Position		**108[a]**	**108[b]**	**108[c]**	**109[a]**	**109[a]**	**109[b]**
1	a	2.48 dd (13.7, 9.0)	2.24 t (13)	2.42 dd (13.4, 10)	2.47 dd (13.3, 9.6)	2.50 dd (13.6, 9)	2.4 dd (13.6, 9.2)
	b	1.84 dd (13.7, 6.8)	1.91 (obsc.)	1.53 dd (13.4, 7.2)	1.87 dd (13.3, 4.9)	2.20 dd (13.6, 7.2)	1.58 dd (13.6, 7.2)
2	a		4.11 m	4.08 dddd (12.9, 10, 7.2, 5.1)		4.31 dddd (12.6, 9, 7.2, 5.1)	4.1 br s
	b	4.31 m ($W_{1/2}$ 26 Hz)			4.28 m ($W_{1/2}$ 28 Hz)		
3	a	2.56 dd (13.7, 12.8)	2.45 dd (14, 9)	2.11 br t (13.4)	2.54 dd (13.3, 12.4)	2.57 t (13.2)	2.20 br t (13.5)
	b	2.19 dd (13.7, 5.1)	1.59 dd (14, 7)	1.84 dd (13.4, 5.1)	1.85 d (12.4)	2.20 dd (13.7, 5.1)	1.92 dd (13.5, 5.2)
4							
5		1.82 d (5.1)	1.95 d (5)	2.18 d (5)	1.83 d (5.6)	1.84 d (5)	1.92 d (5)
6		5.14 dd (5.1, 2.1)	5.08 ddd (5, 5, 1.5)	5.23 ddd (5, 5, 1.7)	5.16 t-like	5.19 ddd (5, 5, 1.6)	5.00 ddd (5, 5, 1.7)
7		6.27 br d	6.20 ddd (5, 1.5)	6.35 ddd (5, 1.7, 1.6)	6.43 d (2.1)	6.46 ddd (5, 1.9, 1.7)	6.13 ddd (5, 1.8, 1.7)
8							
9							
10							
11		6.05 s	5.83 d (1.6)	5.83 d (1.7)	6.09 s	6.12 d (1.7)	5.82 d (1.7)
12							
13							
14		4.86 br s	4.87 d	5.01 ddd (2.3, 1.7, 1.6)	5.32 br s	5.34 ddd (4.1, 1.9, 1.6)	5.21 ddd (4, 1.8, 1.7)
15		2.22 dqq (6.8, 6.8, 2.1)	2.25 m	2.4 sd (6.8, 2.3)	3.39 dq (6.8, 3.9)	3.42 qd (7.1, 4.1)	3.16 qd (7.2, 4)
16		0.98 d (6.8)	0.98 d (6)	1.18 d (6.8)			
17		1.13 d (6.8)	1.20 d (6)	0.97 d (6.8)	1.46 d (6.8)	1.48 d (7.1)	1.38 d (7.2)
18		1.39 s	1.42 s	1.40 s	1.30 s	1.38 s	1.4 s
19							
20		1.29 s	1.28 s	1.24 s	1.36 s	1.32 s	
-OCH_3					3.63 s	3.65 s	3.70 s

[a] Data collected in pyridine-d_5

[b] Data collected in chloroform-*d*

[c] Data collected in methanol-d_4

J-Coupling constants in parenthesis

Table 3. ^{13}C NMR (100 MHz) data for compounds 108 and 109

Reference	Kubo *et al.*, 1991	Bloor *et al.*, 1991	Present data	Ying *et al.*, 1990	Present data	
Position	**108[a]**	**108[b]**	**108[c]**	**109[a]**	**109[a,d]**	**109[b]**
1	41.2	40.2	41.3, CH_2	41.0	41.5, CH_2	40.4, CH_2
2	63.9	64.7	65.3, CH_2	63.9	64.3, CH	64.8, CH_2
3	37.8	36.5	37.7, CH_2	37.6	38.1, CH_2	36.7, CH_2
4	42.8	42.4	44.0, C	42.8	43.2, C	42.5, C
5	45.5	45.7	46.6, CH	45.3	45.7, CH	45.8, CH
6	72.4	72.0	74.1, CH	72.4	72.8, CH	72.0, CH
7	122.4	121.6	123.9, CH	122.5	122.7, CH	121.9, CH
8	133.8	133.8	134.8, C	133.2	133.7, C	132.8, C
9	159.0	158.3	161.3, C	158.8	159.2, C	158.3, C
10	36.1	35.9	37.3, C	36.2	36.6, C	36.2, C
11	113.1	112.8	113.2, CH	113.1	113.6, CH	112.9, CH
12	164.1	165.0	166.8, C	163.5	163.8, C	163.2, C
13						
14	83.0	83.0	85, CH	80.0	80.4, CH	79.5, CH
15	29.8	29.7	31.4, CH	42.4	42.8, CH	42.8, CH
16	16.3	15.1	20.1, CH_2	172.6	173.0, C	172.3, C
17	19.7	19.6	15.6, CH_3	13.8	14.1, CH_3	12.8, CH_3
18	23.4	27.9	28.7, CH_3	28.0	28.4, CH_3	28.2, CH_3
19	181.6	180.6	183.8, C	181.6	181.9, C	180.8, C
20	27.8	23.4	23.7, CH_3	23.3	23.8, CH_3	23.6, CH_3
$-OCH_3$				51.9	52.3, CH_3	52.5, CH_3

[a] Data collected in pyridine-d_5
[b] Data collected in chloroform-*d*
[c] Data collected in methanol-d_4
[d] Part of the assignments of the carbon multiplicities was performed based on their similarities with the reported data (Ying *et al.*, 1990).

Analysis of the splitting patterns of the H-2 resonance in the ^{1}H NMR spectrum and the 2D-NOESY of both compounds showed that the orientation of the hydroxy group should be *β*. The dddd (J = 12.9, 10, 7.2, 5.1 Hz) splitting of H-2 (δ 4.08) for compound **108** showed that two large couplings were present, and this was also reported by the previous authors (Table 2). These coupling patterns were possible only if the H-2 hydroxy group is *β*-oriented (Figure 10). In addition, H-2 of compounds **108** and **109** exhibited NOE cross-peaks with H-3*α* and H-18. Both H-3*α* and H-18 also correlated with H-5 and H-6, while H-1*β* and H-3*β* correlated with the CH_3-20 singlet.

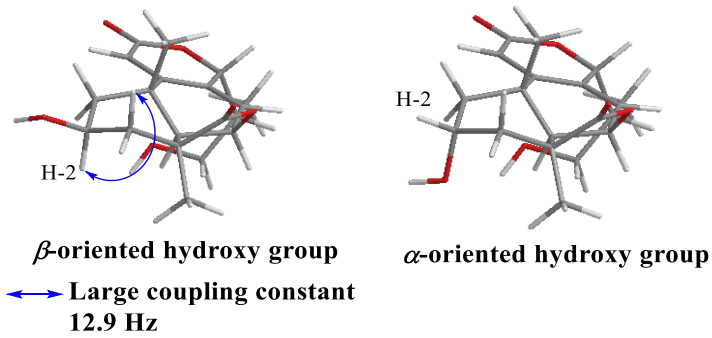

Figure 10. Stable conformation of the 2*α*- and 2*β*-hydroxynagilactone F after MM2 energy minimization

To confirm these assignments, compounds **108** and **109** were crystallized and subjected to X-ray crystallographic analysis. These studies confirmed the 2*β*-OH orientation for both compounds (Figure 11). The ^{1}H and ^{13}C NMR data arising from the A ring are in agreement with the data reported for the tetranor-diterpenoid wentilactone B **(111)**, which has been isolated from the endophytic fungus *Aspergillus wentii* EN-48 (Sun *et al.*, 2012).

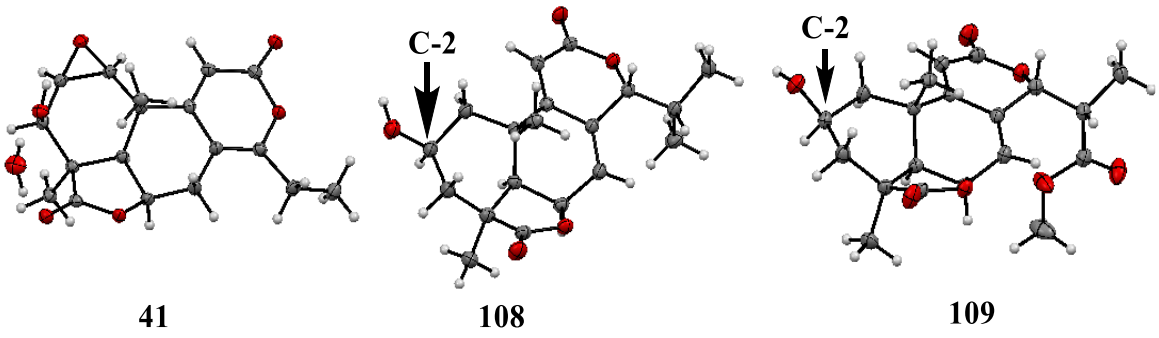

Figure 11. X-ray ORTEP drawing of the crystal structures of 41, 108 and 109

From these evidences, the structure of **108** should be revised to 2*β*-hydroxynagilactone F and the orientation of the C-2 hydroxy group of nagilactone I (**109**), methyl 2*β*-hydroxynagilactone F-16-oate, should be *β* as depicted. The X-ray crystal structure of the

related compound **41**, a bisnor-diterpenoid that is consistent with the reported structure (Kubo *et al.*, 1984), is also shown in Figure 11.

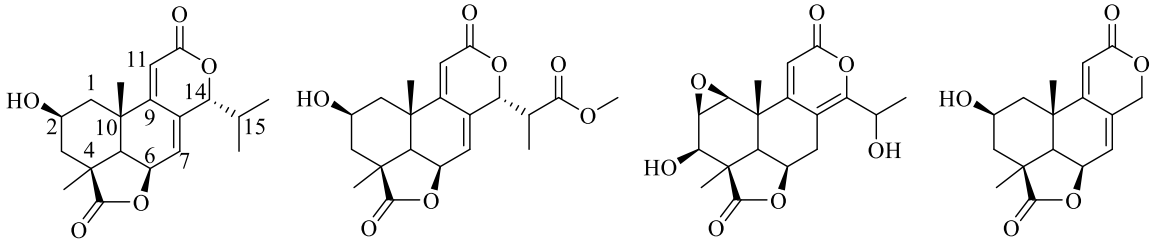

108 **109** **110** **111**

4.4. Structure elucidation of the new compounds PF-1, PF-2 and PF-3

Structure elucidation of compound PF-1

Compound **PF-1** exhibited a sodiated pseudomolecular ion peak $[M+Na]^+$ at *m/z* 355.1500 (calcd. 355.1516) (Figure 27) which in conjunction with the ^{13}C NMR data indicated a molecular formula of $C_{19}H_{24}O_5$, identical to that of **108**. The UV spectrum (Figure 25) showed an absorption band at λ_{max} of 259 nm and the IR stretching at 1762 cm^{-1} (γ-lactone), 1701 cm^{-1} (δ-lactone), 1597 cm^{-1} (weak; C=C conjugated with C=O) (Figure 26) suggested that **PF-1** is a type C nagilactone (Ito and Kodama, 1976). The ^1H NMR spectroscopic data of **PF-1** (Table 4 and Figure 19) were similar to those of **108** except for the absence of H-2α signal (δ 4.08, dddd), the methyl doublet at δ 0.97 of **108** and the presence of two doublet of doublets at δ 3.76 (dd, *J*= 11, 4.4 Hz) and δ 3.47 (dd, *J*= 11, 8 Hz) in addition to multiplets corresponding to three methylenes at δ 2.22–2.15 and 1.84–1.52. The ^{13}C NMR (Table 5 and Figure 20) and HSQC (Figure 22) revealed the presence of 19 carbon resonances with two carbonyl carbons indicative of γ-lactone (δ 183.8, C-19) and δ-lactone (δ 166.6, C-12) moieties, four olefinic carbons, two of which were monosubtituted (δ 112.5, C-11 and δ 124.0, C-7), two oxymethines (δ 73.9, C-6 and

δ 83.5, C-14), an oxymethylene (δ 63.5, C-16), two quaternary carbons (δ 44.4, C-4 and δ 36.6, C-10), three methylenes (δ 31.2, C-1; δ 18.7, C-2 and δ 29.1, C-3), two methines (δ 48.5, C-5 and δ 39.3, C-15) and three methyl carbons at δ 15.2, 24.6 and 25.7 ascribable to C-17, C-18, and C-20, respectively.

Comparison of the ^{1}H and ^{13}C NMR of **PF-1** with those of **108** revealed that the difference between the two compounds was the oxidation states of the ring A and one of the isopropyl methyls at C-15. Two dimensional NMR including, HSQC, ^{1}H-^{1}H COSY, HMBC and NOESY (Figures 21-24) were performed in order to determine the planar structure of **PF-1**. The ^{1}H-^{1}H COSY correlations observed from H-1 to H-3 (Figure 13 and 21) demonstrated the absence of a C-2 hydroxy group in **PF-1**. The long range cross peaks from the two pairs of diastereotopic oxygen-bearing methylene doublet of doublets at δ 3.47 and 3.76 to C-14, C-15 and C-17 permitted the location of the hydroxymethylene group at C-15 (Figure 13 and 23). This is in accordance with the absence in **PF-1** of one isopropyl methyl doublet of **108** (δ 0.97, d, J= 6.8 Hz). The HMBC correlations from the oxygen-bearing methylene protons with C-15, C-17 and C-14 together with that of H-17 with C-16 confirmed that one of the isopropyl methyls (C-16) was substituted. The presence of a γ-lactone moiety was evidenced by the HMBC correlations from H-5 (δ 2.08, d, J= 4.8 Hz) to C-1, C-3, C-9, C-10, C-18 and C-19, from CH_3-18 to C-3, C-4, C-5 and C-19 (δ 183.8) and H-20 to C-1, C-5, C-9 and C-10 while H-11 showed correlation to the δ-lactone carbonyl at C-12 (δ 166.6). The relative configuration of **PF-1** was deduced from the data observed in the 2D-NOESY spectrum (Figure 15 and 24). The orientation of the other substituents of the stereogenic carbons of **PF-1** was deduced to be the same as those in **108** by analysis of the NOE crosspeaks observed in the NOESY spectrum.

Table 4. ^{1}H NMR (400 MHz) data for compounds PF-1, PF-2, PF-3 and 110

Position		PF-1[a]	PF-3[a]	PF-2[b,§]	PF-2[c,§]	110[d]
1	a	1.69 m (Overlapped)[¶]	2.42 dd (13.5, 9.1)	2.43 m (Overlapped)[¶]	1.32 (Overlapped)[¶]	3.57 d (4.2)
	b	1.79 m (Overlapped)[¶]	1.54 dd (13.5, 7.2)	1.45 m (Overlapped)[¶]	2.14 (Overlapped)[¶]	
2	a	1.75 m (Overlapped)[¶]	4.06 dddd (12.6, 9.1, 7.2, 5.1)	2.38 m (Overlapped)[¶]	1.52 br d (11.4)	3.48 dd (6, 4.2)
	b	1.84 m (Overlapped)[¶]		1.58 m (Overlapped)[¶]	1.89 (Overlapped)[¶]	
3	a	1.55 m	2.11 br t (13.5)	2.58 br t (10.5)	1.04 (Overlapped)[¶]	4.45 dd (6, 2.2)
	b	2.18 m	1.84 dd (13.5, 5.1)	1.18 br t (11.6)	2.11 (Overlapped)[¶]	
4						
5		2.08 d (4.8)	2.11 d (5)	2.58 (Overlapped)	1.96 (Overlapped)[¶]	1.88 d (6.4)
6	a	5.22 ddd (4.8,4.8,1.7)	5.22 ddd (5,5, 1.6)	2.98 br d (12.6)	2.00 (Overlapped)[¶]	4.94 dt (9.8, 6.4, 6.4)
	b			2.85 br t (12.6)	2.15 (Overlapped)[¶]	
7	a	6.42 ddd (4.8, 1.9, 1.9)	6.42 ddd (5, 1.8, 1.6)	5.56 br s	4.78 br s	3.54 dd (16.8, 9.8)
	b					2.74 dd (16.8, 6.4)
8						
9						
10						
11		5.79 d (1.9)	5.82 d (1.6)	7.50 s	6.91 s	6.37 s
12						
13						
14		5.09 ddd (2.0, 1.9,1.7)	5.09 ddd (2.0, 1.8, 1.6)			
15		2.39 m	2.37 m	4.29 sep (6.6)	3.56*	4.87 dq (9.5, 6.6)
16	a	3.76 dd (11.0, 4.4)	3.74 dd (11.0, 4.5)	1.88 d (6.6)	1.34 d (7.1)	1.52 d (6.6)
	b	3.47 dd (11.0, 8.0)	3.46 dd (11.0, 8.0)			
17		1.22 d (6.8)		1.77 br s	1.32 d (7.4)	
18		1.33 s	1.40 s	1.59 s		1.43 s
19						
20		1.16 s	1.21 s	1.42 br s		1.28 s
3–OH						3.4 d (2.2)
15–OH						2.26 d (9.5)

[a]Measured in methanol-d_4
[b]Measured in pyridine-d_5
[c]Measured in DMSO-d_6
[d]Measured in chloroform-*d*
[§]Assignment of the monomer
*Overlapped with the water signal
[¶]The overlapped signals were assigned with accurate axis calibration of ^{1}H-^{1}H COSY and HSQC.

From the above data the structure of **PF-1** was deduced to be 16-hydroxynagilactone F (Figure 12).

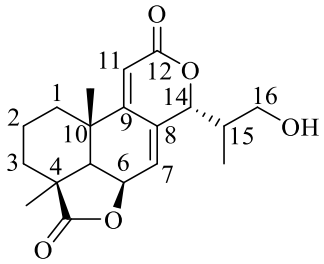

Figure 12. Chemical structure of 16-hydroxynagilactone F (PF-1)

Structure elucidation of compound PF-3

The molecular formula of **PF-3** was determined to be $C_{19}H_{24}O_6$ from the ^{13}C NMR data (Table 5 and Figure 29) and an HRESIMS pseudomolecular ion peak at *m/z* 371.1460 (calcd. for $[M+Na]^+$ 371.1465) (Figure 36). The UV absorption at λ_{max} 261 nm (Figure 34) along with IR (Figure 35) stretching absorption at 1764 cm^{-1} (γ-lactone), 1698 cm^{-1} (δ-lactone) and 1600 cm^{-1} (C=C conjugated with a carbonyl) suggested that **PF-3** also belonged to type C (7(8), 9(11)-dienolide) norditerpene dilactones (Ito and Kodama, 1976). The ^1H NMR spectroscopic data of **PF-3** (Table 5 and Figure 28) were similar to those of **108** except for the absence of one of the isopropyl methyl doublets (δ 0.97) in **PF-3** and appearance of two doublet of doublet signals of hydroxymethylene protons at δ 3.74 and 3.46 ppm which were identical to those of **PF-1**. The ^{13}C NMR and HSQC data (Figure 31) also indicated that **PF-3** had a total of 19 resonances with two disubstituted olefinic carbons (δ 161.3, C-9 and 134.6, C-8), two monosubstituted olefinic carbons (δ 123.9, C-7 and 113.2, C-11), three oxymethine carbons (δ 83.5, C-14; 74.2, C-6 and 65.3, C-2), an oxymethylene carbon (δ 63.4, C-16), two methylene carbons (δ 41.4, C-1 and 37.7, C-3), two methine carbons (δ 46.6, C-5 and 39.5, C-15), and three methyl carbons

(δ 15.2, C-17; 23.7, C-20 and 28.8, C-18) and two quaternary carbons (44.0, C-4 and 37.4, C-10). The remaining two signals at δ 183.8 (C-19) and δ 166.5 (C-12) were typical of the carbonyls of γ-lactone and conjugated δ-lactone moieties, respectively, characteristic of the type C nagilactones.

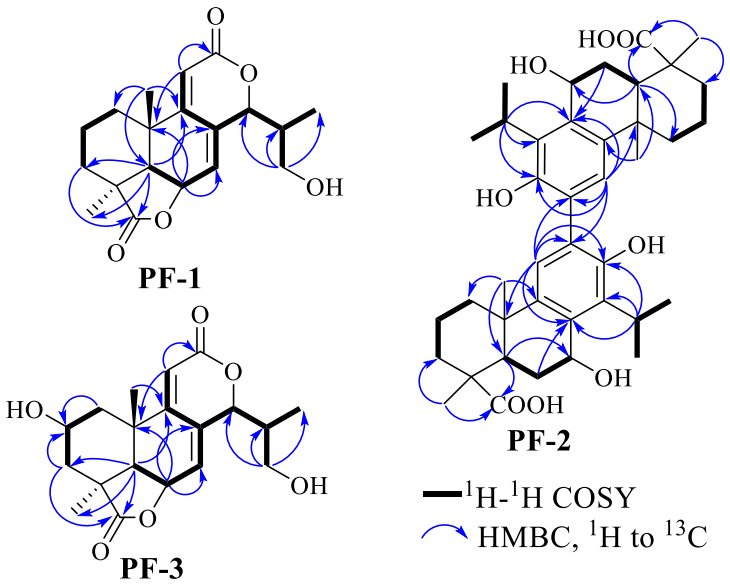

Figure 13. Key HMBC and ^{1}H-^{1}H COSY correlations of the new compounds PF-1, PF-2 and PF-3.

Comparison of the ^{1}H and ^{13}C NMR data of **PF-3** with those of **108** revealed that the only difference was the presence of C-15 hydroxymethylene group in **PF-3** instead of a C-15 methyl group in **108**. This was confirmed by the HMBC correlations from H-16 to C-15, C-17 and C-14 (Figure 13 and 32). The location of the hydroxy group at C-2 was evidenced by the presence of the spin network H-1 (δ 2.42 and 1.54)–H-2 (δ 4.06)–H-3 (δ 2.11 and 1.84) in the COSY spectrum (Figure 13 and 30). The locations of the C-7 and C-9 double bonds were substantiated by the COSY spin system, H-5 (δ 2.11)–H-6 (δ 5.22)–H-7 (δ 6.42)–H-11(δ 5.82) and also from the HMBC correlations from H-6 to C-7 (δ 123.9) and C-8 (δ 134.8) and H-15 to C-8. The assignment of the two lactone rings

was confirmed by comparison of the ^{13}C NMR data of **PF-3** with those of **108** and interpretation of the HMBC spectroscopic data. The determination of the relative configuration of **PF-3** was carried out as follows. The correlation between H-2 (δ 4.06) and the methyl signal at H-18 (δ 1.40, s) in the NOESY spectrum of **PF-3** indicated that the C-2 hydroxy was β-oriented (Figure 15 and 33).

Table 5. ^{13}C NMR (100 MHz) data for compounds PF-1, PF-2, PF-3 and 110

Position	PF-1[a]	PF-3[a]	PF-2[b,*]	PF-2[c,*]	110[d]
1	31.2, CH_2	41.3, CH_2	40.7, CH_2	39.5, CH_2[£]	57.2, CH
2	18.7, CH_2	65.3, CH	21.3, CH_2	20.3, CH_2	50.7, CH
3	29.1, CH_2	37.7, CH_2	38.8, CH_2	37.6, CH_2	67.6, CH
4	44.4, C	44.0, C	44.2, C	42.9, C	48.8, C
5	48.5, CH	46.6, CH	45.9, CH	44.5, CH	50.4, CH
6	73.9, CH	74.1, CH	33.2, CH_2	31.6, CH_2	73.2, CH
7	124.0, CH	123.9, CH	65.6, CH	64.0, CH	24.9, CH_2
8	135.0, C	134.6, C	137.5, C	134.6, C	108.4, C
9	161.9, C	161.3, C	142.6, C	140.9, C	162.5, C[§]
10	36.6, C	37.4, C	39.7, C	38.5, C	37.9, C
11	112.5, CH	113.2, CH	127.6, CH	126.0, CH	106.6, CH
12	166.6, C	166.4, C	130.9, C	130.6, C	162.6, C[§]
13			152.3, C	151.5, C	
14	83.5, CH	83.4, CH	136.6, C	136.0, C	160.7, C[§]
15	39.3, CH	39.5, CH	29.2, CH	27.7, CH	64.7, CH
16	63.5, CH_2	63.4, CH_2	21.8, CH_3	21.4, CH_3	22.0, CH_3
17	15.2, CH_3	15.2, CH_3	22.0, CH_3	21.4, CH_3	
18	24.6, CH_3	28.8, CH_3	29.8, CH_3	28.6, CH_3	25.9, CH_3
19	183.8, C	183.7, C	180.6, C	179.6, C	177.9, C[§]
20	25.7, CH_3	23.7, CH_3	23.7, CH_3	22.9, CH_3	17.7, CH_3

[a]Measured in methanol-d_4
[b]Measured in pyridine-d_5
[c]Measured in DMSO-d_6
[d]Measured in chloroform-*d*
[§]Signal assignments were from HMBC
[£]Overlapped with the solvent signal
*Assignment of the monomer

This was confirmed not only by the splitting pattern of the H-2 resonance which was similar to those in **108** and **109** but also by the NOE correlation between H-3β and CH_3-20 (δ 1.21) which in turn correlated with H-1β. The (14*S*) configuration was deduced by comparison of the ^1H and the ^{13}C NMR chemical shifts of C-14 of **PF-3** with those of **PF-1** and **108**. The key HMBC correlations in support of the structure elucidation of **PF-3** are

shown in Figure 13. Thus, the complete structure of **PF-3** was assigned to be 2*β*,16-dihydroxynagilactone F (Figure 14).

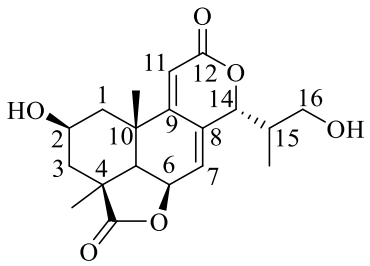

Figure 14. Chemical structure of 2*β*,16-dihydroxynagilactone F (PF-3)

Structure elucidation of compound PF-2

Examination of the UV spectroscopic data (Figure 43) of **PF-2** showed absorptions at λ_{max} 217, 251 and 291 nm which are similar to those of the **15** dimer macrophyllic acid **37** (λ_{max} 220, 251, 291 nm) originally isolated from the heartwood of *P. macrophyllus* D. Don. (Bocks *et al.*, 1963). The IR spectrum exhibited absorption bands and stretch frequencies at 3533, 3500-2400 (broad), 1694,1614 1467, 1259, 1175 cm^{-1} ascribable to hydroxy, carboxylic acid OH, carbonyl, aromatic methine and phenolic hydroxy functions (Figure 44) (Bocks *et al.*, 1963; Pavia *et al.*, 2009). The HRESIMS displayed a sodiated pseudomolecular ion peak $[M+Na]^+$ at *m/z* 685.3727 (calcd. 685.3711) (Figure 45) which in conjunction with the ^{13}C NMR data indicated a molecular formula of $C_{40}H_{54}O_8$ which had two more oxygen atoms than **37**. The difference between **PF-2** and **37** was thus suggested to be the presence of two additional oxygen atoms in **PF-2**.

The ^{13}C NMR (Table 5 and Figure 38) and HSQC (Figure 40) indicated 20 resonances for the monomeric units: a carboxylic acid carbonyl (δ 180.6), an oxygenated aromatic carbon (δ 152.3), four quaternary aromatic carbons (δ 142.6, 137.5, 136.6, 130.9), an aromatic methine carbon (δ 127.6), an oxymethine carbon (δ 65.6), two methine carbons (δ

45.9, 29.2), two quaternary carbons (δ 44.2, 39.7), four methylenes (δ_C 40.7, 38.8, 33.2, 21.3), and four methyl carbons (δ 29.8, 23.7, 22.0, 21.8). With the exception of the carbon resonance at δ 130.9, the ^{13}C NMR spectrum of **PF-2** was similar to that of the inumakinol D (**28**), a known totarane–type monomer isolated from the bark of *P. macrophyllus* D. Don (Sato *et al.*, 2008) (*vs.* 117.3 in **28**). Likewise, the ^{1}H NMR spectroscopic data of **PF-2** was also close to those of **28** except for the absence of the two aromatic doublets of **25** (δ 6.64, d, J = 8.7 Hz and 6.97, d, J = 8.7 Hz) compared to the aromatic singlet at (δ 7.50, s) in **PF-2**. This coupled with the HRESIMS data (Figure 45) with two extra oxygen atoms in **PF-2** and the similarity of the IR and UV spectroscopic data with **37** indicated that **PF-2** was a dimer of **28**.

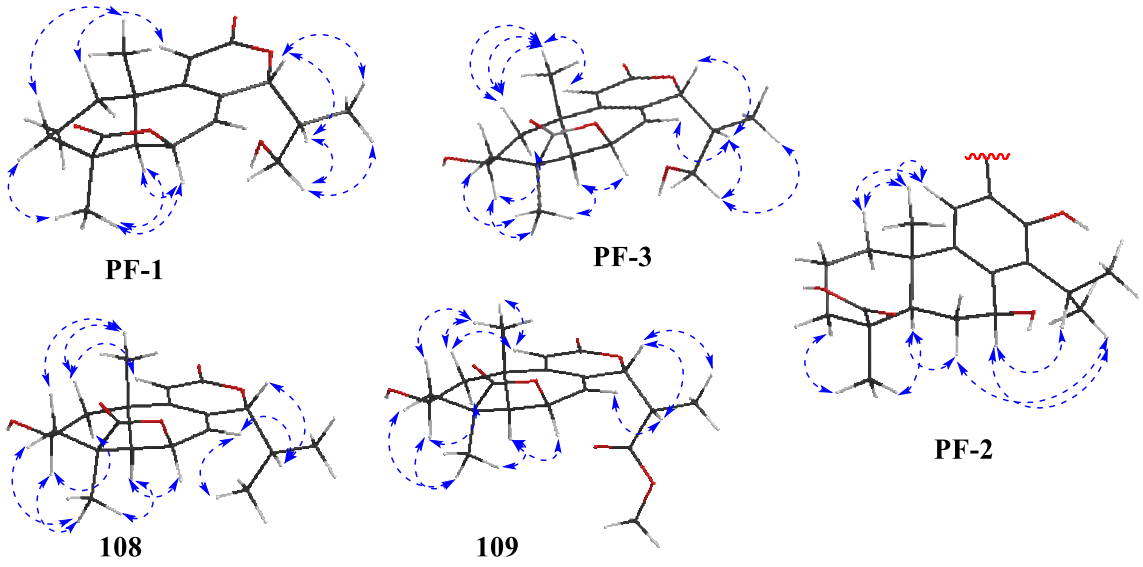

Figure 15. Key NOESY correlations of compounds PF-1, PF-2, PF-3, 108 and 109

Noteworthy, most of the proton and carbon signals in the ^{1}H and ^{13}C NMR spectra of **PF-2** were broadened. To gain more information on the structure of **PF-2** the NMR spectroscopic data of **PF-2** were measured in DMSO-d_6 (Tables 3 and 4). The assignments of all

carbons and protons in **PF-2** as well as the site of the dimerization of the two monomers were successfully achieved by the interpretation of the NMR data obtained from three solvents (methanol-d_4, pyridine-d_5, and DMSO-d_6; (Figures 37–42). The assignment of the oxygen-bearing methine at δ 5.56 (δ_C 65.6) to be at C-7,7′ was determined by the presence of the spin network from H-5,5′ to H-7,7′ [δ 2.58 (H-5,5′), δ_H 2.98 and 2.85 (H-6ab,6′ab), and δ_H 5.56 (H-7,7′)] in the ^{1}H-^{1}H COSY spectrum (Figure 13 and 39). This was in accordance with the similarity of the carbon chemical shifts of C-5,5′, C-6,6′ and C-7,7′ (45.9, 33.2, and 65.6 ppm, respectively) of **PF-2** with those reported for **28**. Apart from the solvent signals (pyridine-d_5), the aromatic region of the ^{1}H NMR spectrum of **PF-2** displayed only one signal (δ 7.50, s) which was attributed to two aromatic methines of two equivalent pentasubstituted aromatic rings. The assignment of the two aromatic methines to be at H-11,11′ was performed by the observation of the NOESY correlation from the signal at δ 7.50 to H-1*a* (δ 2.43) and to the methyl singlet at δ 1.42 (CH_3-20,20′) (Figure 15 and 42). The location of the isopropyl moiety at C-14,14′ of **PF-2** which confirmed its totarane nature was further confirmed by the NOESY correlation from H-7 (δ 5.56, br s) to the isopropyl methine proton septet at δ 4.29 (H-15,15′, sept, J = 6.6 Hz). This was confirmed by the long range cross peak from the isopropyl methyl signals [δ 1.88 (H-16,16′) and δ 1.77 (H-1,17′)] and isopropyl methine (δ 29.2, C-15,15′) and δ 136.6 (C-14,14′) (Figure 13 and 41). The long range correlation from both H-11,11′ and H-15,15′ to the oxygen-bearing aromatic carbon (δ_C 151.8) permitted the location of the hydroxy group at C-13,13′. This was also supported by the correlation of both protons (H-11,11′ and H-15,15′) with the quaternary aromatic carbon C-8. These data indicated that the second monomeric unit must be attached at C-12. The strong HMBC correlation

observed between H-11,11′ and C-12,12′ confirmed the ^{2}J (H-11 to C-12 or H-11′ to C-12′) and ^{3}J (H-11 to C-12′ or H-11′ to C-12) couplings (Figure 13 and 41). Therefore, the structure of **PF-2** named as 7β-hydroxymacrophyllic acid, was elucidated as shown (Figure 16).

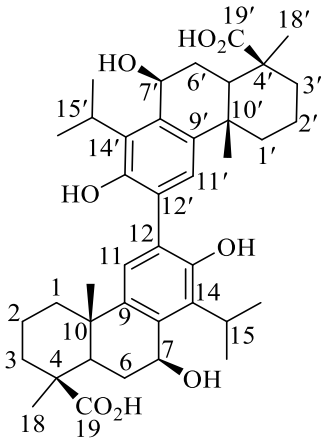

Figure 16. Chemical structure of 7β-hydroxymacrophyllic acid (PF-2)

Besides the new compounds, the structure of the known compounds were determined by comparison of their observed and reported spectroscopic and physical data: inumakiol D (**28**) (Sato *et al.*, 2008), macrophyllic acid (**37**) (Amaro and Dignora Carroz, 1989), nagilactone D (**41**) (Kubo *et al.*, 1984) and ponasterone A (**94**) (Vokac *et al.*, 1998). Except **90**, ^{1}H and ^{13}C NMR data of compounds is given in Tables 6 and 7 and Appendices V, VI, VII and VIII. The chemical shift variation might be due to different solvents used to the NMR which can affect the chemical shift by interactions including hydrogen bonding, the anisotropy of the solvent molecules and polar and van der Waals effect with the solute (Abraham *et al.*, 2006). A summary of physical and spectral data of the ten compounds is given in Appendix I.

Table 6. ^{1}H NMR (400 MHz) data for compounds 28, 37 and 41

Position		28[a]	37[b]	41[b]
1	a	2.23 m (Overlapped) ¶	2.07 br d (12.6)	3.57 d (4.1)
	b	1.37 m (Overlapped) ¶	1.27 (Obscured)	
2	a	2.01 m (Overlapped) ¶	1.94 m (Overlapped) ¶	3.46 dd (6, 4.12)
	b	1.59 br d (14.0)	1.54 br d (13.4)	
3	a	2.24 m (Overlapped) ¶	2.18 br d (13.2)	4.44 dd (6.08, 1.84)
	b	1.15 br t (13.3, 4.1)	1.04 br dt (13.2, 3.7)	
4				
5		2.02 m (Overlapped) ¶	1.46 d (11.9)	1.88 d (6.52)
6	a	2.15 br dt (14.3, 3.4)	2.24 br td (13.4, 5.3)	4.93 dt (9.92, 6.48)
	b	2.26 m (Overlapped) ¶	1.97 m (Overlapped) ¶	
7	a	4.93 br t (2.6)	2.65 ddd (16.8,12.3, 6.2)	3.39 dd (16.4, 9.92)
	b		3.00 dd (16.8, 4.11)	2.8 dd (16.6, 6.4)
8				
9				
10				
11		6.64 d (8.7)	6.84 s	6.3 s
12		6.97 d (8.7)		
13				
14				
15		3.53 sep (7)	3.28 br s	2.58 q (7.56)
16		1.41 d (7)	1.29 d (7)	1.24 t (7.56)
17		1.7 d (7)	1.33 d (7)	
18		1.29 s	1.32 s	1.43 s
19				
20		1.05 s	0.98 s	1.26 s
3-OH				3.4 d (2.2)

[a] Measured in methanol-d_4

[b] Measured in chloroform-*d*

¶ The overlapped signals were assigned with careful axis calibration of ^{1}H-^{1}H COSY and HSQC.

Ponasterone A (90): ^{1}H NMR (CD_3OD, 400 MHz): δ 5.80 (7H, d 2.4), 3.95 (H_a-3, m), 3.84 (H-2, ddd, 12, 4.1, 3.2), 3.33 (H-22-m, Overlapped with solvent signal), 3.15 (H-9, ddd, 10.8, 7.2, 2.2), 2.38 (H-5, dd, 12.4, 4.8), 2.38 (H-17, t, 8.2), 2.12 (H_a-12, ddd,12.9, 12.9, 4.7), 2.05-1.19 (Significantly overlapped area-H-1, H_b-3, H-4, H_b-12, H-15, H-16, H-23, H-24, 25-H). ^{13}C NMR (CD_3OD, 100 MHz): δ 18.2 (C-18), 21.1(C-11), 21.7 (C-18), 21.7 (C-16), 22.9 (C-26), 23.6 (C-27), 24.6 (C-19), 29.4 (C-25), 30.6 (C-24), 31.9 (C-15), 32.7 (C-12), 33.0 (C-4), 35.3 (C-9), 37.5 (C-1), 37.8 (C-23), 39.4 (C-10), 50.6 (C-17), 52.0 (C-5), 68.7 (C-3), 68.9 (C-2), 78.0 (C-20), 78.1 (C-22), 85.4 (C-14), 122.3 (C-7), 168.1 (C-8), 206.6 (C-6).

Table 7. ^{13}C NMR (100 MHz) data for compounds 28, 37 and 41

Position	28[a]	37[c]	41[b]
1	41.2, CH_2	40.5, CH_2	57.3, CH
2	21.5, CH_2	20.2, CH_2	50.7, CH
3	38.7, CH_2	37.1, CH_2	67.6, CH
4	44.5, C	43.8, C	48.8, C
5	46.4, CH	52.5, CH	50.6, CH
6	32.6, CH_2	21.3, CH_2	72.4, CH
7	66.3, CH	30.43, CH_2	25.7, CH_2
8	135.2, C	132.1, C	106.4, C
9	141.2, C	135.2, C	163.8, C
10	39.9, C	38.9, C	37.83, C
11	125.0, CH	125.1, CH	106.9, CH
12	117.9, CH	120.4, C	162.2, C
13	155.7, C	150.3, C	
14	134.3, C	140.9, C	163.1, C
15	29.2, CH	28.3, CH	24.8, CH_2
16	21.1, CH_3	20.4, CH_3	12.0, CH_3
17	21.2, CH_3	20.0, CH_3	
18	29.2, CH_3	28.0, CH_3	25.9, CH_3
19	180.2, C	185.5, C	178.5, C
20	23.0, CH_3	22.5, CH_3	17.69, CH_3

[a] Measured in methanol-d_4
[b] Measured in chloroform-*d*

4.5. Cytotoxicity of the isolated compounds from the roots of *P. falcatus*

The isolated compounds were evaluated for cytotoxicity against human colorectal adenocarcinoma cell line HT-29 and their ED_{50} values are shown in Table 8. From the strong antiproliferative data displayed by all the nagilactones it may be inferred that: (1) the γ-lactone moiety together with the unsaturated δ-lactone unit of nagilactones are responsible for the strong antiproliferative activity, (2) introduction of a lipophilic ester group at C-16/17 slightly lower the activity while hydroxylation of the isopropyl side chain of nagilactones decreases the activity roughly two to three fold and (3) the presence of a C-1/C-2 epoxide moiety marginally decreases the activity (Figure 17).

Table 8. Cytotoxicity of the isolated compounds from the roots of *P. falcatus*

Compound	ED_{50} against HT-29 (µM)[a]
16-Hydroxynagilactone F (**PF-1**)	0.6±0.4
2*β*,16-Dihydroxynagilactone F (**PF-2**)	1.1±0.5
2*β*-Hydroxynagilactone F (**108**)	0.3±0.1
7*β*-hydroxymacrophyllic acid (**PF-3**)	>10
Macrophyllic acid (**37**)	>10
Nagilactone D (**41**)	0.9±0.3
15-Hydroxynagilactone D (**110**)	5.1±0.8
Nagilactone I (**109**)	0.5±0.1
Inumakiol D (**28**)	>10
Ponasterone A (**94**)	>10
Paclitaxel (**7**)	0.00082±0.0003

[a]The values represent the average ± standard deviation from a triplicate.

These observations were in good agreement with a previous report on the structure-activity relationship of natural and synthetic nagilactones against *Yoshida sarcoma* cell line (Hayashi *et al.*, 1979).

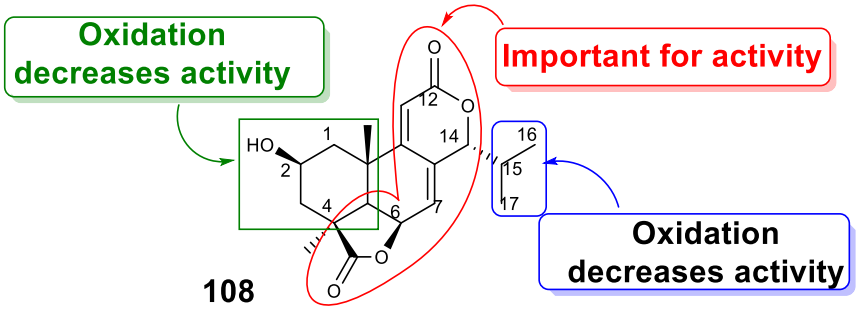

Figure 17. Structure-activity requirement of nagilactones

A study done by Chan *et al.* (2004) indicated that the type A nagilactone, nagilactone C (**40**), is a potent inhibitor of protein synthesis that specifically inhibits eukaryotic translation apparatus and interfere with translation elongation. Since, the nagilactones are the

active compounds isolated from the roots of *P. falcatus* in the present study, they might act by a mechanism similar to nagilactone C thereby causing death cells by deprivation of important proteins. Moreover, since these compounds contain an *α, β, γ, δ* unsaturated lactone, which acts as Michael acceptor, they might irreversibly alkylate important cellular components, such as DNA, enzymes and/or those involved in protein synthesis (Figure 18) (Zhang *et al.*, 2005). These mechanism have been shown to be the main mechanism action of the antitumors mitomycin C (Paz *et al.*, 2012), neratinib and afatinib (Hoelder *et al.*, 2012), bardoxolone methyl (Couch *et al.*, 2005; Wang *et al.*, 2014) and the antimigraine and antitumor parthenolide (Zhang *et al.*, 2005; Skalska *et al.*, 2009; Ghantous *et al.*, 2013). It is also possible that there might be opening of the *γ*- and *δ*-dilactone moiety to occupy/intertwine active sites in enzymes or important proteins and/or to intercalate DNA, thereby making them inactive.

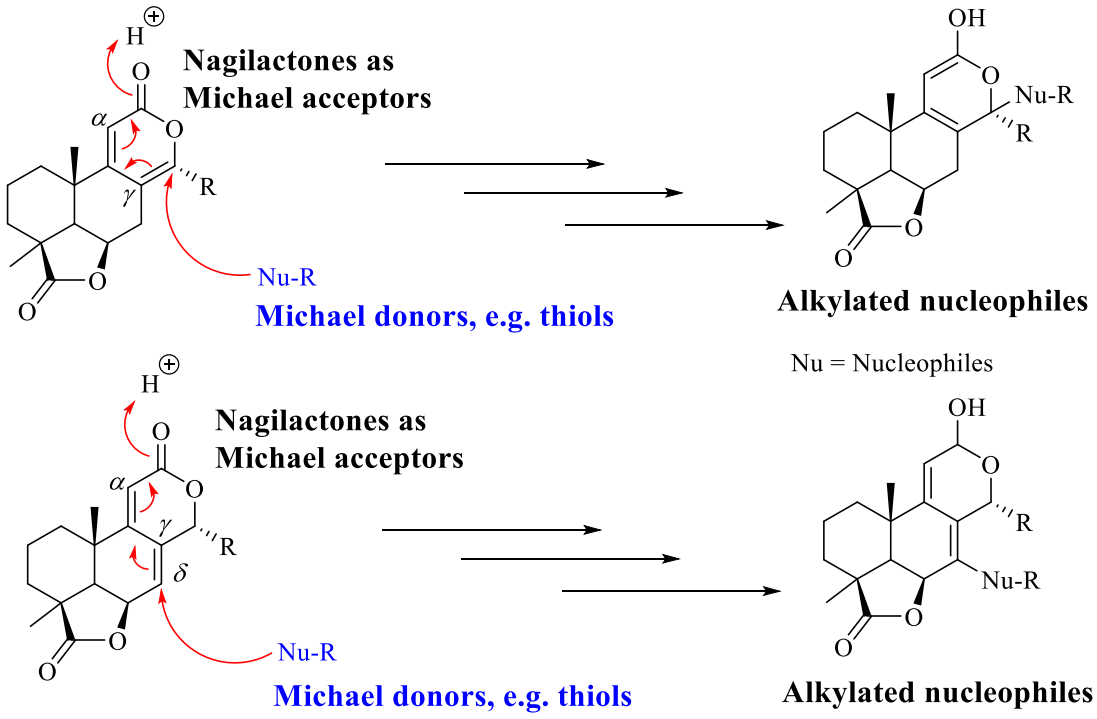

Figure 18. Plausible mechanism of action of nagilactones

5. Conclusion

In summary, the present study led to the isolation of ten bioactive compounds through bioassay guided fractionation and isolation, three of which are new. The nagilactones were shown to be the major active constituents, which is in agreement with a number of reports indicating their activity against various tumor cell lines. Thus, the traditional use of the plant may be justified by its high content of cytotoxic nagilactones, which might contribute for development of new, safe and effective anticancer drugs. The isolation of compounds **PF-1** and **PF-3** from the roots of *P. falcatus* adds number to the rare type C nagilactones, which are the most cytotoxic among the nagilactones.

6. Recommendations

- Since the study was conducted on a single cancer line, the compounds need to be checked for activity against other tumor cell lines.
- Moreover, it is worth to check their selectivity against normal cells which the common drawback of existing anticancer drugs.
- *In vivo* studies should be done to assess their activities in real biological systems.

References

Abdillahi HS, Finnie JF, Van Staden J (2011). Anti-inflammatory, antioxidant, anti-tyrosinase and phenolic contents of four *Podocarpus* species used in traditional medicine in South Africa. *J Ethnopharmacol* **136**(3): 496-503.

Abdillahi HS, Stafford GI, Finnie JF, Van Staden J (2010). Ethnobotany, phytochemistry and pharmacology of *Podocarpus sensu latissimo* (s.l.). *S Afr J Bot* **76**(1): 1-24.

Abdillahi HS, Verschaeve L, Finnie JF, Van Staden J (2012). Mutagenicity, antimutagenicity and cytotoxicity evaluation of South African *Podocarpus* species. *J Ethnopharmacol* **139**(3): 728-738.

Abernethy A, Abrahams E, Barker A, Buetow K, Burkholder R, Dalton WS, Foti M, Frueh F, Gaynor RB, Kean M, Khan Z, Lessor T, Lichtenfeld JL, Mendelsohn J, van't Veer L (2014). Turning the tide against cancer through sustained medical innovation: the pathway to progress. *Clin Cancer Res* **20**(5): 1081-1086.

Abraham RJ, Byrne JJ, Griffiths L, Perez M (2006). ^{1}H chemical shifts in NMR: part 23, the effect of dimethyl sulphoxide versus chloroform solvent on ^{1}H chemical shifts. *Magn Reson Chem* **44**(5): 491-509.

Aerts R (2008). *Afrocarpus falcatus* (Thunb.) C.N.Page Retrieved June 13, 2015, from http://database.prota.org/PROTAhtml/Afrocarpus%20falcatus_En.htm.

Aguirre-Ghiso JA (2007). Models, mechanisms and clinical evidence for cancer dormancy. *Nat Rev Cancer* **7**(11): 834-846.

Amaro JM, Dignora Carroz U (1989). Phytochemistry of the flora of Venezuela. VI. Phenolic diterpenoids of *Decussocarpus rospigliosii*. *Rev Latinoam Quim* **20**(1): 8-10.

Amin A, Gali-Muhtasib H, Ocker M, Schneider-Stock R (2009). Overview of major classes of plant-derived anticancer drugs. *Int J Biomed Sci* **5**(1): 1-11.

Amiri-Kordestani L, Blumenthal GM, Xu QC, Zhang L, Tang SW, Ha L, Weinberg WC, Chi B, Candau-Chacon R, Hughes P, Russell AM, Miksinski SP, Chen XH, McGuinn WD, Palmby T, Schrieber SJ, Liu Q, Wang J, Song P, Mehrotra N, Skarupa L, Clouse K, Al-Hakim A, Sridhara R, Ibrahim A, Justice R, Pazdur R, Cortazar P (2014). FDA approval: ado-trastuzumab emtansine for the treatment of patients with HER2-positive metastatic breast cancer. *Clin Cancer Res* **20**(17): 4436-4441.

Anand P, Kunnumakkara AB, Sundaram C, Harikumar KB, Tharakan ST, Lai OS, Sung B, Aggarwal BB (2008). Cancer is a preventable disease that requires major lifestyle changes. *Pharm Res* **25**(9): 2097-2116.

Andersen OM (1989). Delphinidin-3-neohesperidoside and cyanidin-3-neohesperidoside from receptacles of *Podocarpus* species. *Phytochemistry* **28**(2): 495-497.

Aplin RT, Cambie RC, Rutledge PS (1963). The taxonomic distribution of some diterpene hydrocarbons. *Phytochemistry* **2**(3): 205-214.

Balunas MJ, Kinghorn AD (2005). Drug discovery from medicinal plants. *Life Sci* 78(5): 431-441.

Barkera NP, Mullera EM, Mill RR (2004). A yellowwood by any other name: molecular systematics and the taxonomy of *Podocarpus* and the Podocarpaceae in southern Africa. *S Afr J Sci* **100**: 629-632.

Barok M, Joensuu H, Isola J (2014). Trastuzumab emtansine: mechanisms of action and drug resistance. *Breast Cancer Res* **16**(2): 209.

Barrero AF, Moral JFQ, Herrador MM (2003). Podolactones: a group of biologically active norditerpenoids. Studies in Natural Products Chemistry. Atta-ur-Rahman (Eds.). Elsevier B.V: Dordrecht, The Netherlands. Volume 28, Part I: pages 453-516.

Baxevanis CN, Perez SA, Papamichail M (2009). Combinatorial treatments including vaccines, chemotherapy and monoclonal antibodies for cancer therapy. *Cancer Immunol Immunother* **58**(3): 317-324.

Belpomme D, Irigaray P, Hardell L, Clapp R, Montagnier L, Epstein S, Sasco AJ (2007). The multitude and diversity of environmental carcinogens. *Environ Res* **105**(3): 414-429.

Bendall JG, Cambie RC (1995). Totarol: a non-conventional diterpenoid. *Aust J Chem* **48**(5): 883-917.

Bhakuni D, Bittner M, Silva M, Sammes PG (1973). Nubigenol: an α-hydroxydihydrochalcone from *Podocarpus nubigena*. *Phytochemistry* **12**(11): 2777-2779.

Bhosle J, Hall G (2006). Principles of cancer treatment by chemotherapy. *Surgery (Oxford)* **24**(2): 66-69.

Bhosle J, Hall G (2009). Principles of cancer treatment by chemotherapy. *Surgery (Oxford)* **27**(4): 173-177.

Bloor SJ, Molloy BPJ (1991). Cytotoxic norditerpene lactones from *Ileostylus micranthus*. *J Nat Prod* **54**(5): 1326-1330.

Bocks SM, Cambie RC, Takahashi T (1963). Chemistry of the podocarpaceae-VIII: macrophyllic acid, a bisditerpenoid from *Podocarpus macrophyllus* D. Don. *Tetrahedron* **19**(6): 1109-1116.

Borrello MG, Degl'Innocenti D, Pierotti MA (2008). Inflammation and cancer: the oncogene-driven connection. *Cancer Lett* **267**(2): 262-270.

Brandt CW, Neubauer LG (1939). 221. Miro resin. Part I. Ferruginol. *J Chem Soc*(0): 1031-1037.

Briggs LH, Cain BF (1959). Chemistry of the Podocarpaceae-I: constituents of the heartwood of *Podocarpus spicatus*. *Tetrahedron* **6**(2): 143-144.

Briggs LH, Cambie RC, Hoare JL (1959a). Chemistry of the Podocarpaceae-III: a new lignan, seco-isolariciresinol and further constituents of the heartwood of *Podocarpus spicatus*. *Tetrahedron* **7**(3): 262-269.

Briggs LH, Cambie RC, Hoare JL (1959b). Seco-isolariciresinol, a new lignan from *Podocarpus spicatus*. *Tetrahedron Lett* **1**(4): 14-15.

Briggs LH, Cebalo TP (1959). Chemistry of the Podocarpaceae-II: the isolation of genistein from *Podocarpus spicatus* and the constitution of podospicatin. *Tetrahedron* **6**(2): 145-147.

Brower V (2008). Back to nature: extinction of medicinal plants threatens drug discovery. *J Natl Cancer Inst* **100**(12): 838-839.

Bussmann RW, Swartzinsky P, Worede A, Evangelista P (2011). Plant use in Odo-Bulu and Demaro, Bale region, Ethiopia. *J Ethnobiol Ethnomed* **7**: 28.

Caley A, Jones R (2012). The principles of cancer treatment by chemotherapy. *Surgery (Oxford)* **30**(4): 186-190.

Cambie RC, Cox RE, Sidwell D (1984). Phenolic diterpenoids of *Podocarpus ferrugineus* and other podocarps. *Phytochemistry* **23**(2): 333-336.

Cambie RC, Mander LN (1962). Chemistry of the podocarpaceae-VI : constituents of the heartwood of *Podocorpus totara* G. Benn. *Tetrahedron* **18**(4): 465-475.

Campello JP, Fonseca SF, Chang C-J, Wenkert E (1975). Terpenes of *Podocarpus lambertius*. *Phytochemistry* **14**(1): 243-248.

Candido J, Hagemann T (2013). Cancer-related inflammation. *J Clin Immunol* **33** (Suppl 1): S79-84.

Carman RM, Russell-Maynard JKL, Schumann RC (1985). Isoflavones from *Podocarpus amarus*. *Aust J Chem* **38**(3): 485-496.

Carter GT (2011). Natural products and Pharma 2011: strategic changes spur new opportunities. *Nat Prod Rep* **28**(11): 1783-1789.

Cassady JM, Lightner TK, McCloud TG, Hembree JA, Byrn SR, Chang C (1984). Revised structure of podolactone C, the antileukemic component of *Podocarpus milanjianus* Rendle. *J Org Chem* **49**(5): 942-945.

Chabner BA, Roberts TG, Jr. (2005). Timeline: chemotherapy and the war on cancer. *Nat Rev Cancer* **5**(1): 65-72.

Chan J, Khan SN, Harvey I, Merrick W, Pelletier J (2004). Eukaryotic protein synthesis inhibitors identified by comparison of cytotoxicity profiles. *RNA* **10**(3): 528-543.

Chari RV, Miller ML, Widdison WC (2014). Antibody-drug conjugates: an emerging concept in cancer therapy. *Angew Chem Int Ed Engl* **53**(15): 3796-3827.

Chen C, Zhou J, Ji C (2010). Quercetin: a potential drug to reverse multidrug resistance. *Life Sci* **87**(11-12): 333-338.

Chin AFO, Clarke DB, Hinkley SFR, Perry NB, Weavers RT (2001). Links between the triquinane diterpenes laurenene and waihoensene. *Aust J Chem* **54**(3): 205-211.

Cho WC, Roukos DH (2013). Trastuzumab emtansine for advanced HER2-positive breast cancer and beyond: genome landscape-based targets. *Expert Rev Anticancer Ther* **13**(1): 5-8.

Clarke DB, Hinkley SFR, Weavers RT (1997). Waihoensene. A new laurenene-related diterpene from *Podocarpus totara* var *waihoensis*. *Tetrahedron Lett* **38**(24): 4297-4300.

Couch RD, Browning RG, Honda T, Gribble GW, Wright DL, Sporn MB, Anderson AC (2005). Studies on the reactivity of CDDO, a promising new chemopreventive and

chemotherapeutic agent: implications for a molecular mechanism of action. *Bioorg Med Chem Lett* **15**(9): 2215-2219.

Cox RE, Yamamoto S, Otto A, Simoneit BRT (2007). Oxygenated di- and tri- cyclic diterpenoids of southern hemisphere conifers. *Biochem Syst Ecol* **35**(6): 342-362.

Cragg GM, Newman DJ (2003). Plants as a source of anti-cancer and anti-HIV agents. *Ann Appl Biol* **143**(2): 127-133.

Cragg GM, Newman DJ (2005). Plants as a source of anti-cancer agents. *J Ethnopharmacol* **100**(1-2): 72-79.

Crowden RK (1974). Cyanidin-3-neohesperidoside, a novel anthocyanin from *Podocarpus lawrencii*. *Phytochemistry* **13**: 2877-2878.

Crowden RK, Grubb MJ (1971). Anthocyanins from five species of the Podocarpaceae. *Phytochemistry* **10**(11): 2821-2822.

Dancey JE, Bedard PL, Onetto N, Hudson TJ (2012). The genetic basis for cancer treatment decisions. *Cell* **148**(3): 409-420.

de Jesus MB, Zambuzzi WF, Ruela de Sousa RR, Areche C, Santos de Souza AC, Aoyama H, Schmeda-Hirschmann G, Rodriguez JA, Monteiro de Souza Brito AR, Peppelenbosch MP, den Hertog J, de Paula E, Ferreira CV (2008). Ferruginol suppresses survival signaling pathways in androgen-independent human prostate cancer cells. *Biochimie* **90**(6): 843-854.

de Souza AC, Justo GZ, de Araujo DR, Cavagis AD (2011). Defining the molecular basis of tumor metabolism: a continuing challenge since Warburg's discovery. *Cell Physiol Biochem* **28**(5): 771-792.

Demissew S, Friis I (2009). Podocarpaceae. Flora of Ethiopia and Eritrea. Lycopodiaceae to Pinaceae. I. Hedberg, I. Friis and E. Persson (Eds.). The National Herbarium, Biology Department, Science Faculty, Addis Ababa Univerity, Ethiopia and The Department of Systematic Biology, Uppsala Univeristy, Sweden. 1.

Desai AG, Qazi GN, Ganju RK, El-Tamer M, Singh J, Saxena AK, Bedi YS, Taneja SC, Bhat HK (2008). Medicinal plants and cancer chemoprevention. *Curr Drug Metab* **9**(7): 581-591.

Devkota KP, Ratnayake R, Colburn NH, Wilson JA, Henrich CJ, McMahon JB, Beutler JA (2011). Inhibitors of the oncogenic transcription factor AP-1 from *Podocarpus latifolius*. *J Nat Prod* **74**(3): 374-377.

Dinan L (2001). Phytoecdysteroids: biological aspects. *Phytochemistry* 57(3): 325-339.

Dinan L (2009). The Karlson lecture. Phytoecdysteroids: what use are they? *Arch Insect Biochem Physiol* **72**(3): 126-141.

ECA (2007). Ethiopian Cancer Association: Fight against tobacco to reduce the risk of cancer through antitobacco youth clubs in Ethiopia. Retrieved June 13, 2015, from http://www.yeeca.org/Projects2.html.

Faiella L, Temraz A, Siciliano T, De Tommasi N, Braca A (2012). Terpenoids from the leaves of *Podocarpus gracilior*. *Phytochem Lett* **5**(2): 297-300.

Federico A, Morgillo F, Tuccillo C, Ciardiello F, Loguercio C (2007). Chronic inflammation and oxidative stress in human carcinogenesis. *Int J Cancer* **121**(11): 2381-2386.

Feleke S, Haile F, Alemu A, Abebe S (2012). Characteristics of seed kernel oil from *Podocarpus falcatus*. *J Trop For Sci* **24**(4): 512-516.

Ferlay J, Shin HR, Bray F, Forman D, Mathers C, Parkin DM (2010). Estimates of worldwide burden of cancer in 2008: GLOBOCAN 2008. *Int J Cancer* **127**(12): 2893-2917.

Ferlay J, Soerjomataram I, Dikshit R, Eser S, Mathers C, Rebelo M, Parkin DM, Forman D, Bray F (2015). Cancer incidence and mortality worldwide: sources, methods and major patterns in GLOBOCAN 2012. *Int J Cancer* **136**(5): E359-E386.

Ferlay J, Soerjomataram I, Ervik M, Dikshit R, Eser S, Mathers C, Rebelo M, Parkin D, Forman D, Bray F (2013). GLOBOCAN 2012 v1.0, Cancer Incidence and Mortality Worldwide: IARC CancerBase No. 11 [Internet]. Retrieved June 13, 2015, from http://globocan.iarc.fr/Pages/fact_sheets_cancer.aspx.

Fernando J, Jones R (2015). The principles of cancer treatment by chemotherapy. *Surgery (Oxford)* **33**(3): 131-135.

Flygare JA, Pillow TH, Aristoff P (2013). Antibody-drug conjugates for the treatment of cancer. *Chem Biol Drug Des* **81**(1): 113-121.

Galbraith MN, Horn DHS (1969). Insect moulting hormones: crustecdysone (20-hydroxyecdysone) from *Podocarpus elatus*. *Aust J Chem* **22**(5): 1045-1057.

Galbraith MN, Horn DHS, Ito S, Kodama M, Sasse JM (1972). Structure-activity relationships of podolactones and related compounds. *Agric Biol Chem* **36**(13): 2393-2396.

Galbraith MN, Horn DHS, Sasse JM (1971). Podolactones C and D, terpene sulphoxides from *Podocarpus neriifolius*. *J Chem Soc D* (21): 1362b-1363.

Garg AK (2011). Nocebo side-effects in cancer treatment. *Lancet Oncol* **12**(13): 1181-1182.

Gennari A, D'amico M, Corradengo D (2011). Extending the duration of first-line chemotherapy in metastatic breast cancer: a perspective review. *Ther Adv Med Oncol* **3**(5): 229-232.

Ghantous A, Sinjab A, Herceg Z, Darwiche N (2013). Parthenolide: from plant shoots to cancer roots. *Drug Discov Today* **18**(17–18): 894-905.

Giday M, Asfaw Z, Woldu Z (2010). Ethnomedicinal study of plants used by Sheko ethnic group of Ethiopia. *J Ethnopharmacol* **132**(1): 75-85.

Gordaliza M, García PA, del Corral JMM, Castro MA, Gómez-Zurita MA (2004). Podophyllotoxin: distribution, sources, applications and new cytotoxic derivatives. *Toxicon* **44**(4): 441-459.

Graham JG, Quinn ML, Fabricant DS, Farnsworth NR (2000). Plants used against cancer-an extension of the work of Jonathan Hartwell. *J Ethnopharmacol* **73**(3): 347-377.

Guerram M, Jiang Z-Z, Zhang L-Y (2012). Podophyllotoxin, a medicinal agent of plant origin: past, present and future. *Chin J Nat Med* 10(3): 161-169.

Gurib-Fakim A (2006). Medicinal plants: traditions of yesterday and drugs of tomorrow. *Mol Aspects Med* **27**(1): 1-93.

Haider S, Rizvi M, Rahman W, Okigawa M, Kawano N (1974). Biflavones from *Podocarpus neriifolius*. *Phytochemistry* **13**(9): 1990.

Hameed N, Ilyas M, Rahman W, Okigawa M, Kawano N (1973). Biflavones in the leaves of *Podocarpus taxifolia*. *Phytochemistry* **12**(6): 1497.

Hammann S, Schroder M, Schmidt C, Vetter W (2015). Isolation of two Δ5 polymethylene interrupted fatty acids from *Podocarpus falcatus* by countercurrent chromatography. *J Chromatogr A* **1394**: 89-94.

Han Y, Di XX, Li HZ, Shen T, Ren DM, Lou HX, Wang XN (2014). Podoimbricatin A, a cytotoxic diterpenoid with an unprecedented 6/6/5/6-fused tetracyclic ring system from the twigs and leaves of *Podocarpus imbricatus*. *Bioorg Med Chem Lett* **24**(15): 3326-3328.

Hanahan D, Coussens LM (2012). Accessories to the crime: functions of cells recruited to the tumor microenvironment. *Cancer Cell* **21**(3): 309-322.

Hanahan D, Weinberg RA (2000). The hallmarks of cancer. *Cell* **100**(1): 57-70.

Hanahan D, Weinberg RA (2011). Hallmarks of cancer: the next generation. *Cell* **144**(5): 646-674.

Hanessian S, Boyer N, Reddy GJ, Deschenes-Simard B (2009). Total synthesis of oidiodendrolides and related norditerpene dilactones from a common precursor:

metabolites CJ-14,445, LL-Z1271gamma, oidiolactones A, B, C, and D, and nagilactone F. *Org Lett* **11**(20): 4640-4643.

Harvey AL, Edrada-Ebel R, Quinn RJ (2015). The re-emergence of natural products for drug discovery in the genomics era. *Nat Rev Drug Discov* **14**(2): 111-129.

Hayashi T, Kakisawa H, Itô S, Chen YP, Hsū H-Y (1972a). Structure of the further norditerpenoids of *Podocarpus macrophyllus*. Inumakilactone A glucoside, a plant growth inhibitor and inumakilactone E. *Tetrahedron Lett* **13**(33): 3385-3388.

Hayashi Y, Matsumoto T (1982). Reaction and interconversion of norditerpenoid dilactones, biologically active principles isolated from *Podocarpus* plants. *J Org Chem* **47**(18): 3421-3428.

Hayashi Y, Matsumoto T, Tashiro T (1979). Antitumor activity of norditerpenoid dilactones in *Podocarpus* plants: structure-activity relationship on *in vitro* cytotoxicity against *Yoshida sarcoma*. *Gan* **70**(3): 365-369.

Hayashi Y, Matsumoto T, Uemura M, Koreeda M (1980). Carbon-13 NMR studies of the biologically active norditerpenoid dilactones from *Podocarpus* plants. *Org Magn Reson* **14**(2): 86-91.

Hayashi Y, Sakan T (1975). Antitumor activity of nagilactones. *Gan* **66**(5): 587-588.

Hayashi Y, Takahashi S, Ona H, Sakan T (1968). Structures of nagilactone A, B, C, and D, novel nor- and bis-norditerpenoids. *Tetrahedron Lett* **9**(17): 2071-2076.

Hayashi Y, Yokoi J, Watanabe Y, Sakan T, Masuda Y, Yamamoto R (1972b). Structures of nagilactone E and F, and biological activity of nagilactones as plant growth regulator. *Chem Lett* **1**(9): 759-762.

Hayashi Y, Yuki YI, Matsumoto T, Sakan T (1977a). New congeners of cytotoxic nor-diterpenoid dilactones in *Podocarpus nagi*: three highly polar components with α-pyrone ring. *Tetrahedron Lett* **18**(34): 2953-2956.

Hayashi Y, Yuki YI, Matsumoto T, Sakan T (1977b). New congeners of cytotoxic nor-diterpenoid dilactones in *Podocarpus nagi*: two C_{19} lactones from seed extract. *Tetrahedron Lett* **18**(41): 3637-3640.

Hayashia Y, Kima K, Hayashia Y, Chairula (1992). Nagilactones as an anti-feedant from *Podocarpus nagi* for herbivorous mammals. *Biosci Biotech Biochem* **56**(8): 1302-1303.

Hembree JA, Chang C-J, McLaughlin JL, Cassady JM, Watts DJ, Wenkert E, Fonseca SF, Campello JDP (1979). The cytotoxic norditerpene dilactones of *Podocarpus milanjianus* and *Podocarpus sellowii*. *Phytochemistry* **18**(10): 1691-1694.

Ho JW, Cheung MW (2014). Combination of phytochemicals as adjuvants for cancer therapy. *Recent Pat Anticancer Drug Discov* **9**(3): 297-302.

Hoelder S, Clarke PA, Workman P (2012). Discovery of small molecule cancer drugs: successes, challenges and opportunities. *Mol Oncol* **6**(2): 155-176.

Holohan C, Van Schaeybroeck S, Longley DB, Johnston PG (2013). Cancer drug resistance: an evolving paradigm. *Nat Rev Cancer* **13**(10): 714-726.

Imai S, Fujioka S, Murata E, Sasakawa Y, Nakanishi K (1968a). The structures of three additional phytoecdysones from *Podocarpus macrophyllus*, makisterone B, C and D. *Tetrahedron Lett* **9**(36): 3887-3890.

Imai S, Hori M, Fujioka S, Murata E, Goto M, Nakanishi K (1968b). Isolation of four new phytoecdysones, makisterone A, B, C, D and the structure of makisterone A, A C_{28} steroid. *Tetrahedron Lett* **9**(36): 3883-3886.

Ito S, Kodama M (1976). Norditerpene dilactones from *Podocarpus* species. *Heterocycles* **4**(3): 595-624.

Ito S, Kodama M, Sunagawa M, Koreeda M, Nakanishi K (1971). Structure of the norditerpene ponalactone A and its glucoside, plant growth inhibitors. *J Chem Soc D* (15): 855-856.

Itokawa H, Morris-Natschke SL, Akiyama T, Lee KH (2008). Plant-derived natural product research aimed at new drug discovery. *J Nat Med* **62**(3): 263-280.

Ji H-F, Li X-J, Zhang H-Y (2009). Natural products and drug discovery. Can thousands of years of ancient medical knowledge lead us to new and powerful drug combinations in the fight against cancer and dementia? *EMBO Reports* **10**(3): 194-200.

Ji S, Orlikova B, Diederich M (2014). Non-edible plants as an attractive source of compounds with chemopreventive potential. *J Cancer Prev* **19**(1): 1-6.

Jiang WG, Ablin RJ (2011). Cancer metastasis, challenges, progress and the opportunities. *Front Biosci (Elite Ed)* **3**: 391-394.

Jones PA, Baylin SB (2007). The epigenomics of cancer. *Cell* **128**(4): 683-692.

Kanavos P (2006). The rising burden of cancer in the developing world. *Ann Oncol* **17**(Suppl 8): viii15-viii23.

Kelch D (1998). Phylogeny of Podocarpaceae: comparison of evidence from morphology and 18S rDNA. *Am J Bot* **85**(7): 986.

Khan N, Afaq F, Mukhtar H (2010). Lifestyle as risk factor for cancer: evidence from human studies. *Cancer Lett* **293**(2): 133-143.

Kibria G, Hatakeyama H, Harashima H (2014). Cancer multidrug resistance: mechanisms involved and strategies for circumvention using a drug delivery system. *Arch Pharm Res* **37**(1): 4-15.

Kingston DG (2011). Modern natural products drug discovery and its relevance to biodiversity conservation. *J Nat Prod* **74**(3): 496-511.

Kingston DGI (2007). The shape of things to come: structural and synthetic studies of taxol and related compounds. *Phytochemistry* **68**(14): 1844-1854.

Kingston DGI (2009). Tubulin-interactive natural products as anticancer agents. *J Nat Prod* 72(3): 507-515.

Kita M, Kigoshi H (2015). Marine natural products that interfere with multiple cytoskeletal protein interactions. *Nat Prod Rep* **32**(4): 534-542.

Kitamura T, Qian BZ, Pollard JW (2015). Immune cell promotion of metastasis. *Nat Rev Immunol* **15**(2): 73-86.

Klepsch F, Jabeen I, Chiba P, Ecker GF (2010). Pharmacoinformatic approaches to design natural product type ligands of ABC-transporters. *Curr Pharm Des* **16**(15): 1742-1752.

Krauze-Baranowska M, Baczek T, Głód D, Kaliszan R, Wollenweber E (2004). HPLC separation of *O*-acylated flavonoids and biflavones from some species of Gymnospermae. *Chromatographia* **60**(1-2): 9-15.

Krepkowski J, Bräuning A, Gebrekirstos A (2012). Growth dynamics and potential for cross-dating and multi-century climate reconstruction of *Podocarpus falcatus* in Ethiopia. *Dendrochronologia* **30**(4): 257-265.

Kubo I, Himejima M, Ying B-P (1991a). An antifungal norditerpene dilactone from *Podocarpus nagi*. *Phytochemistry* **30**(5): 1467-1469.

Kubo I, Matsumoto T, Klocke JA (1984). Multichemical resistance of the conifer *Podocarpus gracilior* (Podocarpaceae) to insect attack. *J Chem Ecol* **10**(4): 547-559.

Kubo I, Muroi H, Himejima M (1992a). Antibacterial activity of totarol and its potentiation. *J Nat Prod* **55**(10): 1436-1440.

Kubo I, Sutisna M, Kah-Siew T (1991b). Effects of nagilactones on the growth of lettuce seedlings. *Phytochemistry* **30**(2): 455-456.

Kubo I, Ying B-P, Castillo M, Brinen LS, Clardy J (1992b). Podoandin, a molluscicidal sesquiterpene lactone from *Podocarpus andina*. *Phytochemistry* **31**(5): 1545-1548.

Kundu JK, Surh YJ (2008). Inflammation: gearing the journey to cancer. *Mutat Res* **659**(1-2): 15-30.

Kundu JK, Surh YJ (2012). Emerging avenues linking inflammation and cancer. *Free Radic Biol Med* **52**(9): 2013-2037.

Kuo YJ, Hwang SY, Wu MD, Liao CC, Liang YH, Kuo YH, Ho HO (2008). Cytotoxic constituents from *Podocarpus fasciculus*. *Chem Pharm Bull (Tokyo)* **56**(4): 585-588.

Kupchan SM, Baxter RL, Ziegler MF, Smith PM, Bryan RF (1975). Podolide, a new antileukemic norditerpene dilactone from *Podocarpus gracilior*. *Experientia* **31**(2): 137-138.

Kupchan SM, Komoda Y, Branfman AR, Sneden AT, Court WA, Thomas GJ, Hintz HP, Smith RM, Karim A, Howie GA, Verma AK, Nagao Y, Dailey RG, Jr., Zimmerly VA, Sumner WC, Jr. (1977). The maytansinoids. Isolation, structural elucidation, and chemical interrelation of novel ansa macrolides. *J Org Chem* **42**(14): 2349-2357.

Kupchan SM, Komoda Y, Court WA, Thomas GJ, Smith RM, Karim A, Gilmore CJ, Haltiwanger RC, Bryan RF (1972). Maytansine, a novel antileukemic ansa macrolide from *Maytenus ovatus*. *J Am Chem Soc* **94**(4): 1354-1356.

Kupchan SM, Smith RM (1977). Maytoline, maytine, and maytolidine, novel nicotinoyl sesquiterpene alkaloids from *Maytenus serrata* (Hochst., ex A. Rich.) R. Wilczek. *J Org Chem* **42**(1): 115-118.

Laekeman G, Vlietinck A (2013). Phytoecdysteroids: phytochemistry and pharmacological activity. Natural Products. K. G. Ramawat and J.-M. Mérillon (Eds.). Springer Berlin Heidelberg: pages 3827-3849.

Li Y, Revalde JL, Reid G, Paxton JW (2010). Interactions of dietary phytochemicals with ABC transporters: possible implications for drug disposition and multidrug resistance in cancer. *Drug Metab Rev* **42**(4): 590-611.

Little DP, Knopf P, Schulz C (2013). DNA barcode identification of Podocarpaceae-the second largest conifer family. *PLoS One* **8**(11): e81008.

Livshits Z, Rao RB, Smith SW (2014). An approach to chemotherapy-associated toxicity. *Emerg Med Clin North Am* **32**(1): 167-203.

Lorence A, Nessler CL (2004). Camptothecin, over four decades of surprising findings. *Phytochemistry* **65**(20): 2735-2749.

LoRusso PM, Weiss D, Guardino E, Girish S, Sliwkowski MX (2011). Trastuzumab emtansine: a unique antibody-drug conjugate in development for human epidermal growth factor receptor 2-positive cancer. *Clin Cancer Res* **17**(20): 6437-6447.

Lowry JB (1968). Anthocyanin from a malayan member of the podocarpaceae. *Phytochemistry* **7**(10): 1897-1898.

Lowry JB (1972). Anthocyanins of the Podocarpaceae. *Phytochemistry* 11(2): 725-731.

Lulekal E, Asfaw Z, Kelbessa E, Van Damme P (2014). Ethnoveterinary plants of Ankober District, North Shewa Zone, Amhara Region, Ethiopia. *J Ethnobiol Ethnomed* **10**: 21

Lulekal E, Kelbessa E, Bekele T, Yineger H (2008). An ethnobotanical study of medicinal plants in Mana Angetu district, southeastern Ethiopia. *J Ethnobiol Ethnomed* **4**: 10.

Luo J, Solimini NL, Elledge SJ (2009). Principles of cancer therapy: oncogene and non-oncogene addiction. *Cell* **136**(5): 823-837.

Luqmani YA (2005). Mechanisms of drug resistance in cancer chemotherapy. *Med Princ Pract* **14** (Suppl 1): 35-48.

Mabberley D (1997). The Plant-Book, a Portable Dictionary of the Higher Plants. Cambridge University Press Cambridge, England.

Macias FA, Simonet AM, Pacheco PC, Barrero AF, Cabrera E, Jimenez-Gonzalez D (2000). Natural and synthetic podolactones with potential use as natural herbicide models. *J Agric Food Chem* **48**(7): 3003-3007.

Mamadalieva NZ (2013). Occurrence of phytoecdysteroids in plant species. Natural compounds-Phytoecdysteroids. S. S. Azimova (Eds.). Springer Science+Business Media, New York: pages 27-29.

Marín A, Martín M, Liñán O, Alvarenga F, López M, Fernández L, Büchser D, Cerezo L (2015). Bystander effects and radiotherapy. *Rep Pract Oncol Radiother* **20**(1): 12-21.

Matlin SA, Bittner M, Silva M (1984). Lignan and norditerpene dilactone constituents of *Podocarpus saligna*. *Phytochemistry* **23**(12): 2867-2870.

Mesfin F, Demissew S, Teklehaymanot T (2009). An ethnobotanical study of medicinal plants in Wonago Woreda, SNNPR, Ethiopia. *J Ethnobiol Ethnomed* **5**: 28.

Micol V, Mateo CR, Shapiro S, Aranda FJ, Villalain J (2001). Effects of (+)-totarol, a diterpenoid antibacterial agent, on phospholipid model membranes. *Biochim Biophys Acta* **1511**(2): 281-290.

Mill RR (2014). A monographic revision of the genus *Podocarpus* (Podocarpaceae): I. Historical review. *Edinb J Bot* **71**(03): 309-360.

Miller MJ, Foy KC, Kaumaya PT (2013). Cancer immunotherapy: present status, future perspective, and a new paradigm of peptide immunotherapeutics. *Discov Med* **15**(82): 166-176.

Miura H, Kihara T, Kawano N (1968). New bisflavones from *Podocarpus* and *Chamaecyparis* plants. *Tetrahedron Lett* **9**(19): 2339-2342.

Morrison KC, Hergenrother PJ (2014). Natural products as starting points for the synthesis of complex and diverse compounds. *Nat Prod Rep* **31**(1): 6-14.

Mosby TT, Cosgrove M, Sarkardei S, Platt KL, Kaina B (2012). Nutrition in adult and childhood cancer: role of carcinogens and anti-carcinogens. *Anticancer Res* **32**(10): 4171-4192.

Muroi H, Kubo I (1994). Bactericidal effects of anacardic acid and totarol on methicillin-resistant *Staphylococcus aureus* (MRSA). *Biosci Biotechnol Biochem* **58**(10): 1925-1926.

Nabekura T (2010). Overcoming multidrug resistance in human cancer cells by natural compounds. *Toxins (Basel)* **2**(6): 1207-1224.

Nakanishi K, Koreeda M, Chang ML, Hsu HY (1968). Insect hormones V. The structures of ponasterones B and C. *Tetrahedron Lett* **9**(9): 1105-1110.

Nakanishi K, Koreeda M, Sasaki S, Chang ML, Hsu HY (1966). Insect hormones. The structure of ponasterone A, insect-moulting hormone from the leaves of *Podocarpus nakaii* Hay. *Chem Commun (London)* (24): 915-917.

Newman DJ (2008). Natural products as leads to potential drugs: an old process or the new hope for drug discovery? *J Med Chem* **51**(9): 2589-2599.

Newman DJ, Cragg GM (2012). Natural products as sources of new drugs over the 30 years from 1981 to 2010. *J Nat Prod* **75**(3): 311-335.

Newman DJ, Cragg GM (2014). Marine-sourced anti-cancer and cancer pain control agents in clinical and late preclinical development. *Marine Drugs* **12**(1): 255-278.

Newman DJ, Cragg GM, Snader KM (2000). The influence of natural products upon drug discovery. *Nat Prod Rep* **17**(3): 215-234.

Ono M, Yamamoto M, Masuoka C, Ito Y, Yamashita M, Nohara T (1999). Diterpenes from the fruits of *Vitex rotundifolia*. *J Nat Prod* **62**(11): 1532-1537.

Ouyang L, Luo Y, Tian M, Zhang SY, Lu R, Wang JH, Kasimu R, Li X (2014). Plant natural products: from traditional compounds to new emerging drugs in cancer therapy. *Cell Prolif* **47**(6): 506-515.

Pan L, Chai H, Kinghorn AD (2010a). The continuing search for antitumor agents from higher plants. *Phytochem Lett* **3**(1): 1-8.

Pan L, Chai HB, Kinghorn AD (2012). Discovery of new anticancer agents from higher plants. *Front Biosci (Schol Ed)* **4S**(1): 142-156.

Pan L, Kardono LB, Riswan S, Chai H, Carcache de Blanco EJ, Pannell CM, Soejarto DD, McCloud TG, Newman DJ, Kinghorn AD (2010b). Isolation and characterization of minor analogues of silvestrol and other constituents from a large-scale re-collection of *Aglaia foveolata*. *J Nat Prod* **73**(11): 1873-1878.

Pankhurst A (2000). Awliyaw: the largest and oldest tree in Ethiopia? Retrieved June 4, 2015, from http://www.conifers.org/refs/pankhurst00.htm.

Park H-S, Kai N, Fukaya H, Aoyagi Y, Takeya K (2004a). New cytotoxic norditerpene dilactones from leaves of *Podocarpus macrophyllus* var *maki*. *Heterocycles* **63**(2): 347-357.

Park H-S, Yoda N, Fukaya H, Aoyagi Y, Takeya K (2004b). Rakanmakilactones A–F, new cytotoxic sulfur-containing norditerpene dilactones from leaves of *Podocarpus macrophyllus* var *maki*. *Tetrahedron* **60**(1): 171-177.

Patridge E, Gareiss P, Kinch MS, Hoyer D (2015). An analysis of FDA-approved drugs: natural products and their derivatives. *Drug Discov Today Article in Press*.

Pavia D, Lampman G, Kriz G, Vyvyan J (2009). Introduction to Spectroscopy. Brooks/Cole, Cengage Learning USA.

Paz MM, Zhang X, Lu J, Holmgren A (2012). A new mechanism of action for the anticancer drug mitomycin C: mechanism-based inhibition of thioredoxin reductase. *Chem Res Toxicol* **25**(7): 1502-1511.

Perez HL, Cardarelli PM, Deshpande S, Gangwar S, Schroeder GM, Vite GD, Borzilleri RM (2014a). Antibody-drug conjugates: current status and future directions. *Drug Discov Today* **19**(7): 869-881.

Perez LB, Still PC, Naman CB, Ren Y, Pan L, Chai HB, Carcache de Blanco EJ, Ninh TN, Van Thanh B, Swanson SM, Soejarto DD, Kinghorn AD (2014b). Investigation of Vietnamese plants for potential anticancer agents. *Phytochem Rev* **13**(4): 727-739.

Poojari RJ, Patil AG, Gota VS (2012). Development of botanical principles for clinical use in cancer: where are we lacking? *J Postgrad Med* **58**(1): 63-67.

Qurishi Y, Hamid A, Majeed R, Hussain A, Qazi AK, Ahmed M, Zargar MA, Singh SK, Saxena AK (2011). Interaction of natural products with cell survival and signaling pathways in the biochemical elucidation of drug targets in cancer. *Future Oncol* **7**(8): 1007-1021.

Rebucci M, Michiels C (2013). Molecular aspects of cancer cell resistance to chemotherapy. *Biochem Pharmacol* **85**(9): 1219-1226.

Reuter S, Gupta SC, Chaturvedi MM, Aggarwal BB (2010). Oxidative stress, inflammation, and cancer: how are they linked? *Free Radic Biol Med* **49**(11): 1603-1616.

Reynolds M, Chaturvedula VS, Ratovoson F, Andriantsiferana R, Rasamison VE, Guza RC, Kingston DG (2006). Cytotoxic diterpenoids from *Podocarpus madagascariensis* from the Madagascar rainforest. *Nat Prod Res* **20**(6): 606-610.

Rodriguez JA, Theoduloz C, Yanez T, Becerra J, Schmeda-Hirschmann G (2006). Gastroprotective and ulcer healing effect of ferruginol in mice and rats: assessment of its mechanism of action using *in vitro* models. *Life Sci* **78**(21): 2503-2509.

Roy SK, Qasim MA, Kamil M, Ilyas M (1987). Biflavones from the genus *Podocarpus*. *Phytochemistry* **26**(7): 1985-1987.

Russell GB, Fenemore PG, Singh P (1973). Structure of hallactones A and B, insect toxins from *Podocarpus hallii*. *J Chem Soc Chem Commun* (5): 166-167.

Saklani A, Kutty SK (2008). Plant-derived compounds in clinical trials. *Drug Discov Today* **13**(3-4): 161-171.

Sasse JM, Rowan KS, Galbraith MN (1981). Distribution of podolactone-type plant growth inhibitors in the coniferae. *Phytochemistry* **20**(9): 2195-2204.

Sato K, Inaba Y, Park HS, Akiyama T, Koyama T, Fukaya H, Aoyagi Y, Takeya K (2009a). Cytotoxic bisnor- and norditerpene dilactones having 7α,8α-epoxy-9,11-enolide substructure from *Podocarpus macrophyllus* D. DON. *Chem Pharm Bull (Tokyo)* **57**(7): 668-679.

Sato K, Sugawara K, Takeuchi H, Park H-S, Akiyama T, Koyama T, Fukaya H, Aoyagi Y, Takeya K (2009b). New cytotoxic nor- and bis-norditerpene dilactones, makilactones A-D, from *Podocarpus macrophyllus* D. Don. *Heterocycles* **78**(6): 1453-1462.

Sato K, Sugawara K, Takeuchi H, Park HS, Akiyama T, Koyama T, Aoyagi Y, Takeya K, Tsugane T, Shimura S (2008). Antibacterial novel phenolic diterpenes from *Podocarpus macrophyllus* D. Don. *Chem Pharm Bull (Tokyo)* **56**(12): 1691-1697.

Schwab M (2012). Cancer. Encyclopedia of Cancer (3rd edition). M. Schwab (Eds.). Springer Berlin Heidelberg: pages 461-463.

Shrestha K, Banskota AH, Kodata S, Shrivastava SP, Strobel G, Gewali MB (2001). An antiproliferative norditerpene dilactone, nagilactone C, from *Podocarpus neriifolius*. *Phytomedicine* **8**(6): 489-491.

Silva M, Bittner M, Sammes PG (1973). Diterpenoids of *Podocarpus nubigena*. *Phytochemistry* **12**(4): 883-886.

Simmons TL, Andrianasolo E, McPhail K, Flatt P, Gerwick WH (2005). Marine natural products as anticancer drugs. *Mol Cancer Ther* **4**(2): 333-342.

Singh M, Singh P, Shukla Y (2012). New strategies in cancer chemoprevention by phytochemicals. *Front Biosci (Elite Ed)* **4**: 426-452.

Skalska J, Brookes PS, Nadtochiy SM, Hilchey SP, Jordan CT, Guzman ML, Maggirwar SB, Briehl MM, Bernstein SH (2009). Modulation of cell surface protein free thiols: a potential novel mechanism of action of the sesquiterpene lactone parthenolide. *PLoS ONE* **4**(12): e8115.

Sosa MS, Bragado P, Aguirre-Ghiso JA (2014). Mechanisms of disseminated cancer cell dormancy: an awakening field. *Nat Rev Cancer* **14**(9): 611-622.

Strobl S, Fetene M, Beck E (2011). Analysis of the "shelter tree-effect" of natural and exotic forest canopies on the growth of young *Podocarpus falcatus* trees in southern Ethiopia. *Trees* **25**(5): 769-783.

Sun H-F, Li X-M, Meng L, Cui C-M, Gao S-S, Li C-S, Huang C-G, Wang B-G (2012). Asperolides A-C, tetranorlabdane diterpenoids from the marine alga-derived endophytic fungus *Aspergillus wentii* EN-48. *J Nat Prod* **75**(2): 148-152.

Sung B, Prasad S, Yadav VR, Lavasanifar A, Aggarwal BB (2011). Cancer and diet: how are they related? *Free Radic Res* **45**(8): 864-879.

Tadele D, Fetene M (2013). Growth and ecophysiology of seedlings of *Podocarpus falcatus* in plantations of exotic species and in a natural montane forest in Ethiopia. *J Trop For Sci* **24**(1): 29-35.

Tassone P, Goldmacher VS, Neri P, Gozzini A, Shammas MA, Whiteman KR, Hylander-Gans LL, Carrasco DR, Hideshima T, Shringarpure R, Shi J, Allam CK, Wijdenes J, Venuta S, Munshi NC, Anderson KC (2004). Cytotoxic activity of the maytansinoid immunoconjugate B-B4-DM1 against CD138+ multiple myeloma cells. *Blood* **104**(12): 3688-3696.

Taylor JLS, Rabe T, McGaw LJ, Jäger AK, van Staden J (2001). Towards the scientific validation of traditional medicinal plants. *Plant Growth Regul* **34**(1): 23-37.

Teketay D (2011). Natural regeneration and management of *Podocarpus falcatus* (Thunb.) Mirb. in the Afromontane forests of Ethiopia. Silviculture in the Tropics. S.

Günter, M. Weber, B. Stimm and R. Mosandl (Eds.). Springer Berlin Heidelberg. Volume 8: pages 325-337.

Teklehaymanot T (2009). Ethnobotanical study of knowledge and medicinal plants use by the people in Dek Island in Ethiopia. *J Ethnopharmacol* **124**(1): 69-78.

Torre LA, Bray F, Siegel RL, Ferlay J, Lortet-Tieulent J, Jemal A (2015). Global cancer statistics, 2012. *CA Cancer J Clin* **65**(2): 87-108.

Torrisi JM, Schwartz LH, Gollub MJ, Ginsberg MS, Bosl GJ, Hricak H (2011). CT findings of chemotherapy-induced toxicity: What radiologists need to know about the clinical and radiologic manifestations of chemotherapy toxicity. *Radiology* **258**(1): 41-56.

Ulubelen A, Birman H, Oksuz S, Topcu G, Kolak U, Barla A, Voelter W (2002). Cardioactive diterpenes from the roots of *Salvia eriophora*. *Planta Med* **68**(9): 818-821.

Umar A, Dunn BK, Greenwald P (2012). Future directions in cancer prevention. *Nat Rev Cancer* **12**(12): 835-848.

Vanneman M, Dranoff G (2012). Combining immunotherapy and targeted therapies in cancer treatment. *Nat Rev Cancer* **12**(4): 237-251.

Verma S, Miles D, Gianni L, Krop IE, Welslau M, Baselga J, Pegram M, Oh DY, Dieras V, Guardino E, Fang L, Lu MW, Olsen S, Blackwell K (2012). Trastuzumab emtansine for HER2-positive advanced breast cancer. *N Engl J Med* **367**(19): 1783-1791.

Vokac K, Budesinsky M, Harmatha J, Kohoutova J (1998). Plant substances. 58. Ecdysteroid constituents of the mushroom *Tapinella panuoides*. *Phytochemistry* **49**(7): 2109-2114.

Wang H, Khor TO, Shu L, Su ZY, Fuentes F, Lee JH, Kong AN (2012). Plants *vs*. cancer: a review on natural phytochemicals in preventing and treating cancers and their druggability. *Anticancer Agents Med Chem* **12**(10): 1281-1305.

Wang YY, Yang YX, Zhe H, He ZX, Zhou SF (2014). Bardoxolone methyl (CDDO-Me) as a therapeutic agent: an update on its pharmacokinetic and pharmacodynamic properties. *Drug Des Devel Ther* **8**: 2075-2088.

Wani MC, Horwitz SB (2014). Nature as a remarkable chemist: a personal story of the discovery and development of taxol. *Anti-Cancer Drugs* **25**(5): 482-487.

WHO (2015). Cancer. Fact sheet No. 297. Retrieved June 4, 2015, from http://www.who.int/mediacentre/factsheets/fs297/en/.

Woldeamanuel YW, Girma B, Teklu AM (2013). Cancer in Ethiopia. *Lancet Oncol* **14**(4): 289-290.

Wolff R, Pédrono F, Marpeau A, Gunstone F (1999). The seed fatty acid composition and the distribution of Δ5-olefinic acids in the triacylglycerols of some taxares (*Cephalotaxus* and *Podocarpus*). *J Am Oil Chem Soc* **76**(4): 469-473.

Wondimu T, Asfaw Z, Kelbessa E (2007). Ethnobotanical study of medicinal plants around 'Dheeraa' town, Arsi Zone, Ethiopia. *J Ethnopharmacol* 112(1): 152-161.

Wu CP, Ohnuma S, Ambudkar SV (2011). Discovering natural product modulators to overcome multidrug resistance in cancer chemotherapy. *Curr Pharm Biotechnol* **12**(4): 609-620.

Yeh P-H, Shieh Y-D, Hsu L-C, Kuo L-MY, Lin J-H, Liaw C-C, Kuo Y-H (2012). Naturally occurring cytotoxic [3′→8″]-biflavonoids from *Podocarpus nakaii*. *J Tradit Complement Med* **2**(3): 220-226.

Yineger H, Yewhalaw D, Teketay D (2008). Ethnomedicinal plant knowledge and practice of the Oromo ethnic group in southwestern Ethiopia. *J Ethnobiol Ethnomed* **4**: 11-11.

Ying B-P, Kubo I (1991). Complete ^{1}H and ^{13}C NMR assignments of totarol and its derivatives. *Phytochemistry* **30**(6): 1951-1955.

Ying BP, Kubo I, Chairul, Matsumoto T, Hayashi Y (1990). Congeners of norditerpene dilactones from *Podocarpus nagi*. *Phytochemistry* **29**(12): 3953-3955.

Yokota J (2000). Tumor progression and metastasis. *Carcinogenesis* **21**(3): 497-503.

Zhang C, Cao S, Toole BP, Xu Y (2015). Cancer may be a pathway to cell survival under persistent hypoxia and elevated ROS: a model for solid-cancer initiation and early development. *Int J Cancer* **136**(9): 2001-2011.

Zhang L-C, Wu X-D, He J, Li Y, Zhang R-P, Zhao Q-S (2013). Three new abietane diterpenoids from *Podocarpus fleuryi*. *Phytochem Lett* **6**(3): 364-367.

Zhang M, Ying B-P, Kubo I (1992). Nagilactones from *Podocarpus nagi* and their effects on the feeding and growth of tobacco budworm. *J Nat Prod* **55**(8): 1057-1062.

Zhang S, Won Y-K, Ong C-N, Shen H-M (2005). Anti-cancer potential of sesquiterpene lactones: Bioactivity and molecular mechanisms. *Curr Med Chem Anticancer Agents* **5**(3): 239-249.

Zhang Y, Tang C, Sob SVT, Ke C, Ye Y (2012). Two new cyclopeptides from *Podocarpus nagi*. *Chin J Chem* **30**(6): 1361-1364.

Appendices

Appendix I: Summary of physical and spectral data of isolated compounds

16-Hydroxynagilactone F (PF-1): fine colorless needles; $[\alpha]_D^{20}$ −78 (*c* 0.1, MeOH); IR (KBr) ν_{max} 3388 (OH), 1762 (*γ*-lactone), 1701 (*δ*- lactone), 1597 (conjugated C=C) cm^{-1}; UV (MeOH) λ_{max} (log *ε*) 259 (3.7); ^{1}H and ^{13}C NMR data, see Table 4 and Table 5 and Appendix II; HRESIMS $[M + Na]^+$ *m/z* 355.1500 (calcd for $C_{19}H_{24}O_5Na^+$, 355.1516) (Appendix II).

2*β*,16-Dihydroxynagilactone F (PF-3): fine colorless needles; $[\alpha]_D^{20}$ −75 (*c* 0.2, MeOH); IR (KBr) ν_{max} 3390 (OH), 1764 (*γ*-lactone), 1698 (*δ*-lactone), 1600 (conjugated C=C) cm^{-1}; UV (MeOH) λ_{max} (log *ε*) 261 (4.06); ^{1}H and ^{13}C NMR data, see Table 4 and Table 5 and Appendix III; HRESIMS $[M + Na]^+$ *m/z* 371.1460 (calcd for $C_{19}H_{24}O_6Na^+$, 371.1465) (Appendix III).

7*β*-Hydroxymacrophyllic acid (PF-2): white, amorphous solid; $[\alpha]_D^{20}$ +66.9 (*c* 0.2, MeOH); IR (KBr) ν_{max} 3533, 3359−2400 (broad), 2958, 2932, 2872, 1694, 1467, 1453, 1259, 1175 cm^{-1}; UV λ_{max} (MeOH) (log *ε*) 217 (4.45), 251 (3.96), 291 (3.67) nm; ^{1}H and ^{13}C NMR data, see Table 5 and Table 5 and Appendix IV; HRESIMS $[M + Na]^+$ *m/z* 685.3727 (calcd for $C_{40}H_{54}O_8Na^+$, 685.3711) (Appendix IV).

Inumakiol D (28): whitish, amorphous solid; $[\alpha]_D^{20}$, IR and UV: *Not done do you to small amount that was submitted for bioassay*; ^{1}H and ^{13}C NMR data, see Table 6 and Table 7 and Appendix V; HRESIMS $[M + Na]^+$ *m/z* 355.1880 (calcd for $C_{20}H_{28}O_4Na^+$,355.1880) (Appendex V).

Macrophyllic acid (37): yellowish, amorphous solid; $[\alpha]_D^{20}$ +85 (*c* 0.1, MeOH); IR (KBr) ν_{max} 3527, 3350−2400 (broad), 2956, 2929, 2872, 2852, 1693, 1467, 1449, 1251, 1181 cm^{-1}; UV λ_{max} (MeOH) (log ε) 215 (4.47), 251 (3.93), 287 (3.68) nm; ^1H and ^{13}C NMR data, see Table 6 and Table 7 and Appendix VI; HRESIMS $[M + Na]^+$ *m/z* 653.3832 (calcd for $C_{40}H_{55}O_6Na^+$, 653.3813) (Appendix VI).

Nagilactone D (41): colorless crystals; $[\alpha]_D^{20}$ +12 (*c* 0.1, MeOH); IR (KBr) ν_{max} 3502 (OH), 1766 (γ-lactone), 1716 (δ-lactone), 1636 (conjugated C=C) cm^{-1}; UV (MeOH) λ_{max} (log ε) 302 (3.8); ^1H and ^{13}C NMR data, see Table 6 and Table 7 and Appendix VII; HRESIMS $[M + Na]^+$ *m/z* 355.1162 (calcd for $C_{18}H_{21}O_6Na^+$, 355.1152) (Appendix VII).

Ponasterone A (94): White, fine colorless needles; $[\alpha]_D^{20}$ +51 (*c* 0.1, MeOH); IR (KBr) ν_{max} 3554, 3293 (OH); 1638 (C=O); 1049 (C–O) cm^{-1}; UV (MeOH) λ_{max} (log ε) 242 (4); ^1H and ^{13}C NMR data, see Page 50 for summarized data and Appendix IX; HRESIMS $[M + Na]^+$ *m/z* 487.3037 (calcd for $C_{27}H_{44}O_6Na^+$, 487.3030) (Appendix IX).

2*β*-Hydroxynagilactone F (108): colorless crystals; $[\alpha]_D^{20}$ −38 (*c* 0.1, MeOH); IR (KBr) ν_{max} 3446 (OH), 1769 (γ-lactone), 1711 (δ- lactone), 1601 (conjugated C=C) cm^{-1}; UV (MeOH) λ_{max} (log ε) 259 (4.4); ^1H and ^{13}C NMR data, see Table 2 and Table 3 and Appendix VIII; HRESIMS $[M + Na]^+$ *m/z* 355.1512 (calcd for $C_{19}H_{24}O_5Na^+$, 355.1516) (Appendix VIII).

Nagilactone I (109): colorless crystals; $[\alpha]_D^{20}$ −64 (*c* 0.1, MeOH); IR (KBr) ν_{max} 3438 (OH), 1766 (γ-lactone), 1732 (ester carbonyl), 1709 (δ- lactone), 1600 (conjugated C=C) cm^{-1}; UV (MeOH) λ_{max} (log ε) 260 (3.9); ^1H and ^{13}C NMR data, see Table 2 and Table 3

and Appendix X; HRESIMS $[M + Na]^+$ *m/z* 399.1414 (calcd for $C_{20}H_{25}O_7Na^+$, 399.1404) (Appenedix X).

15-Hydroxynagilactone D (110): fine colorless needles; $[\alpha]_D^{20}$ +38 (*c* 0.1, MeOH); IR (KBr) ν_{max} 3399 (OH), 1763 (γ-lactone), 1712 (δ-lactone), 1634 (conjugated C=C) cm^{-1}; UV (MeOH) λ_{max} (log ε) 299 (4.1); ^1H and ^{13}C NMR data, see Table 4 and Table 5 and Appendix XI; HRESIMS $[M + Na]^+$ *m/z* 371.1105 (calcd for $C_{18}H_{21}O_7Na^+$, 371.1101) (Appendix XI).

Appendix II: ^{1}H and ^{13}C NMR, ^{1}H-^{1}H COSY, HSQC, HMBC, 2D-NOESY, UV, IR and HRESIMS of 16-hydroxynagilactone F (PF-1)

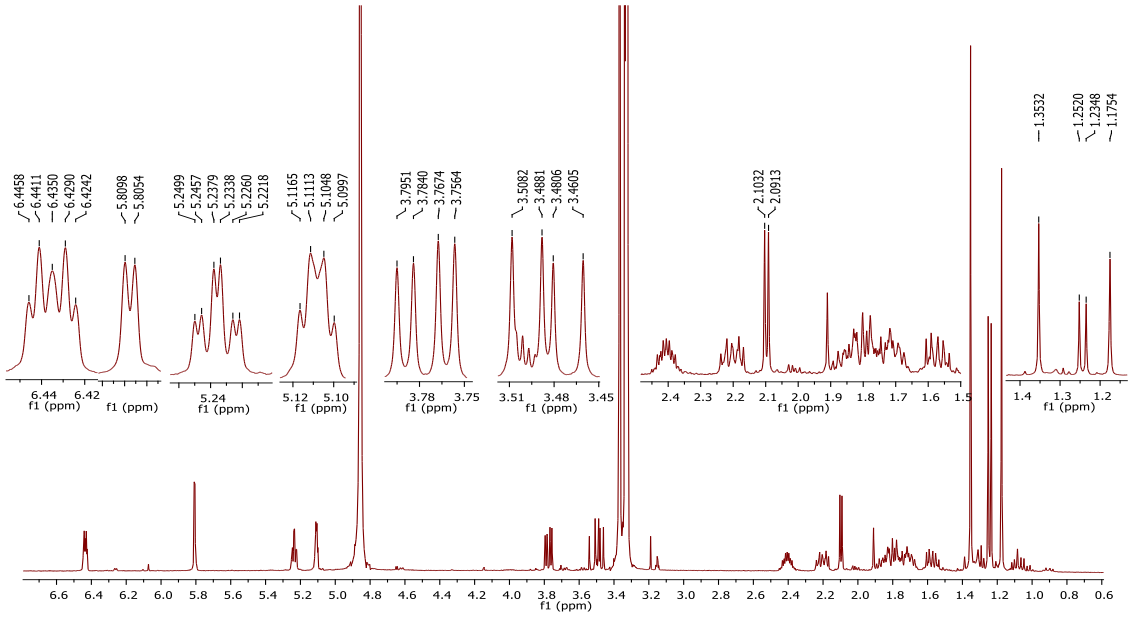

Figure 19. ^{1}H NMR spectrum of 16-hydroxynagilactone F (PF-1) (CD_3OD, 400 MHz)

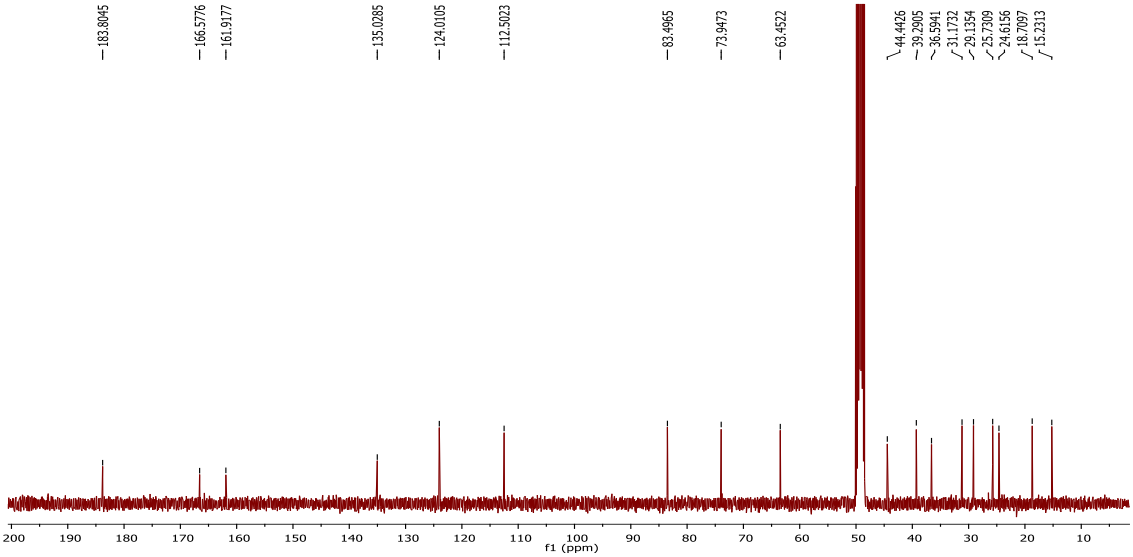

Figure 20. ^{13}C NMR spectrum of 16-hydroxynagilactone F (PF-1) (CD_3OD, 100 MHz)

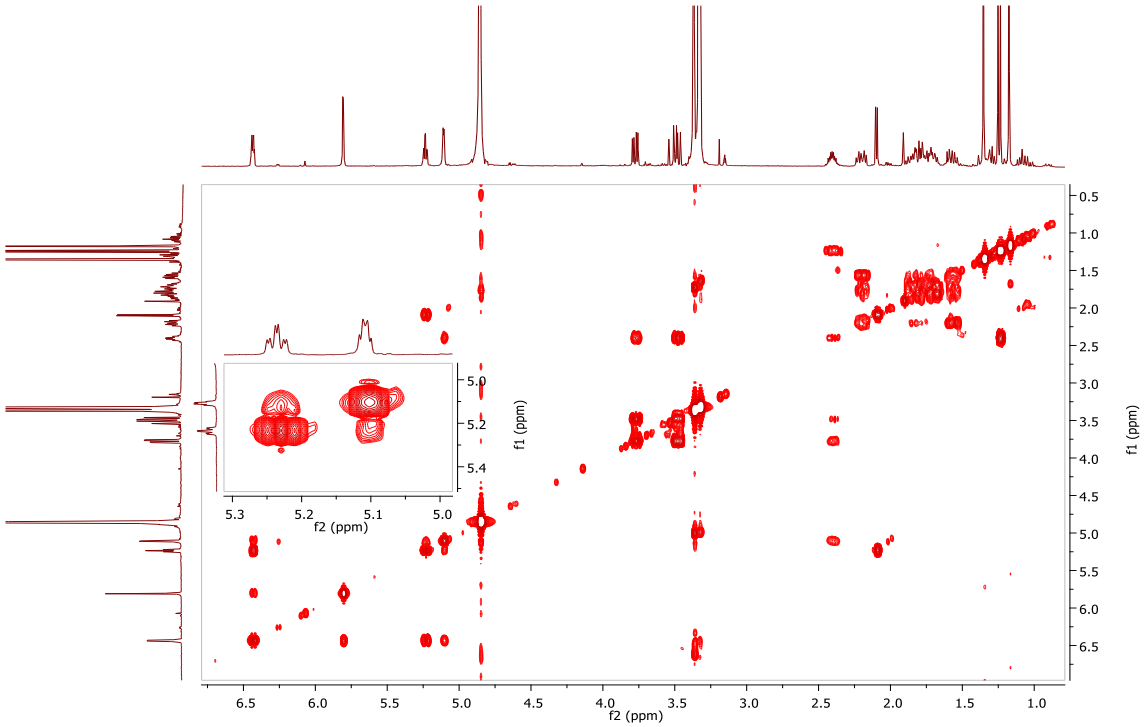

Figure 21. ^{1}H-^{1}H COSY spectrum of 16-hydroxynagilactone F (PF-1) (CD_3OD, 400 MHz)

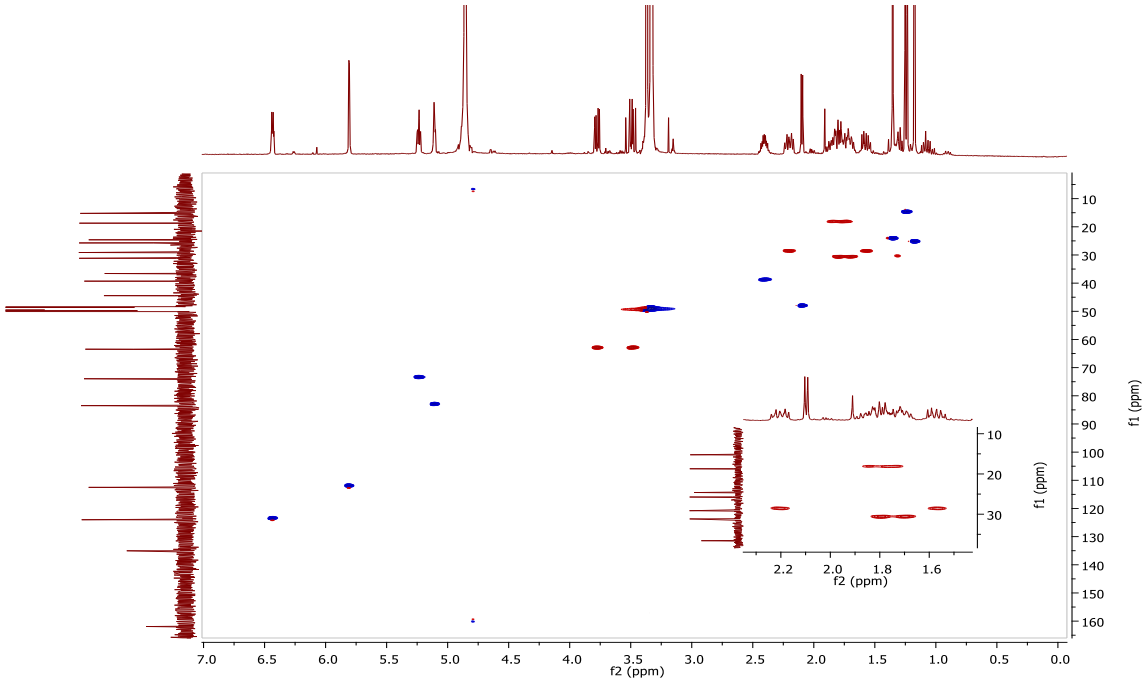

Figure 22. HSQC spectrum of 16-hydroxynagilactone F (PF-1) (CD_3OD, 400 MHz)

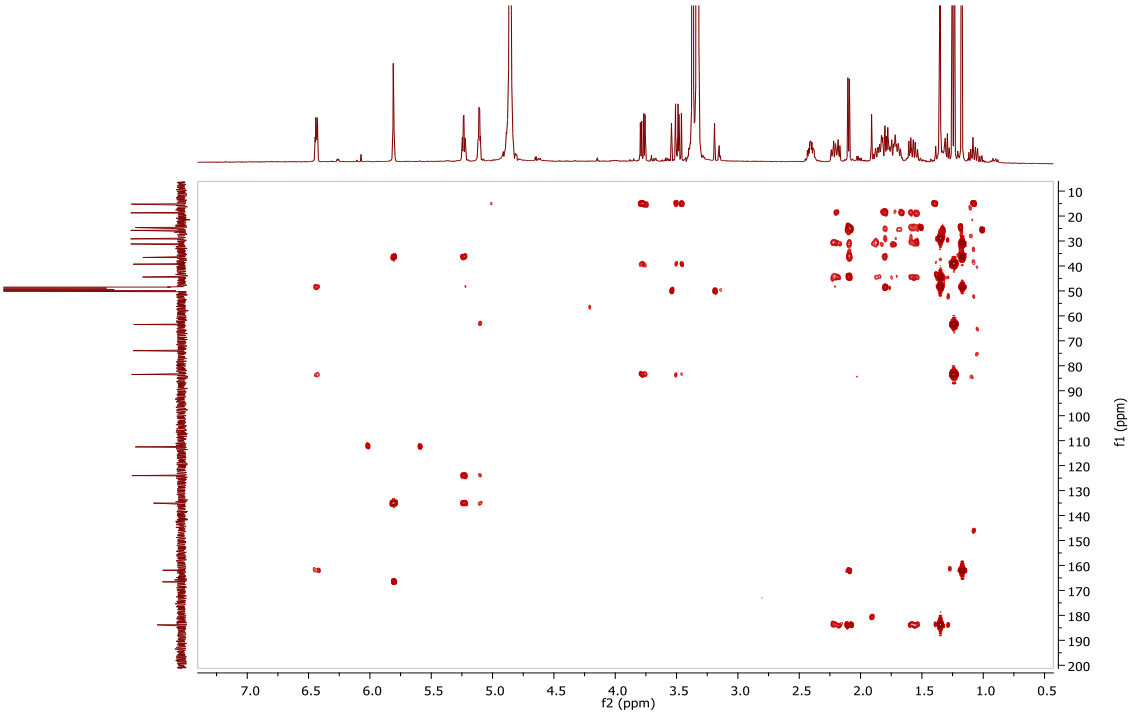

Figure 23. HMBC spectrum of 16-hydroxynagilactone F (PF-1) (CD_3OD, 400 MHz)

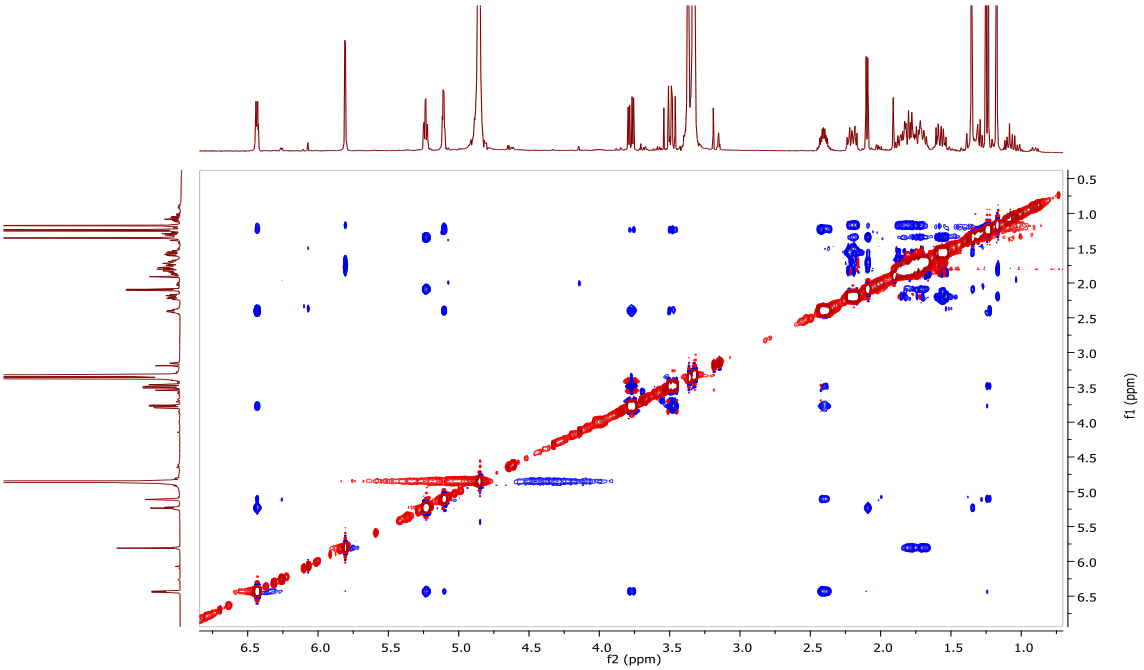

Figure 24. 2D-NOESY spectrum of 16-hydroxynagilactone F (PF-1) (CD_3OD, 400 MHz)

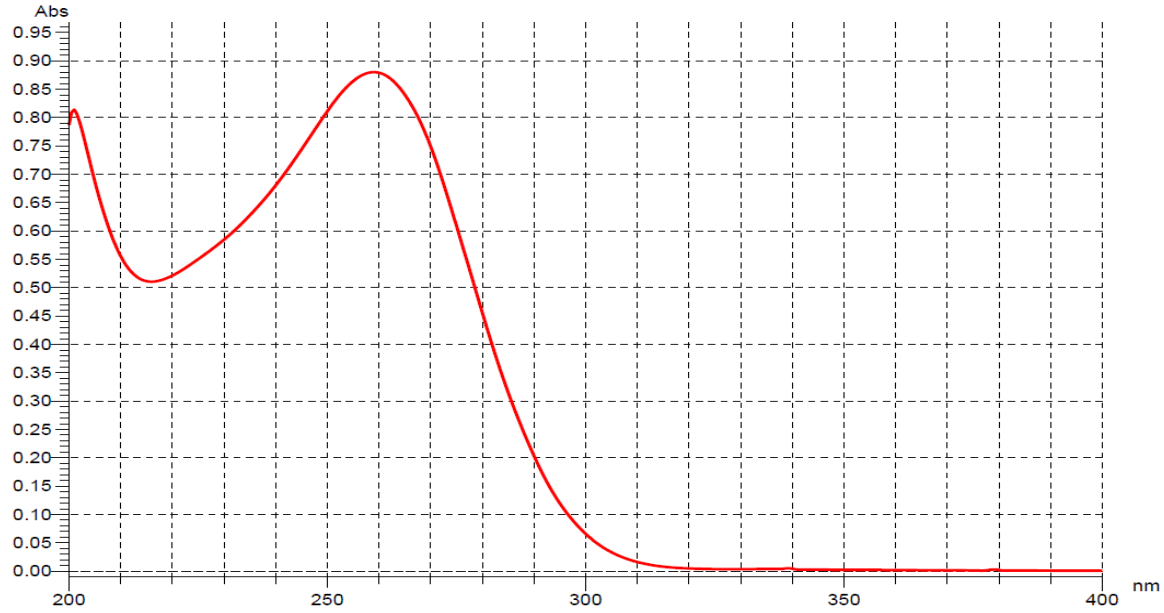

Figure 25. UV spectrum of 16-hydroxynagilactone F (PF-1)

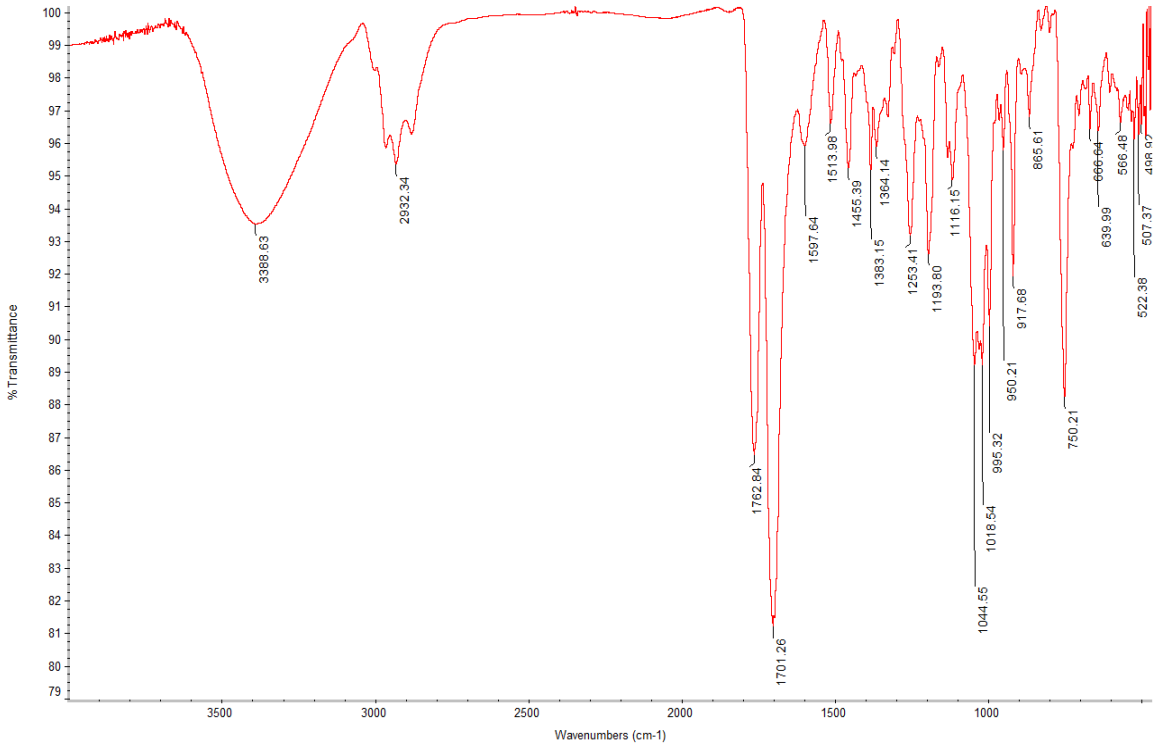

Figure 26. IR spectrum of 16-hydroxynagilactone F (PF-1) (KBr)

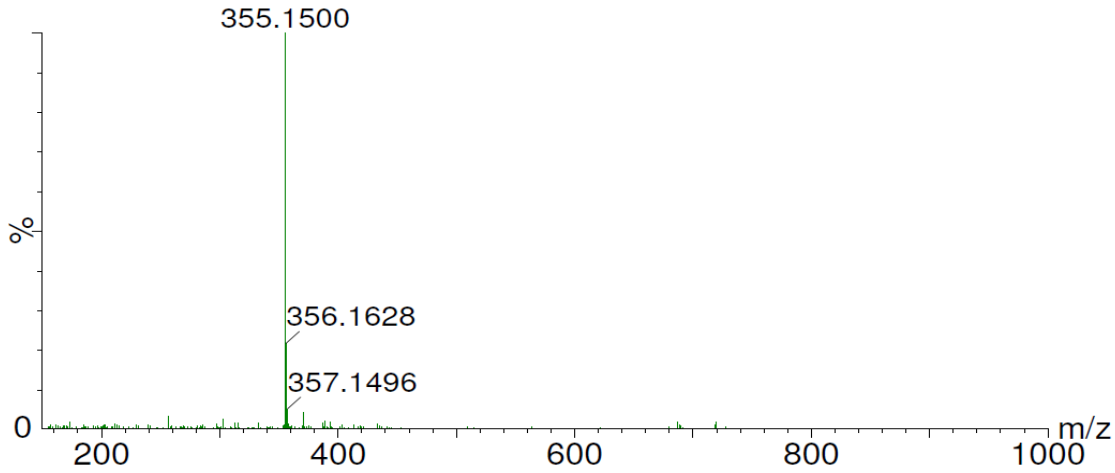

Figure 27. HRESIMS of 16-hydroxynagilactone F (PF-1)

Appendix III: ^{1}H and ^{13}C NMR, ^{1}H-^{1}H COSY, HSQC, HMBC, 2D-NOESY, UV, IR and HRESIMS of 2*β*,16-dihydroxynagilactone F (PF-3)

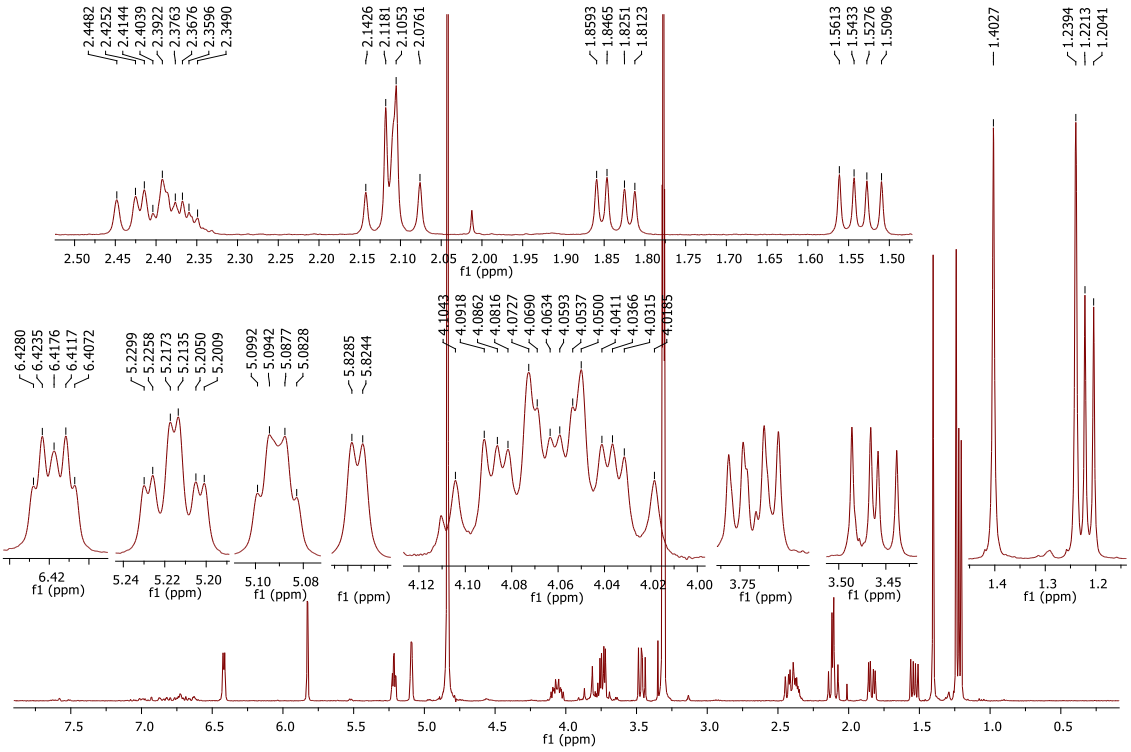

Figure 28. ^{1}H NMR spectrum of 2*β*,16-dihydroxynagilactone F (PF-3) (CD_3OD, 400 MHz)

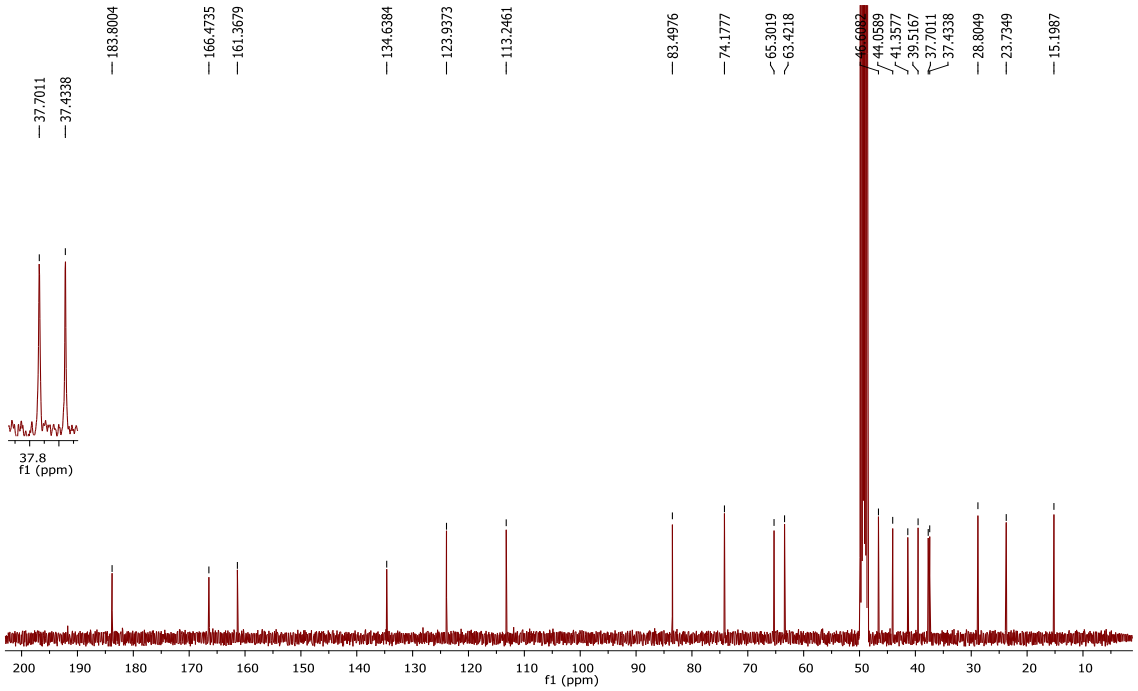

Figure 29. ^{13}C NMR spectrum of 2*β*,16-dihydroxynagilactone F (PF-3) (CD_3OD, 100 MHz)

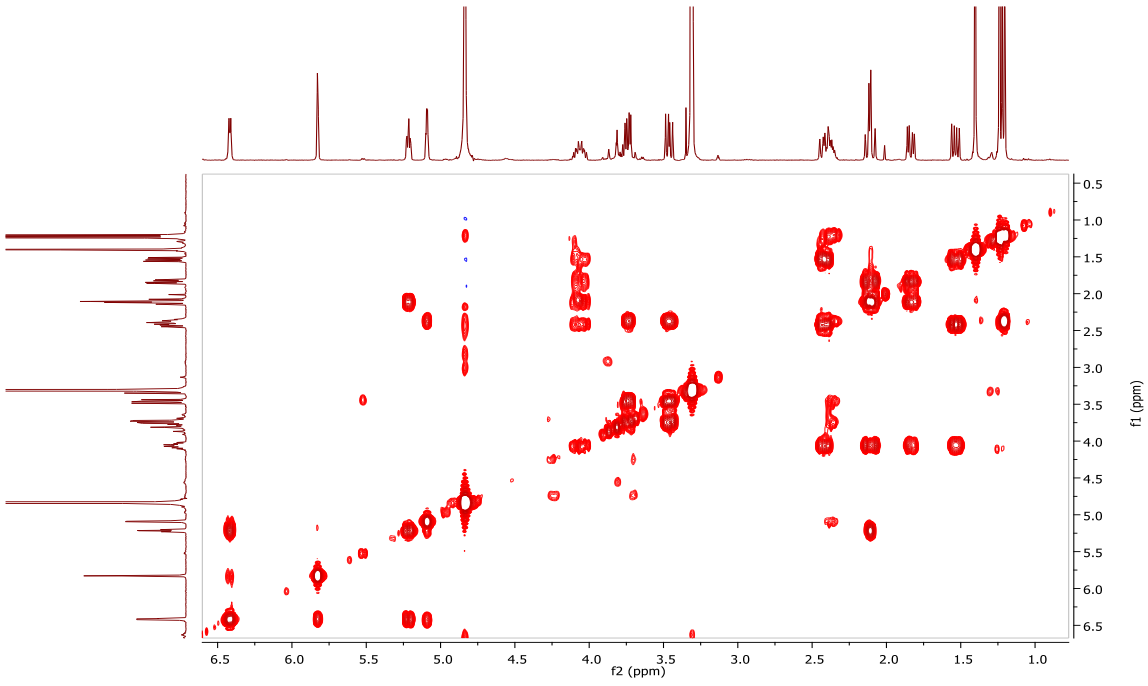

Figure 30. ^{1}H-^{1}H COSY spectrum of 2*β*,16-dihydroxynagilactone F (PF-3) (CD_3OD, 400 MHz)

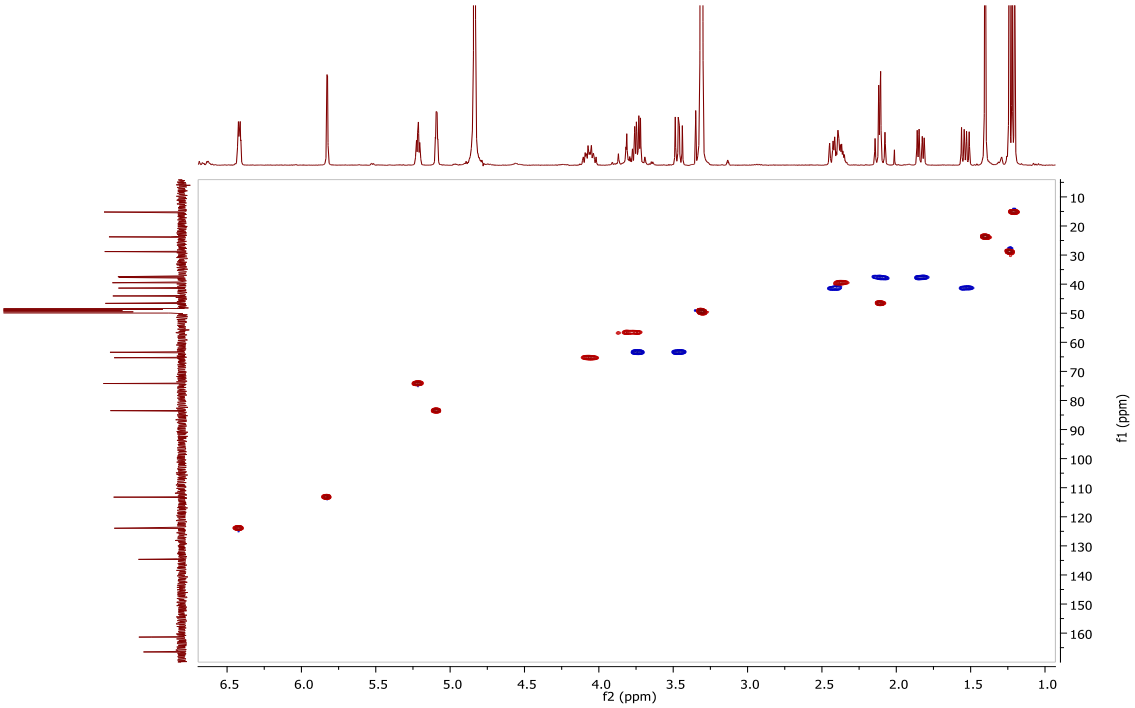

Figure 31. HSQC spectrum of 2*β*,16-dihydroxynagilactone F (PF-3) (CD_3OD, 400 MHz)

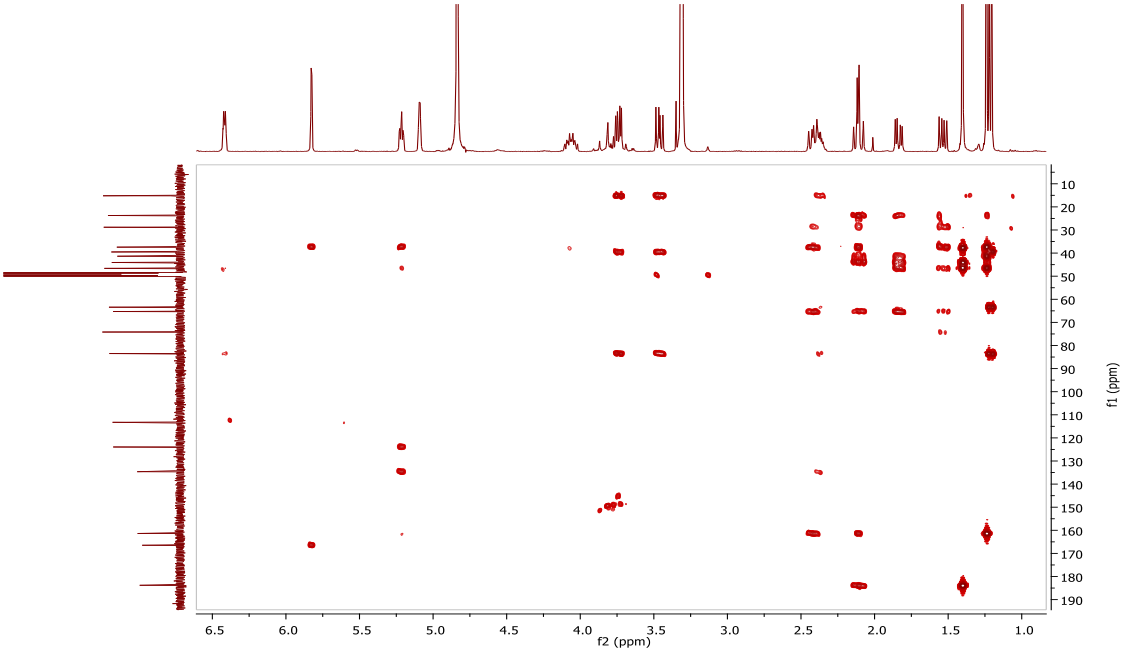

Figure 32. HMBC spectrum of 2*β*,16-dihydroxynagilactone F (PF-3) (CD_3OD, 400 MHz)

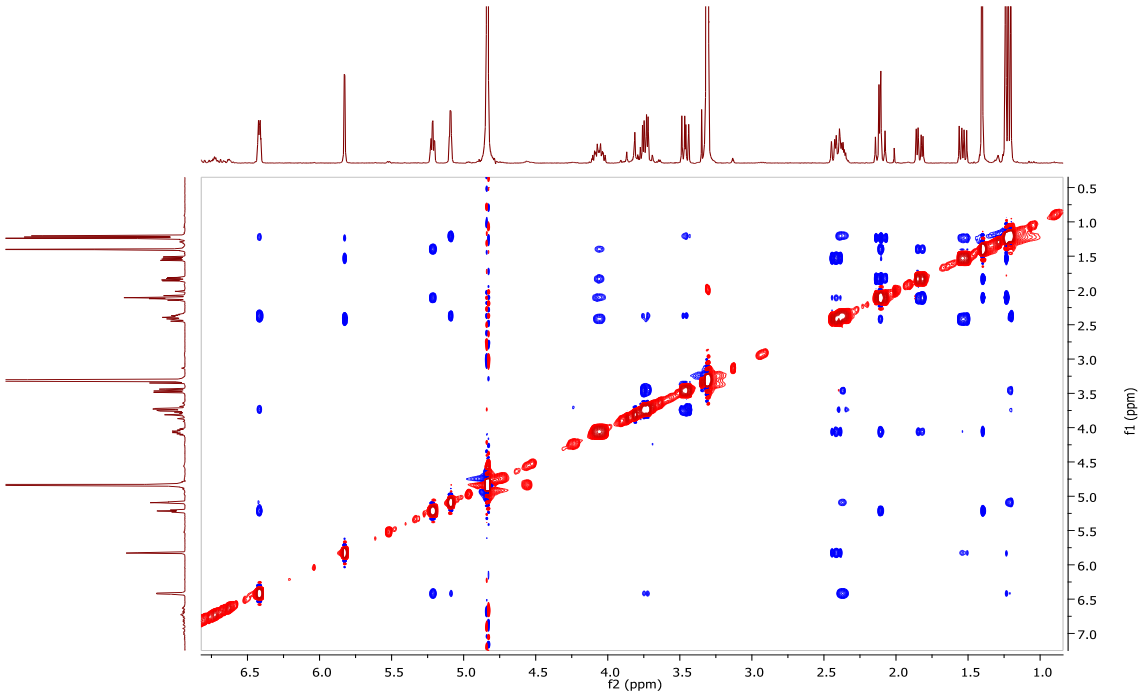

Figure 33. 2D-NOESY spectrum of 2*β*,16-dihydroxynagilactone F (PF-3) (CD_3OD, 400 MHz)

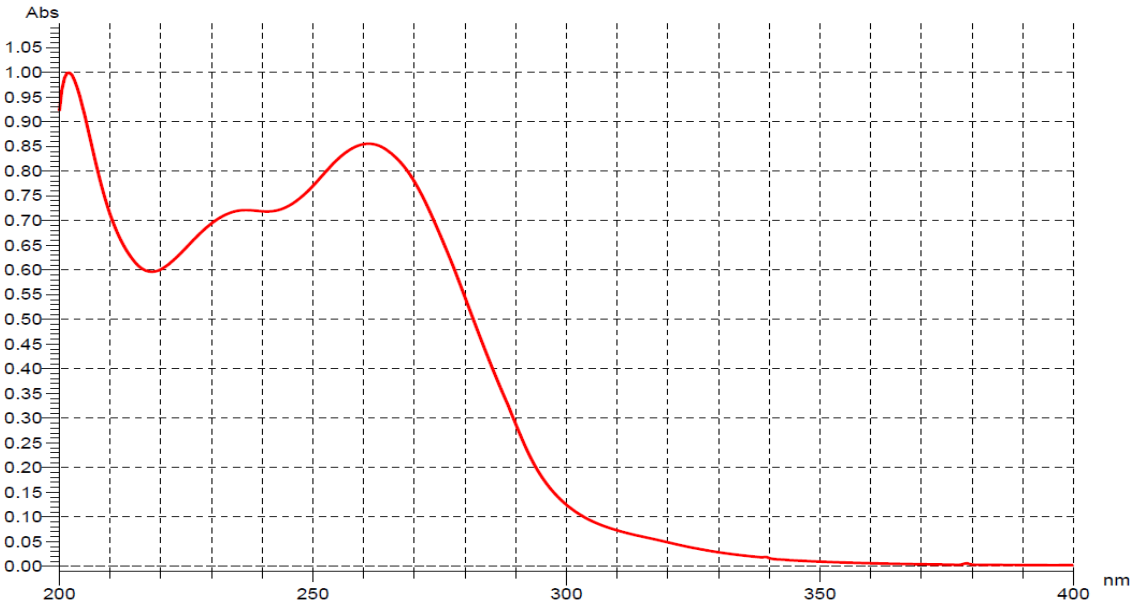

Figure 34. UV spectrum of 2*β*,16-dihydroxynagilactone F (PF-3)

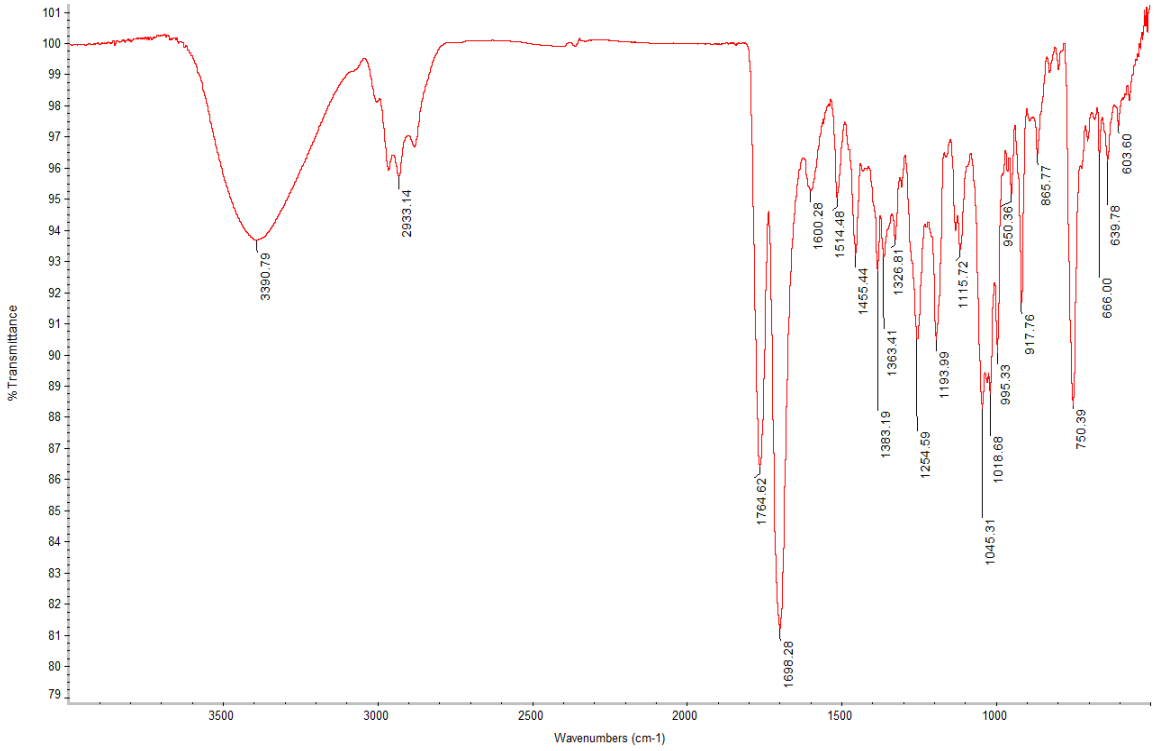

Figure 35. IR spectrum of 2*β*,16-dihydroxynagilactone F (PF-3) (KBr)

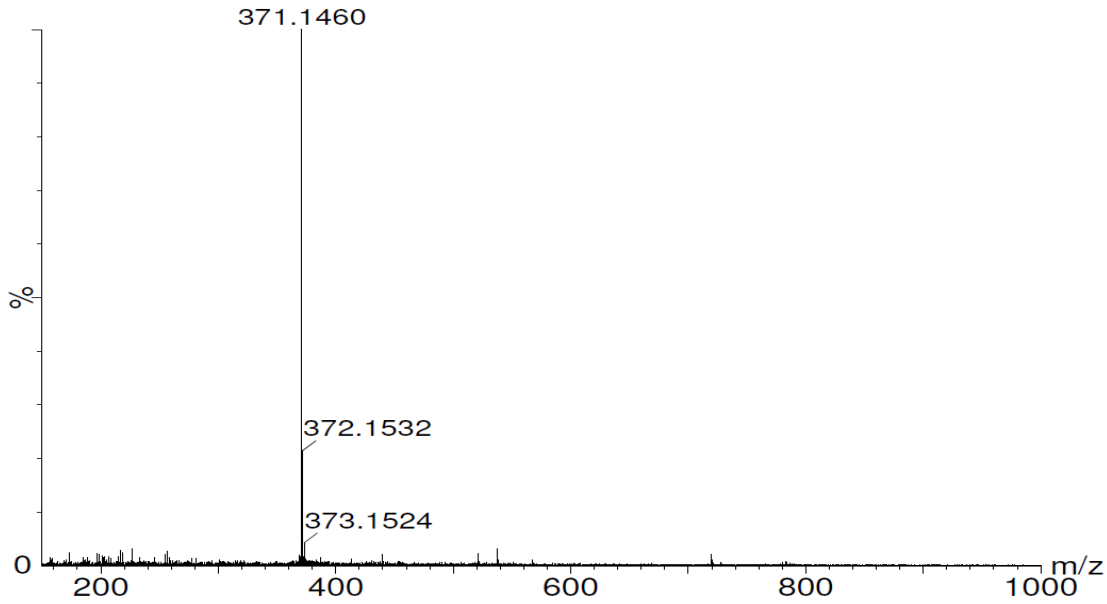

Figure 36. HRESIMS of 2*β*,16-dihydroxynagilactone F (PF-3)

Appendix IV: ^{1}H and ^{13}C NMR, ^{1}H-^{1}H COSY, HSQC, HMBC, 2D-NOESY, UV, IR and HRESIMS of 7*β*-hydroxymacrophyllic acid (PF-2)

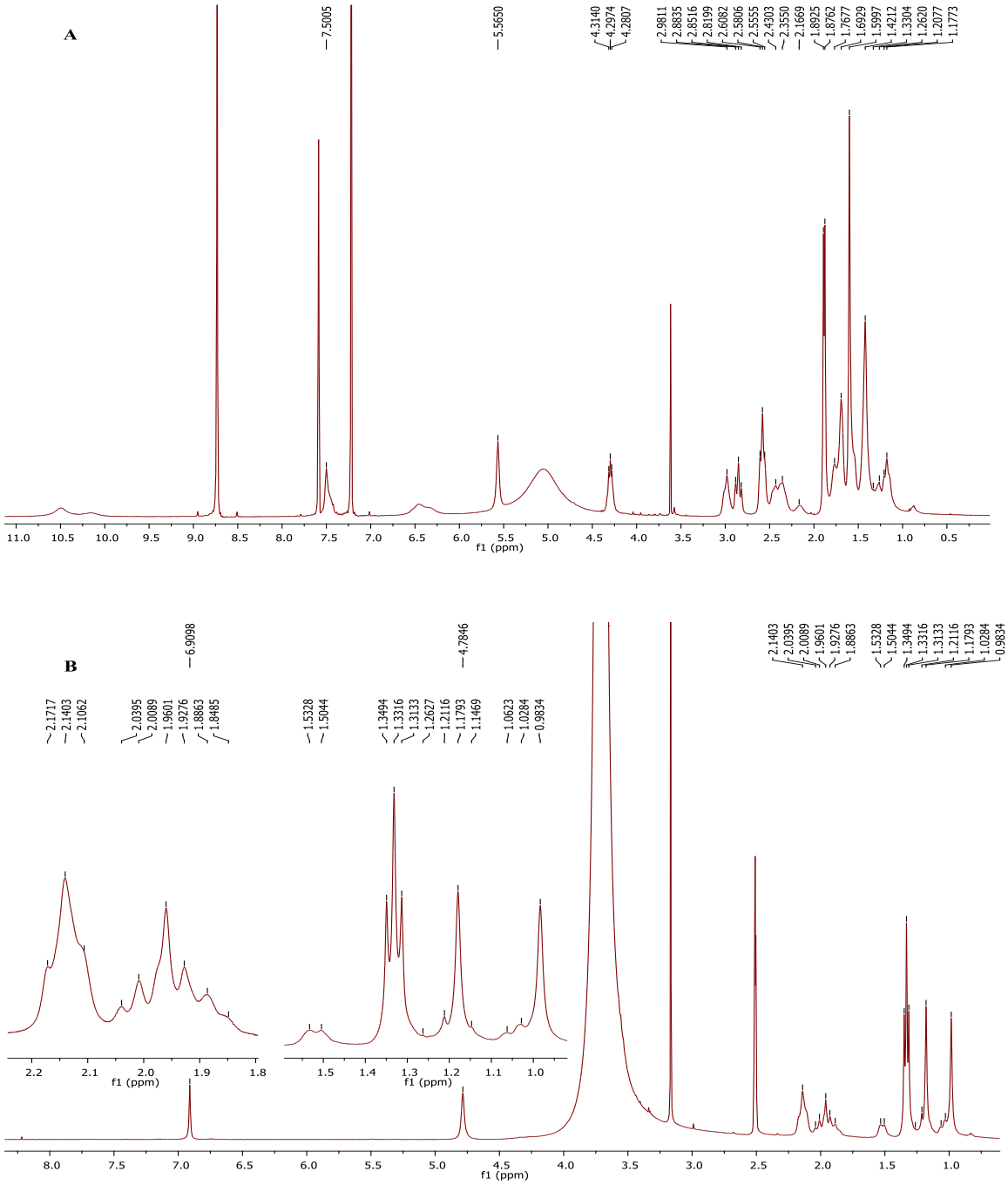

Figure 37. ^{1}H NMR spectrum of 7*β*-hydroxymacrophyllic acid (PF-2) (A. Pyridine-d_5, B. DMSO-d_6, 400 MHz)

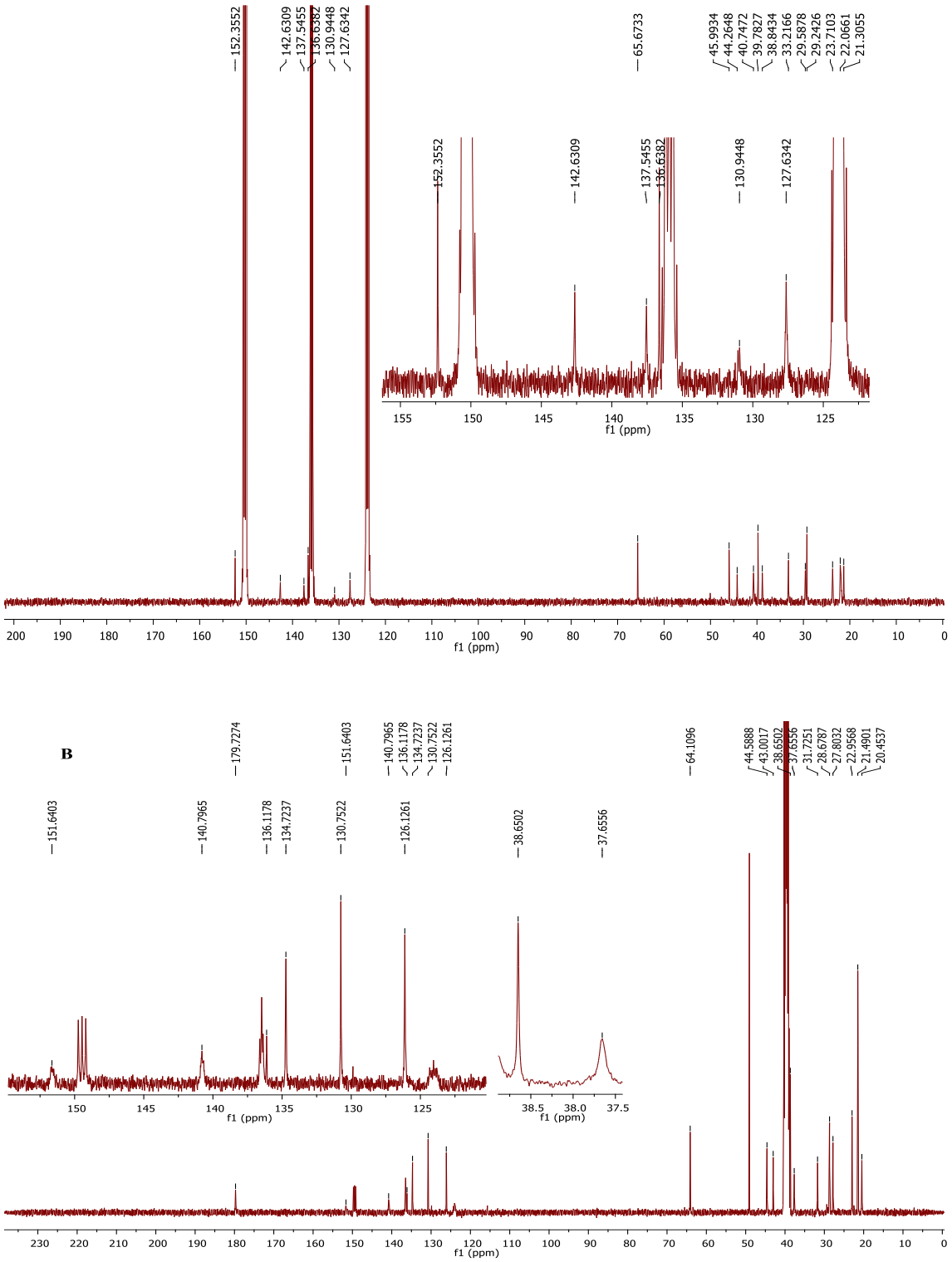

Figure 38. ^{13}C NMR spectrum of 7*β*-hydroxymacrophyllic acid (PF-2) (A. Pyridine-*d*$_5$, B. DMSO-*d*$_6$, 100 MHz)

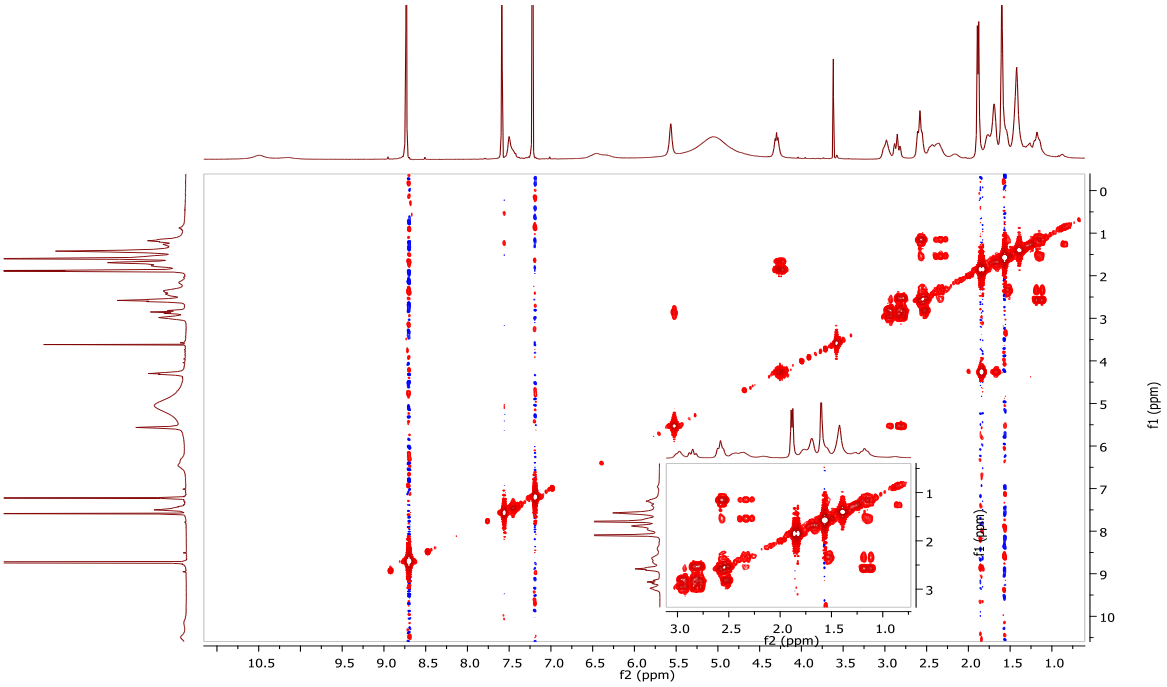

Figure 39. ^{1}H-^{1}H COSY spectrum of 7*β*-hydroxymacrophyllic acid (PF-2) (Pyridine-*d*$_5$, 400 MHz)

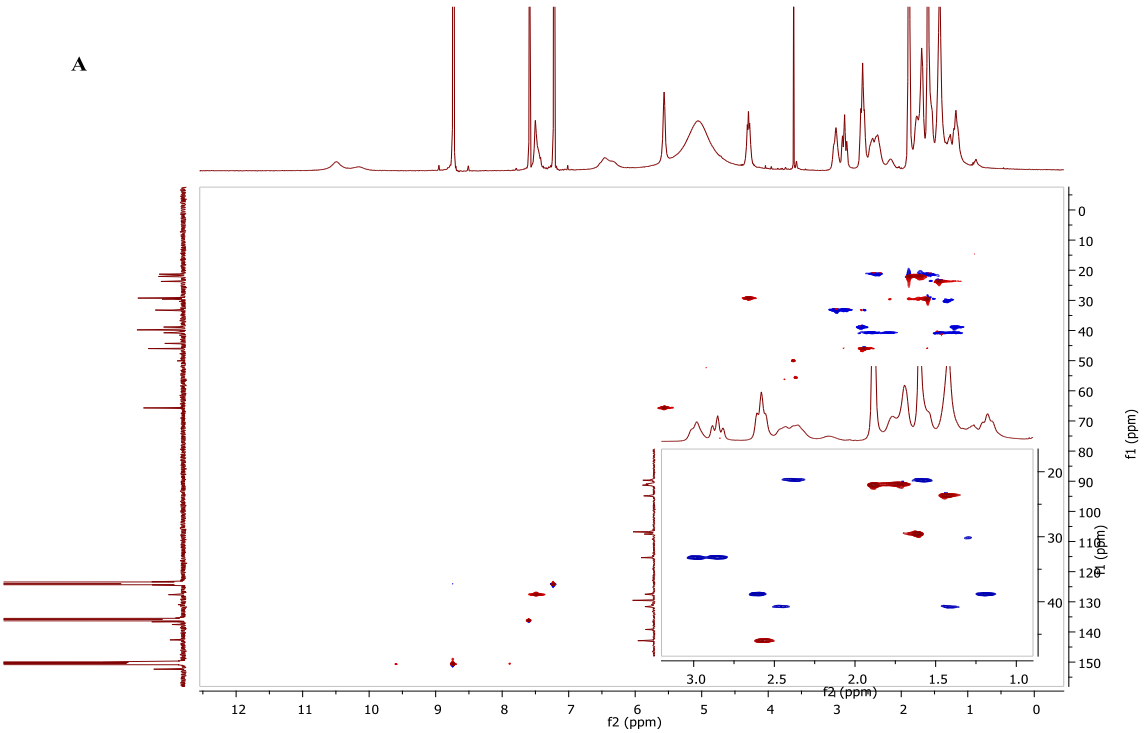

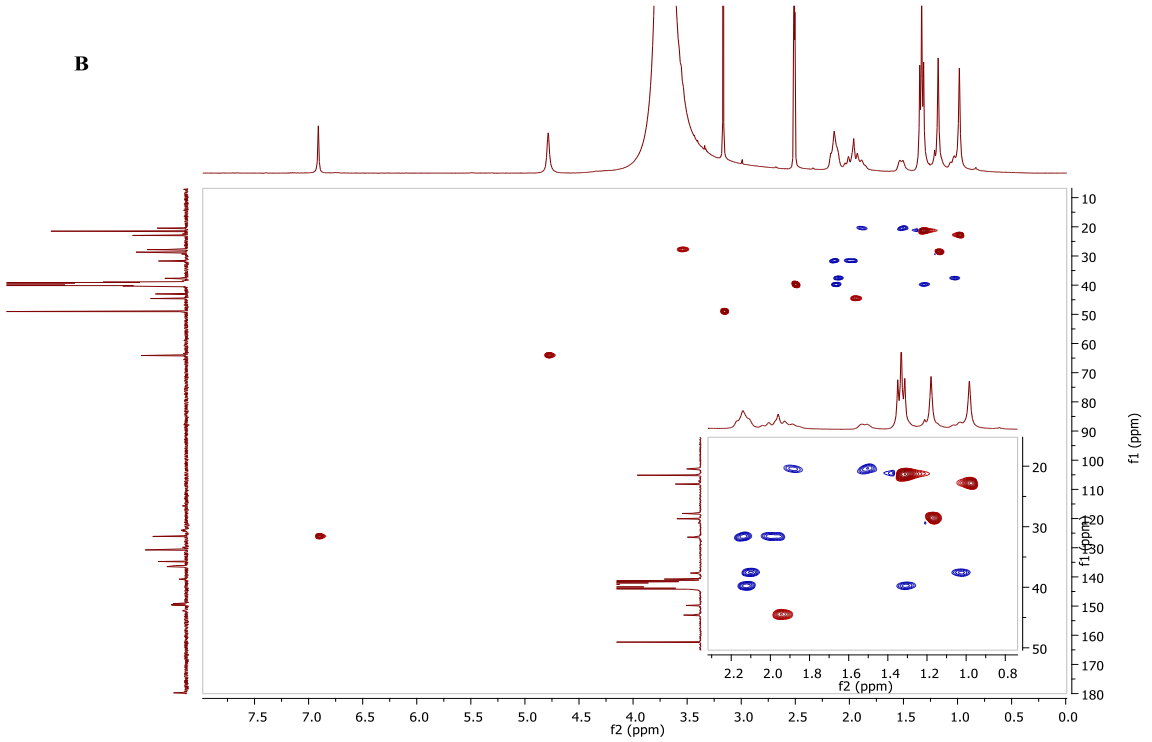

Figure 40. HSQC spectrum of 7*β*-hydroxymacrophyllic acid (PF-2) (A. Pyridine-d_5, B. DMSO-d_6, 400 MHz)

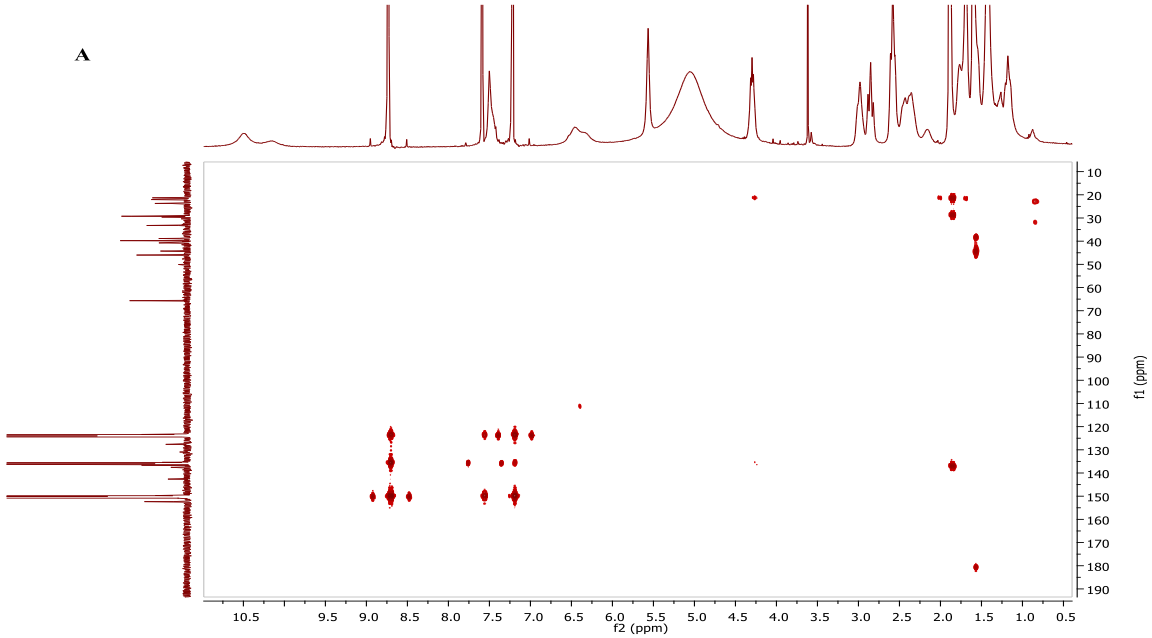

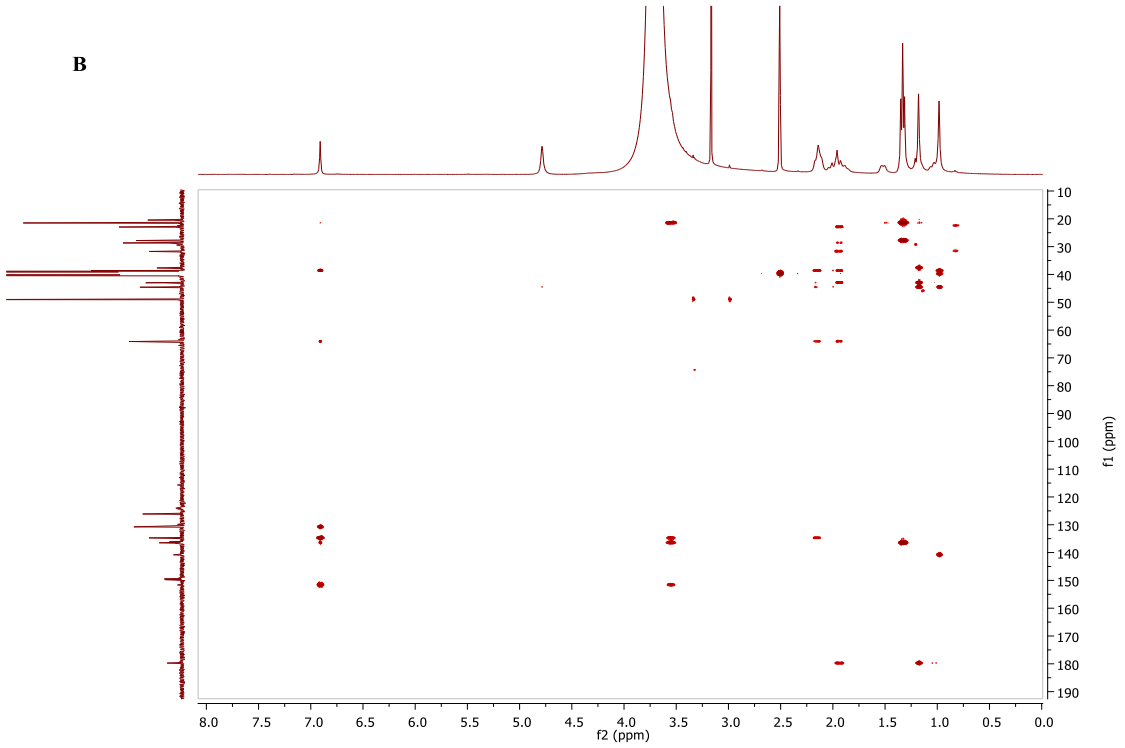

Figure 41. HMBC spectrum of 7*β*-hydroxymacrophyllic acid (PF-2) (A. Pyridine-d_5, B. DMSO-d_6, 400 MHz)

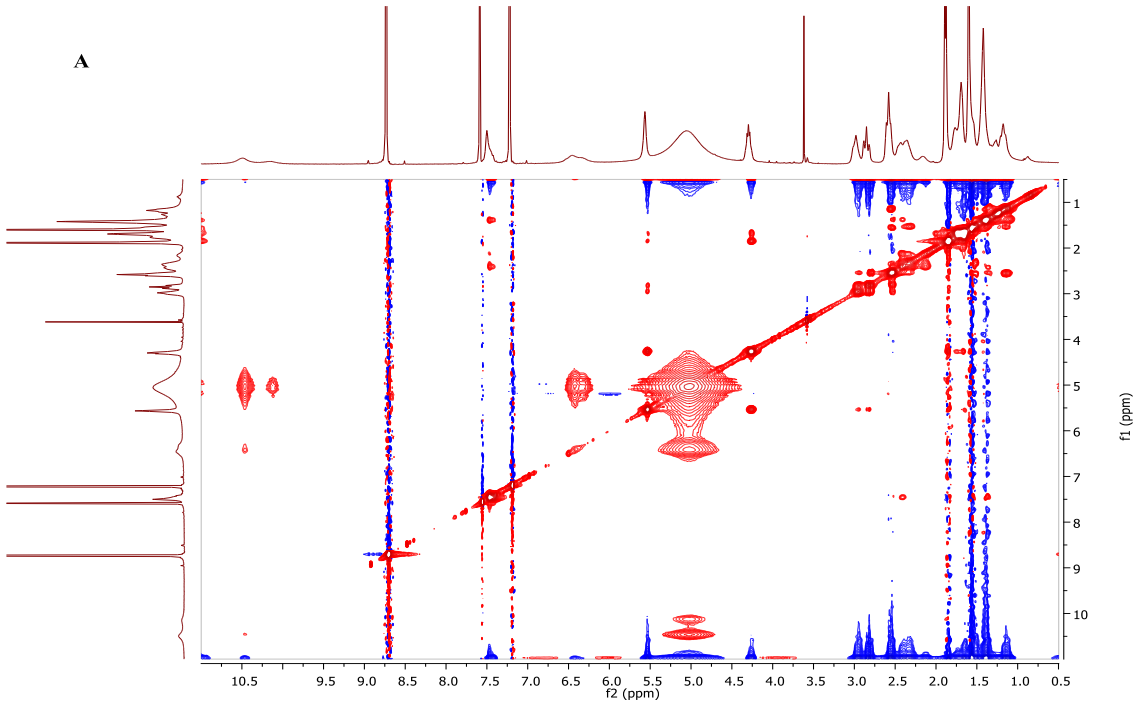

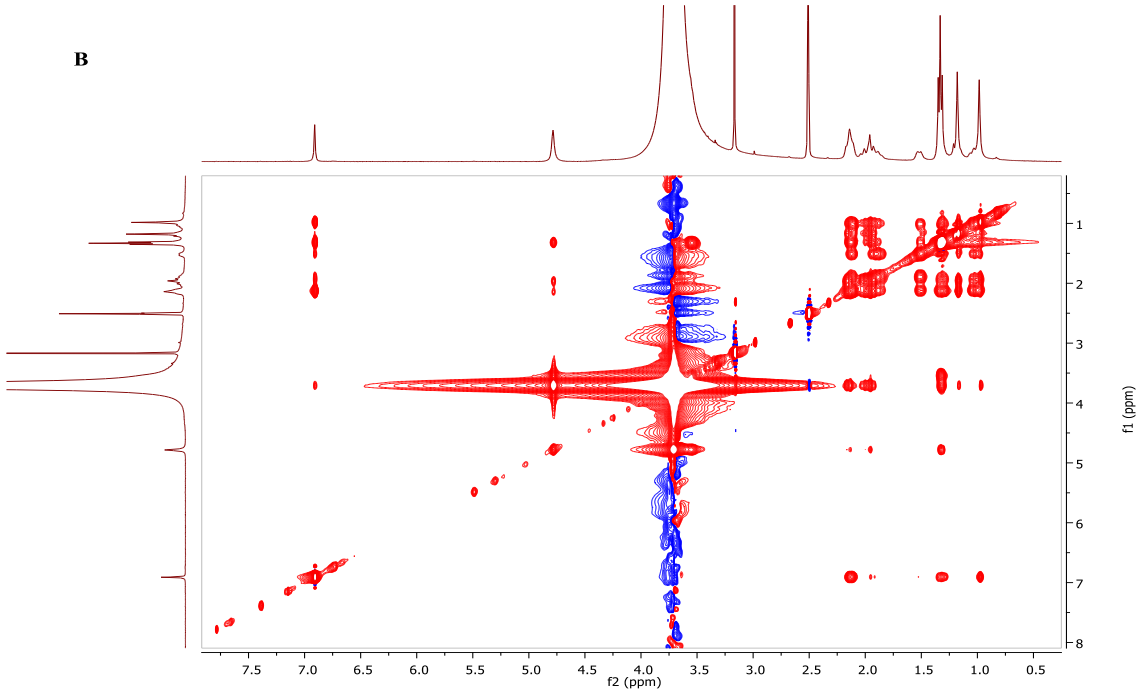

Figure 42. 2D-NOESY spectrum of 7*β*-hydroxymacrophyllic acid (PF-2) (A. Pyridine-d_5, B. DMSO-d_6, 400 MHz)

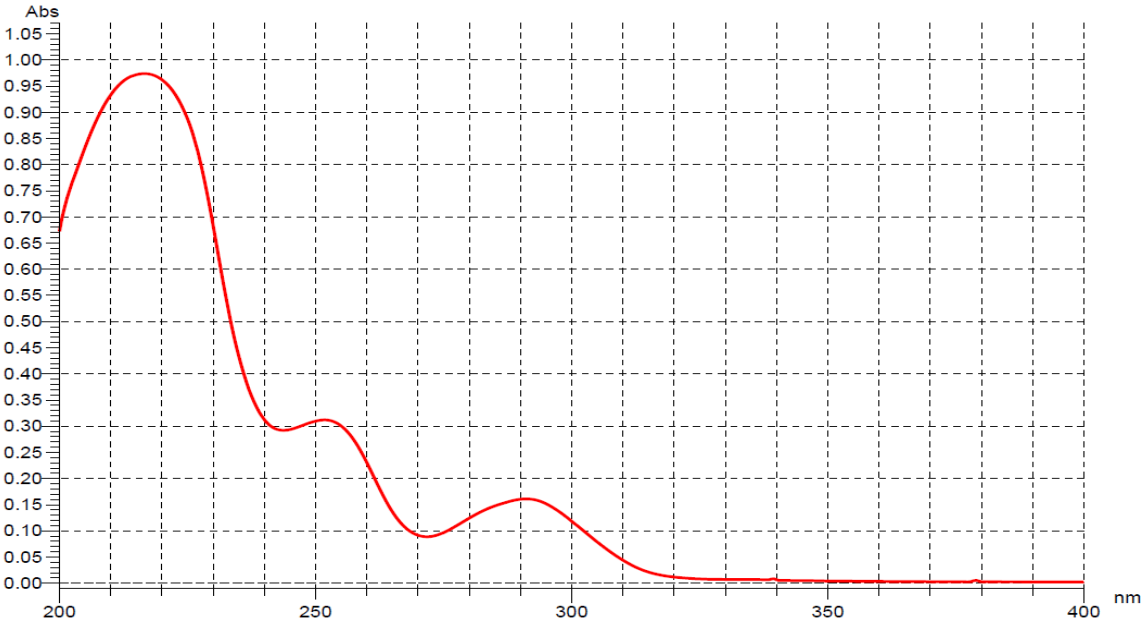

Figure 43. UV spectrum of 7*β*-hydroxymacrophyllic acid (PF-2)

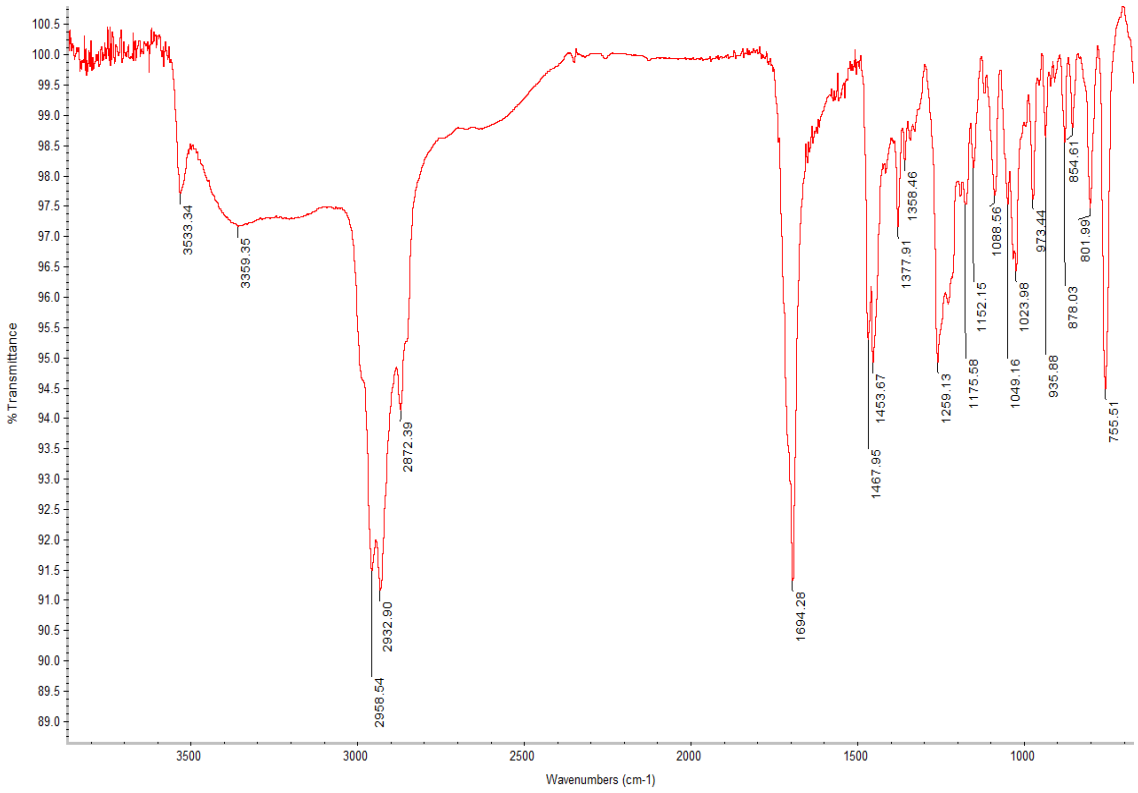

Figure 44. IR spectrum of 7*β*-hydroxymacrophyllic acid (PF-2) (KBr)

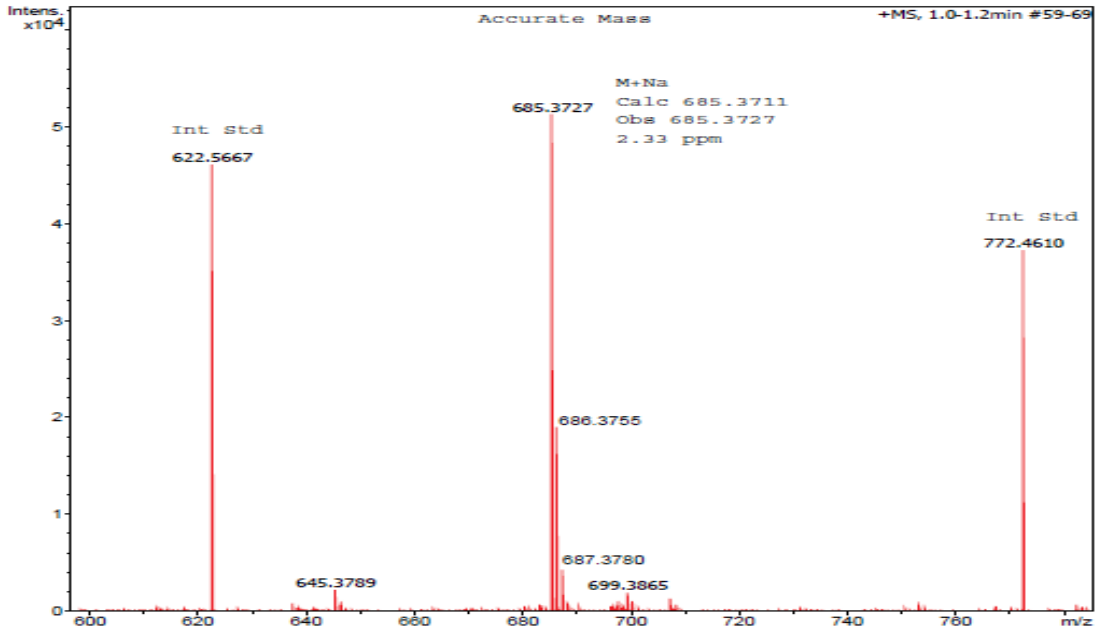

Figure 45. HRESIMS of 7*β*-hydroxymacrophyllic acid (PF-2)

Appendix V: ^{1}H and ^{13}C NMR, ^{1}H-^{1}H COSY, HSQC, HMBC, 2D-NOESY, UV, IR and HRESIMS of inumakiol D (28)

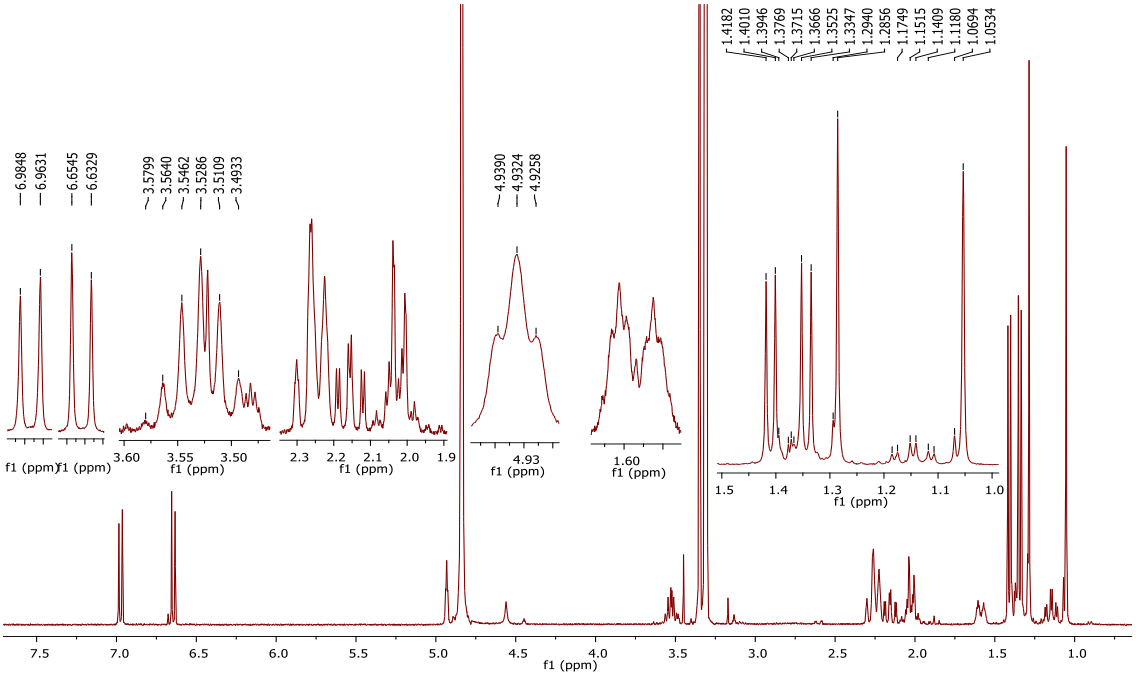

Figure 46. ^{1}H NMR spectrum of inumakiol D (28) (CD_3OD, 400 MHz)

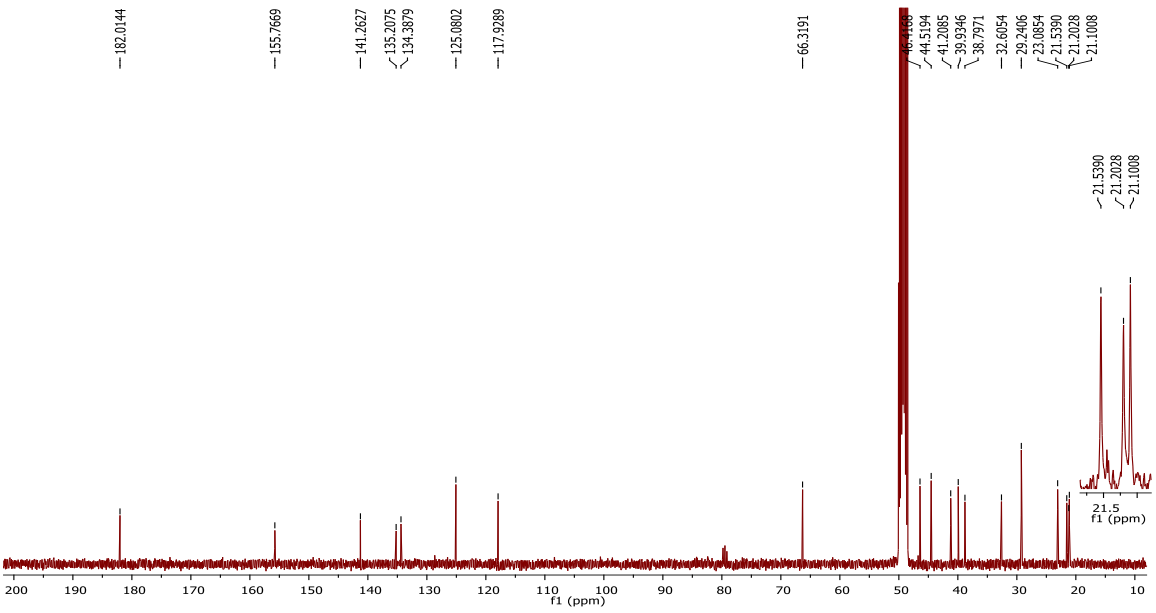

Figure 47. ^{13}C NMR spectrum of inumakiol D (28) (CD_3OD, 100 MHz)

Appendix VI: ^{1}H and ^{13}C NMR, ^{1}H-^{1}H COSY, HSQC, HMBC, 2D-NOESY, UV, IR and HRESIMS of macrophyllic acid (37)

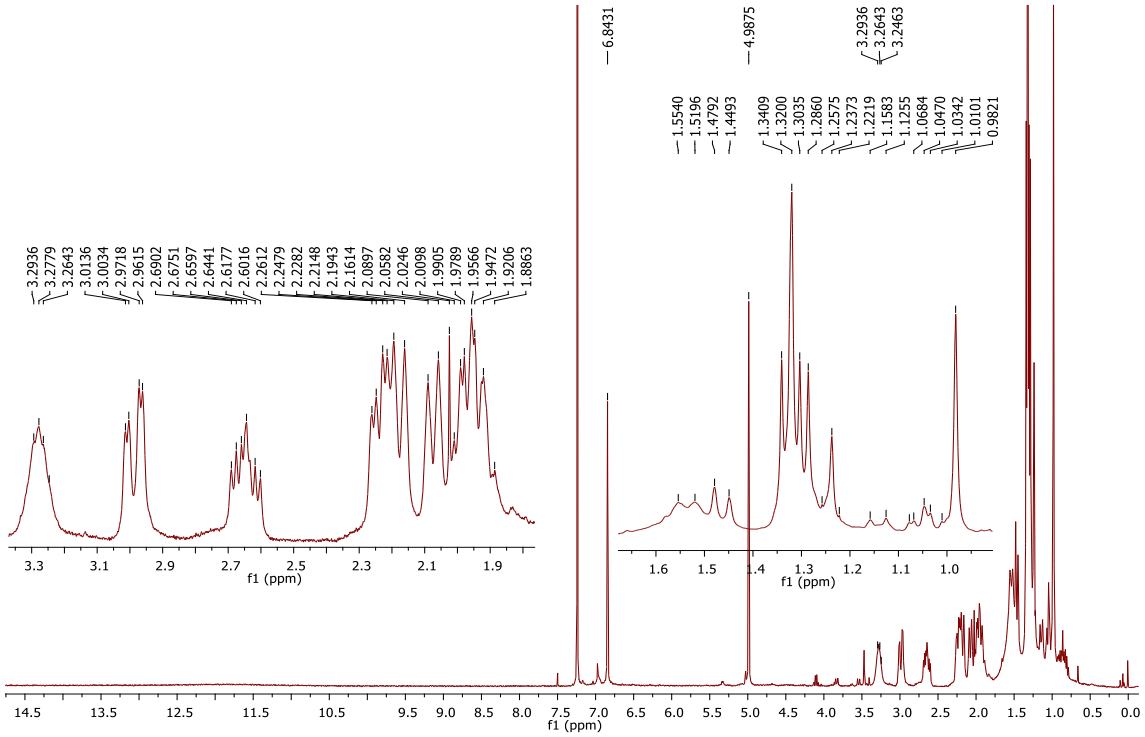

Figure 48. ^{1}H NMR spectrum of macrophyllic acid (37) ($CDCl_3$, 400 MHz)

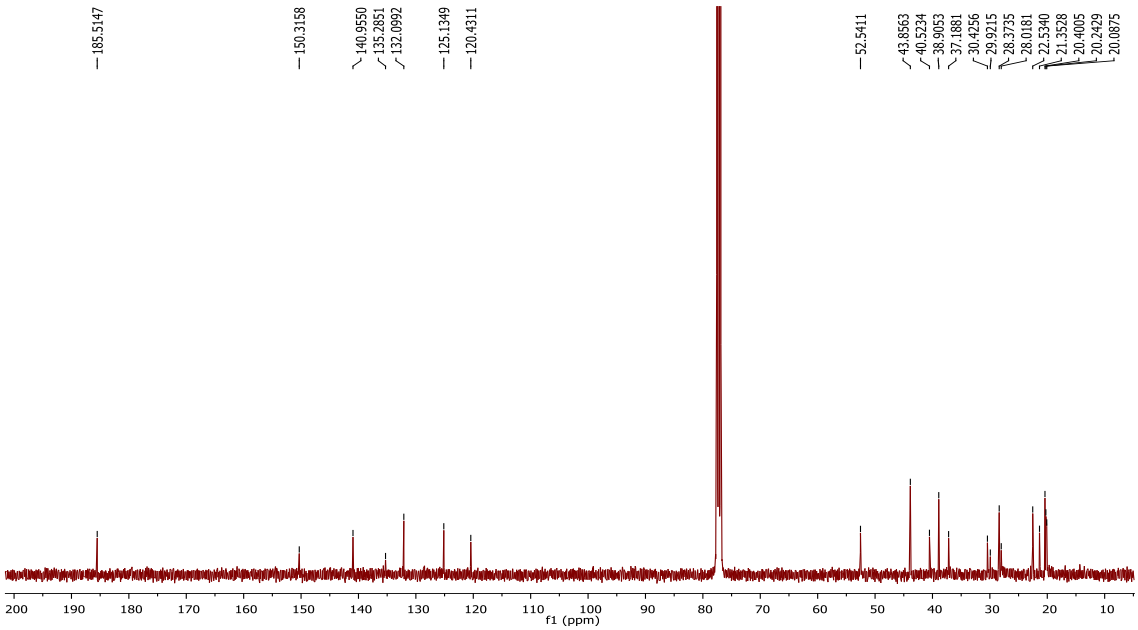

Figure 49. ^{13}C NMR spectrum of macrophyllic acid (37) ($CDCl_3$, 100 MHz)

Appendix VII: ^{1}H and ^{13}C NMR, ^{1}H-^{1}H COSY, HSQC, HMBC, 2D-NOESY, UV, IR and HRESIMS of nagilactone D (41)

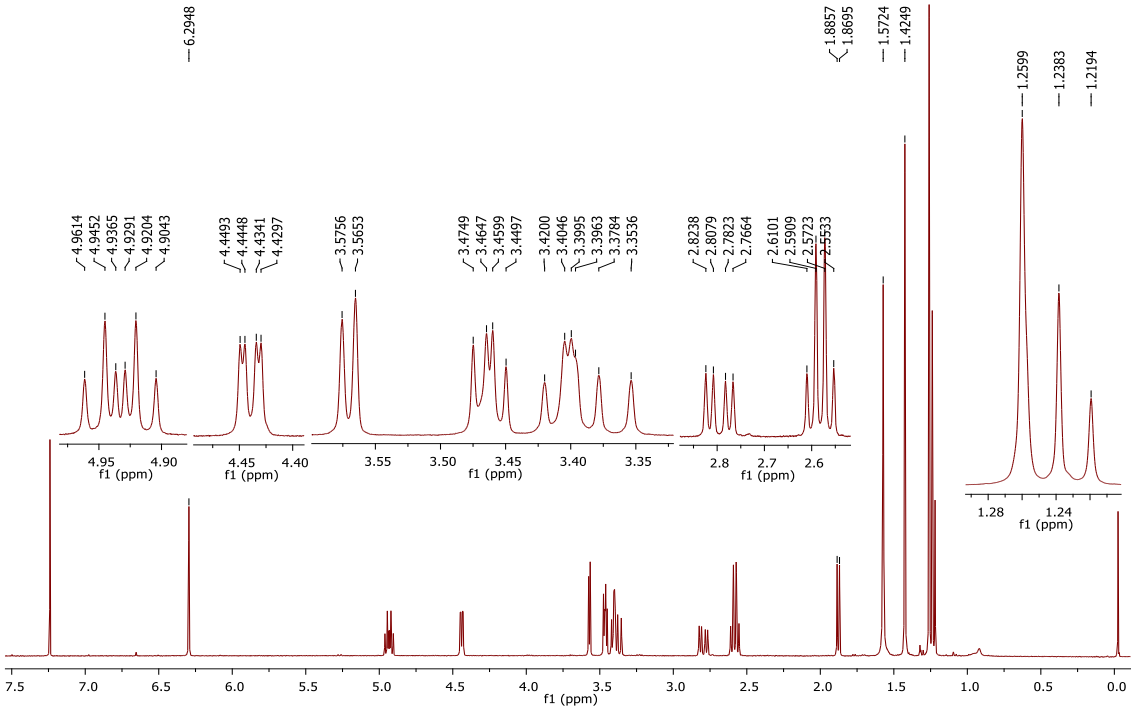

Figure 50. ^{1}H NMR spectrum of nagilactone D (41) ($CDCl_3$, 400 MHz)

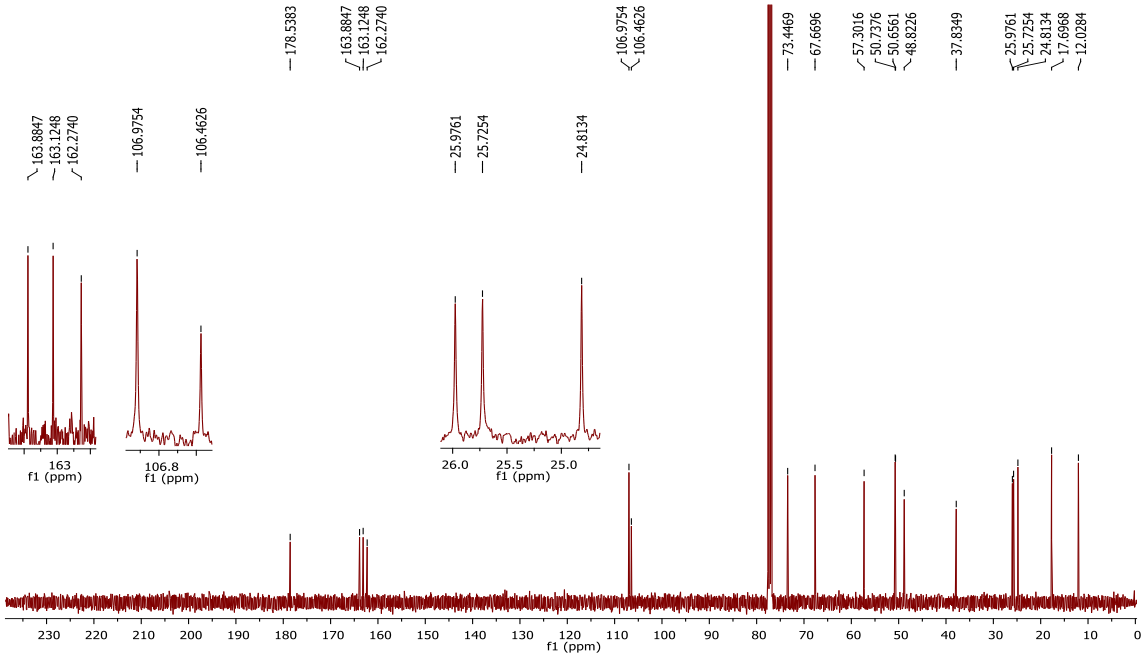

Figure 51. ^{13}C NMR spectrum of nagilactone D (41) ($CDCl_3$, 100 MHz)

Appendix VIII: ^{1}H and ^{13}C NMR, ^{1}H-^{1}H COSY, HSQC, HMBC, 2D-NOESY, UV, IR and HRESIMS of ponasterone A (94)

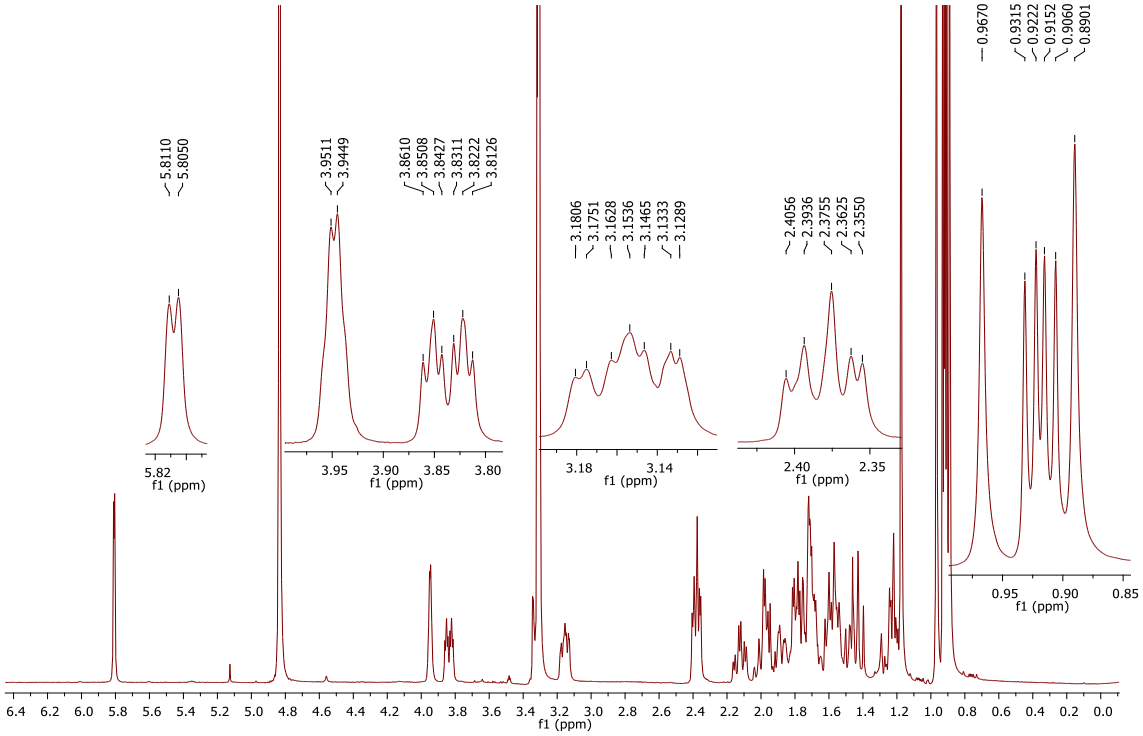

Figure 52. ^{1}H NMR spectrum of ponasterone A (94) (CD_3OD, 400 MHz)

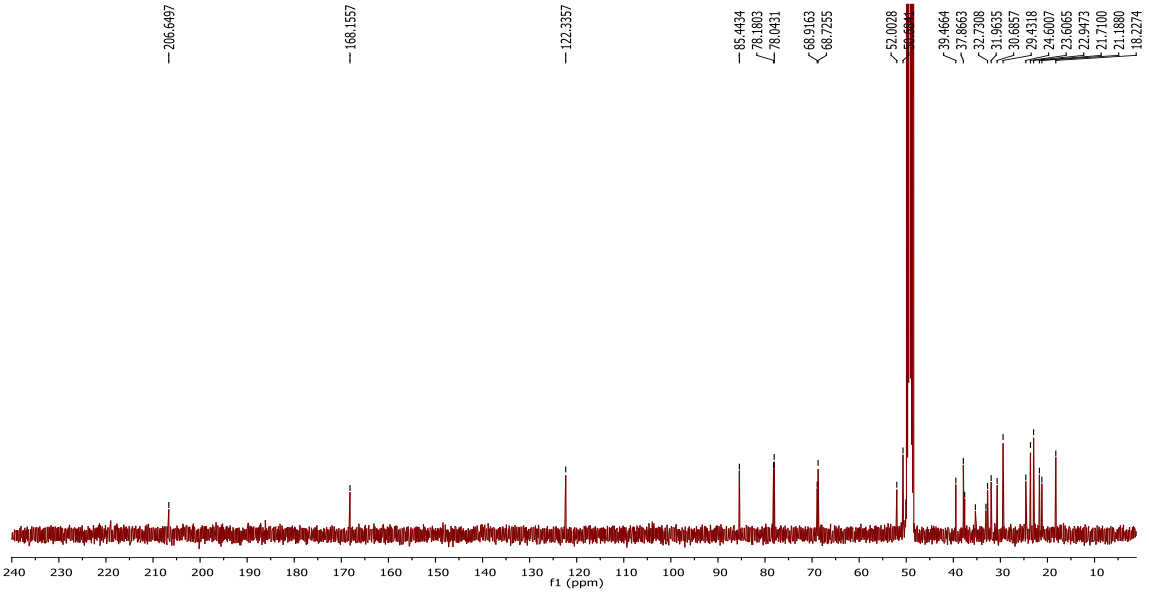

Figure 53. ^{13}C NMR spectrum of ponasterone A (94) (CD_3OD, 100 MHz)

Appendix IX: ^{1}H and ^{13}C NMR, ^{1}H-^{1}H COSY, HSQC, HMBC, 2D-NOESY, UV, IR and HRESIMS of 2*β*-hydroxynagilactone F (108)

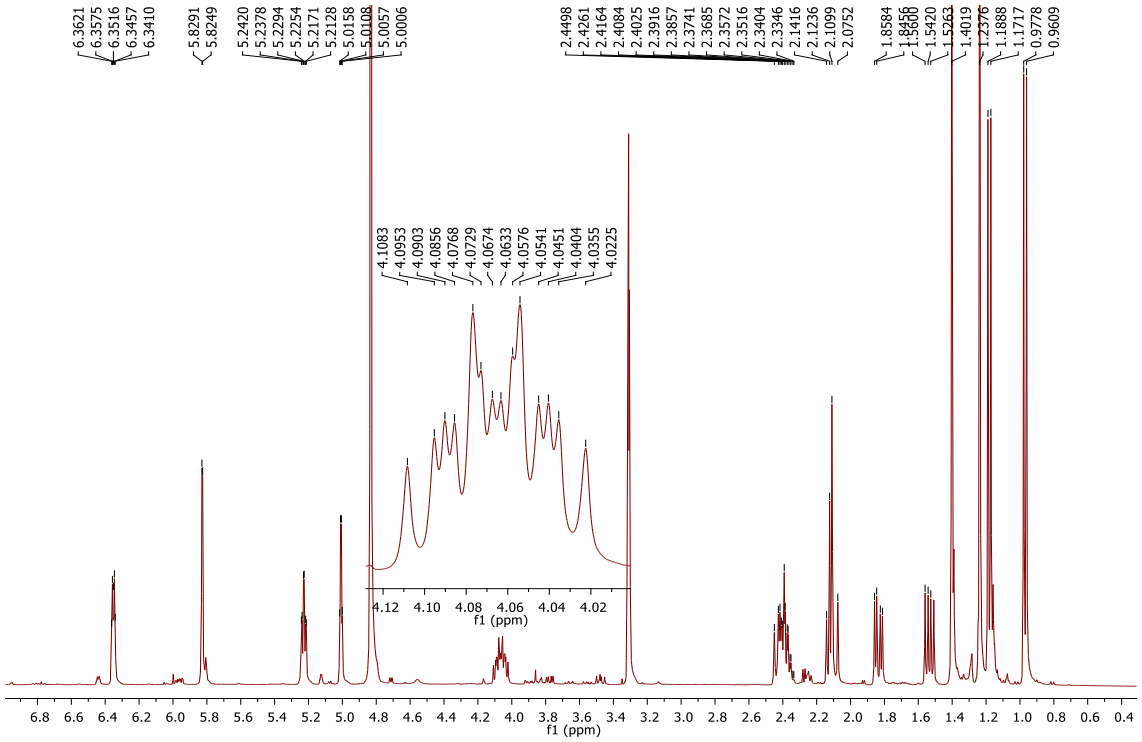

Figure 54. ^{1}H NMR spectrum of 2*β*-hydroxynagilactone F (108) (CD_3OD, 400 MHz)

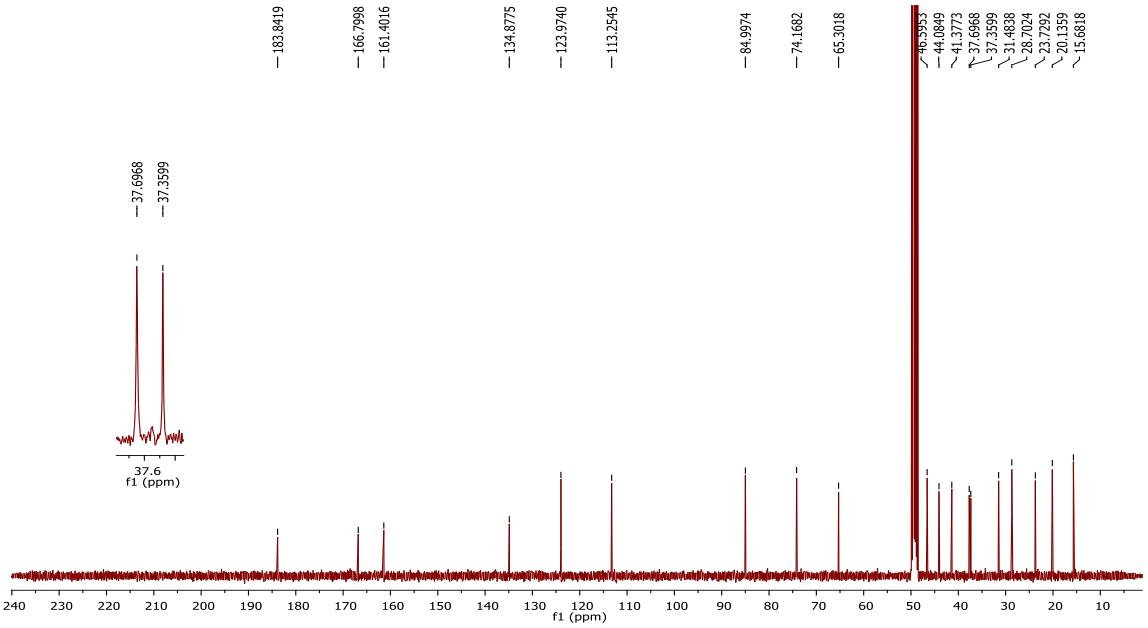

Figure 55. ^{13}C NMR spectrum of 2*β*-hydroxynagilactone F (108) (CD_3OD, 100 MHz)

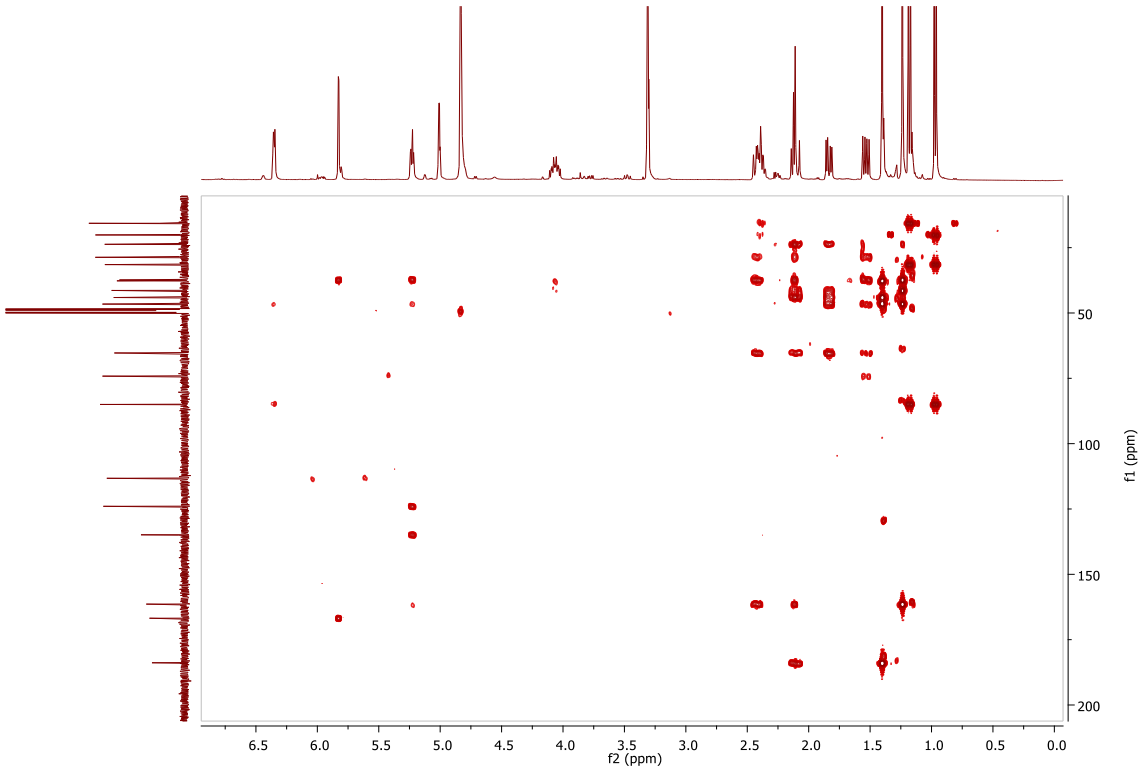

Figure 56. HMBC spectrum of 2*β*-hydroxynagilactone F (108) (CD_3OD, 400 MHz)

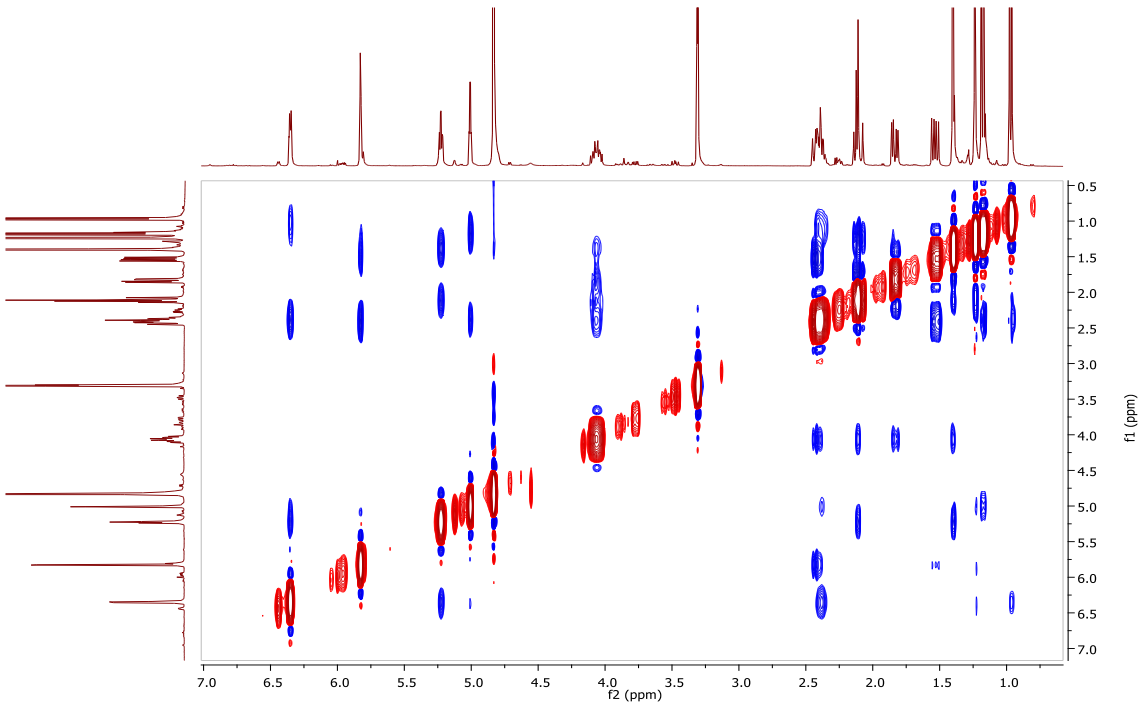

Figure 57. 2D-NOESY spectrum of 2*β*-hydroxynagilactone F (108) (CD_3OD, 400 MHz)

Appendix X: ^{1}H and ^{13}C NMR, ^{1}H-^{1}H COSY, HSQC, HMBC, 2D-NOESY, UV, IR and HRESIMS of nagilactone I (109)

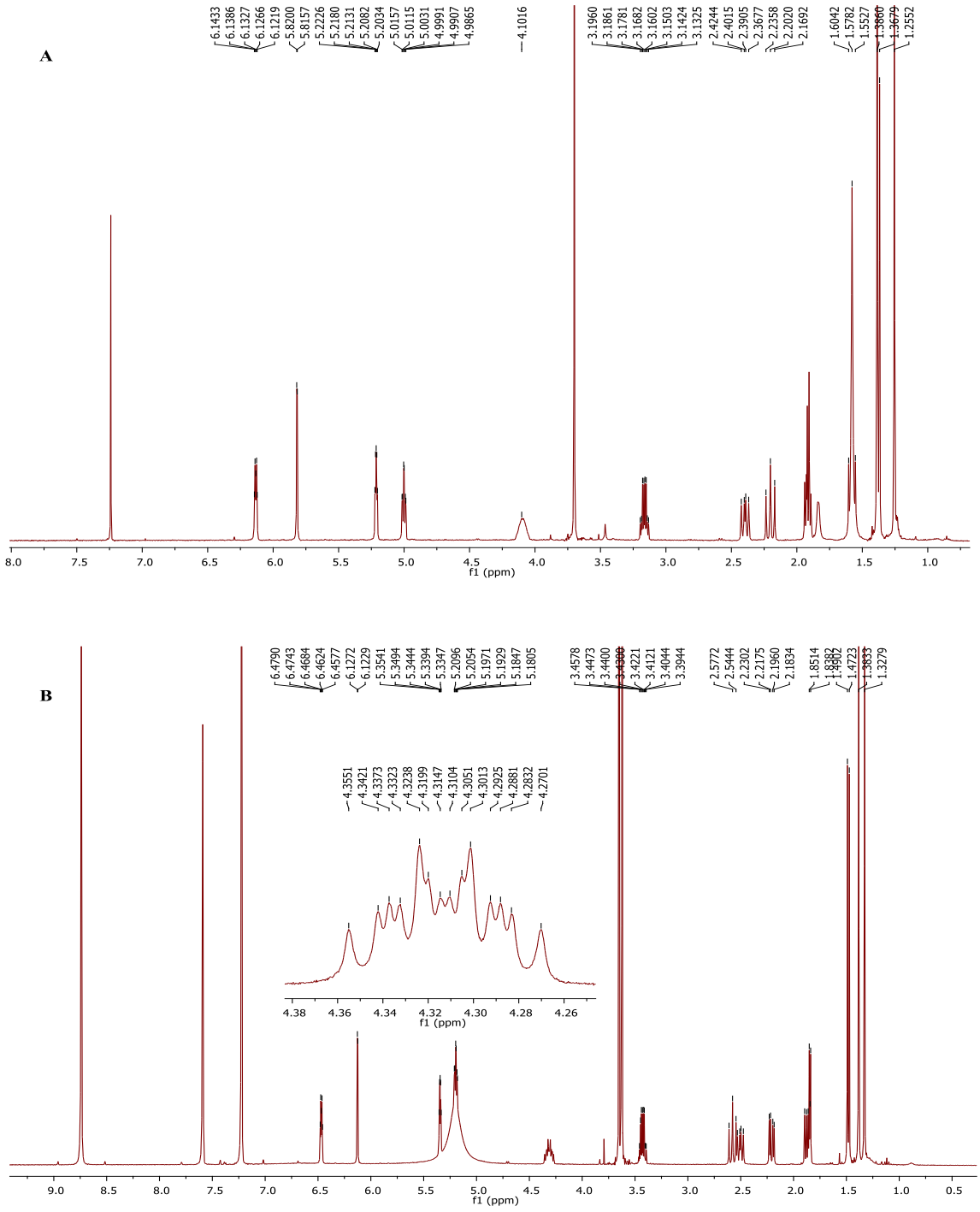

Figure 58. ^{1}H NMR spectrum of nagilactone I (109) (A. $CDCl_3$, B. Pyridine-d_5, 400 MHz)

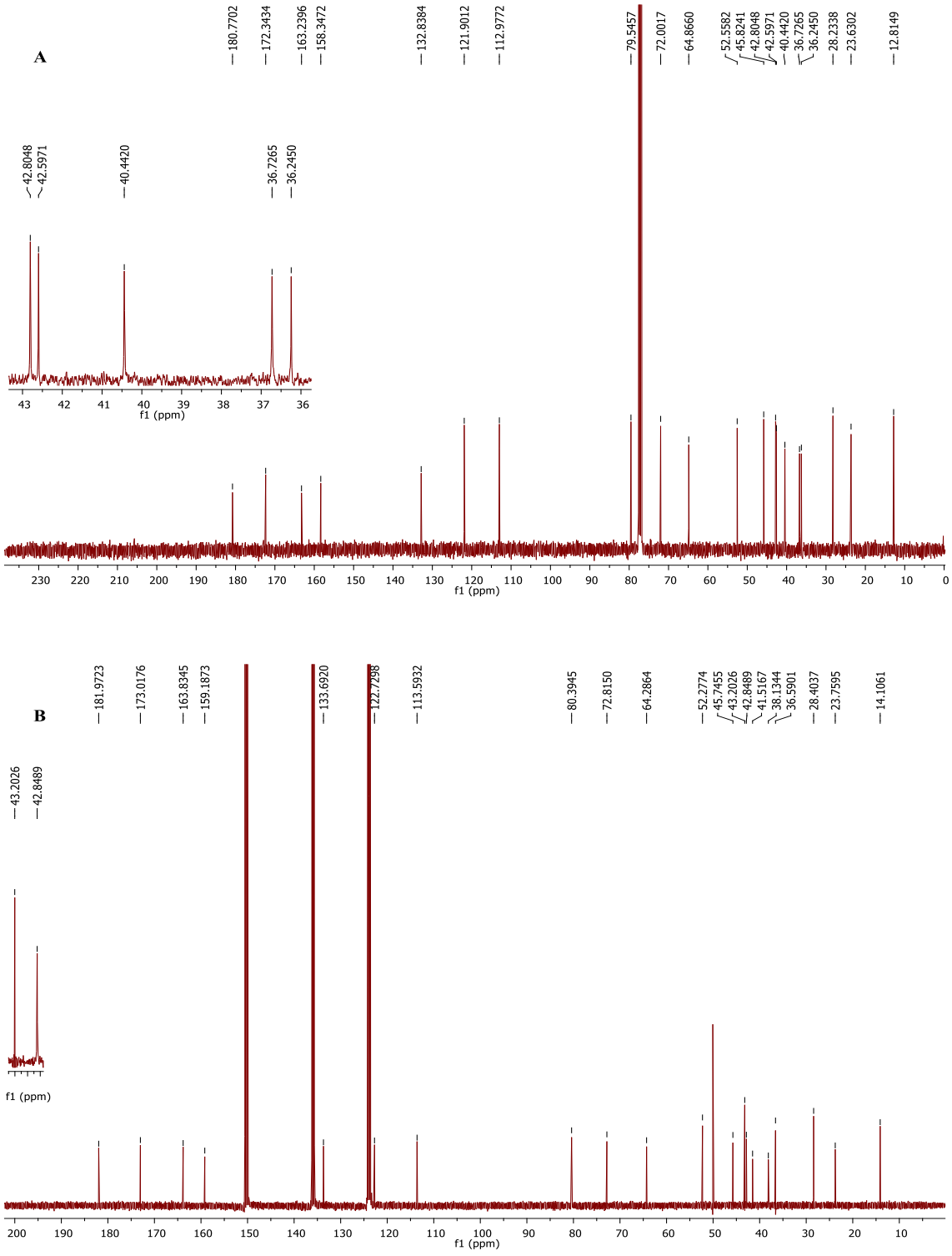

Figure 59. ^{13}C NMR spectrum of nagilactone I (109) (A. $CDCl_3$, B. Pyridine-d_5, 100 MHz)

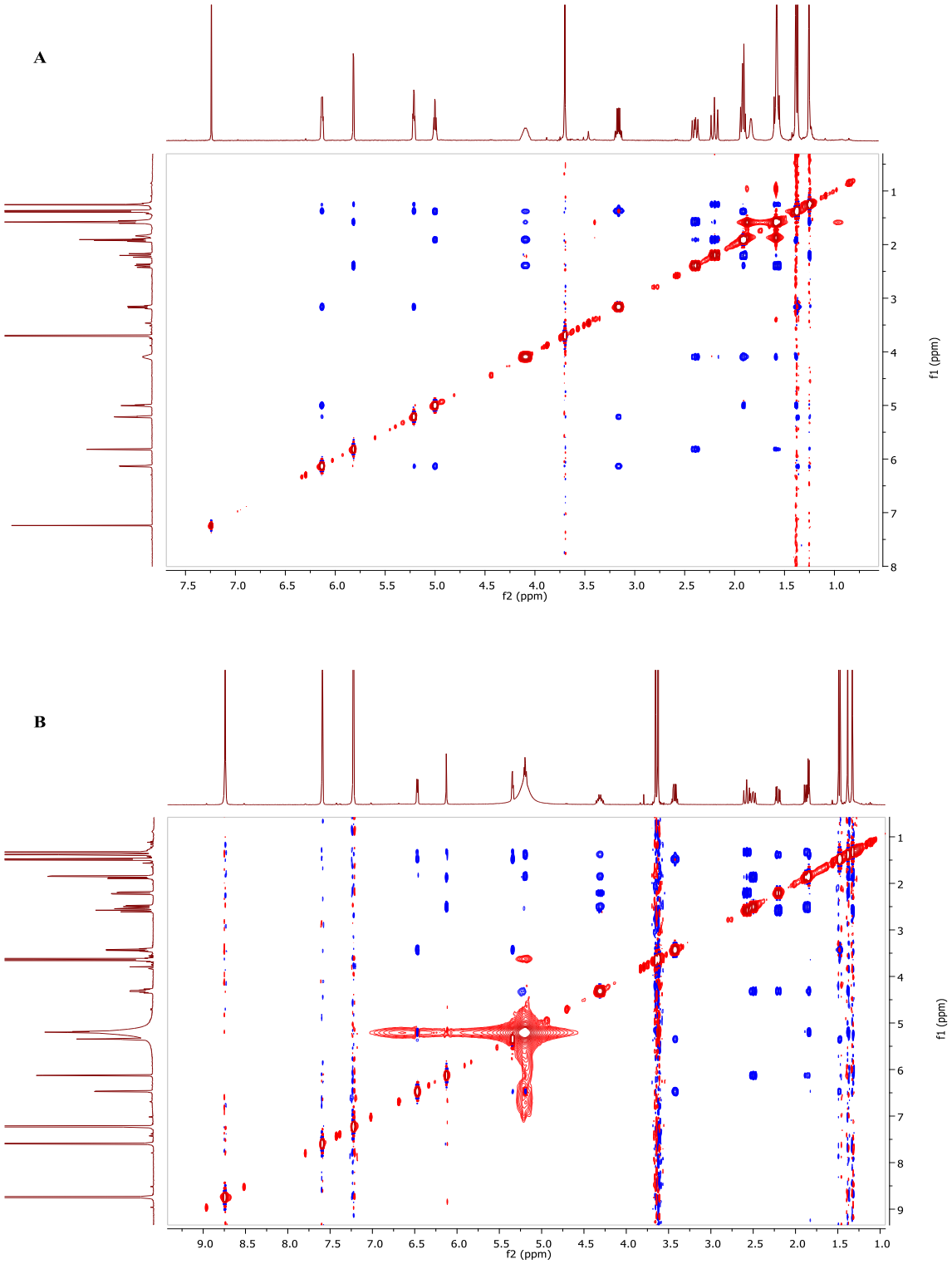

Figure 60. 2D-NOESY spectrum of nagilactone I (109) (A. $CDCl_3$, B. Pyridine-d_5, 400 MHz)

Appendix XI: ^{1}H and ^{13}C NMR, ^{1}H-^{1}H COSY, HSQC, HMBC, 2D-NOESY, UV, IR and HRESIMS of 15-hydroxynagilactone D (110)

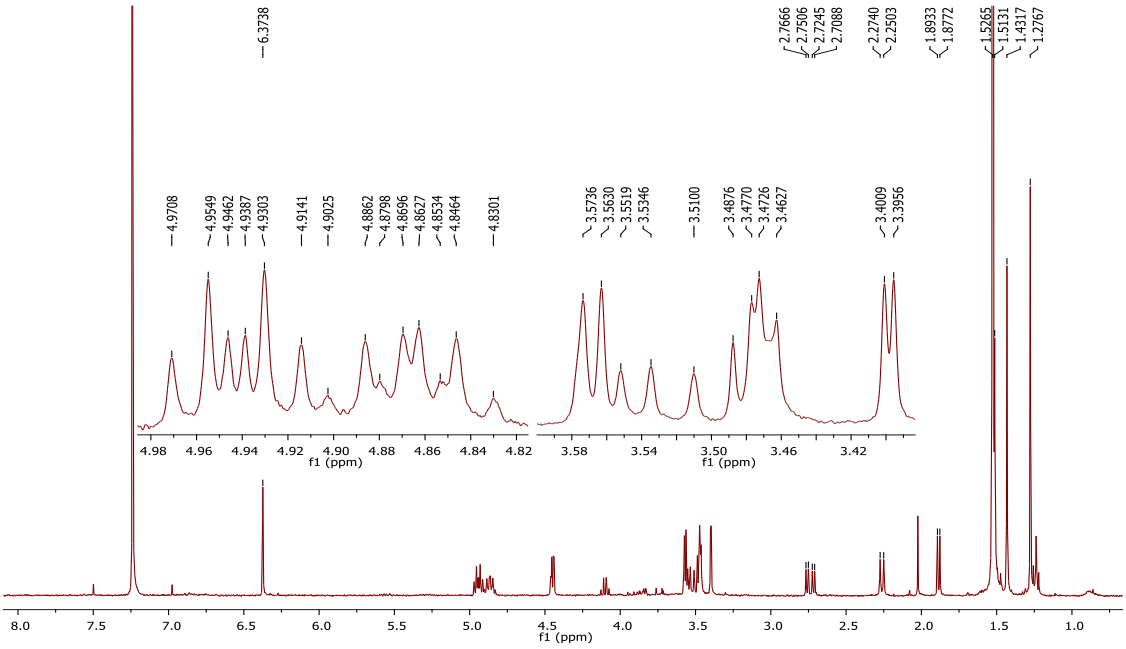

Figure 61. ^{1}H NMR spectrum of 15-hydroxynagilactone D (110) ($CDCl_3$, 400 MHz)

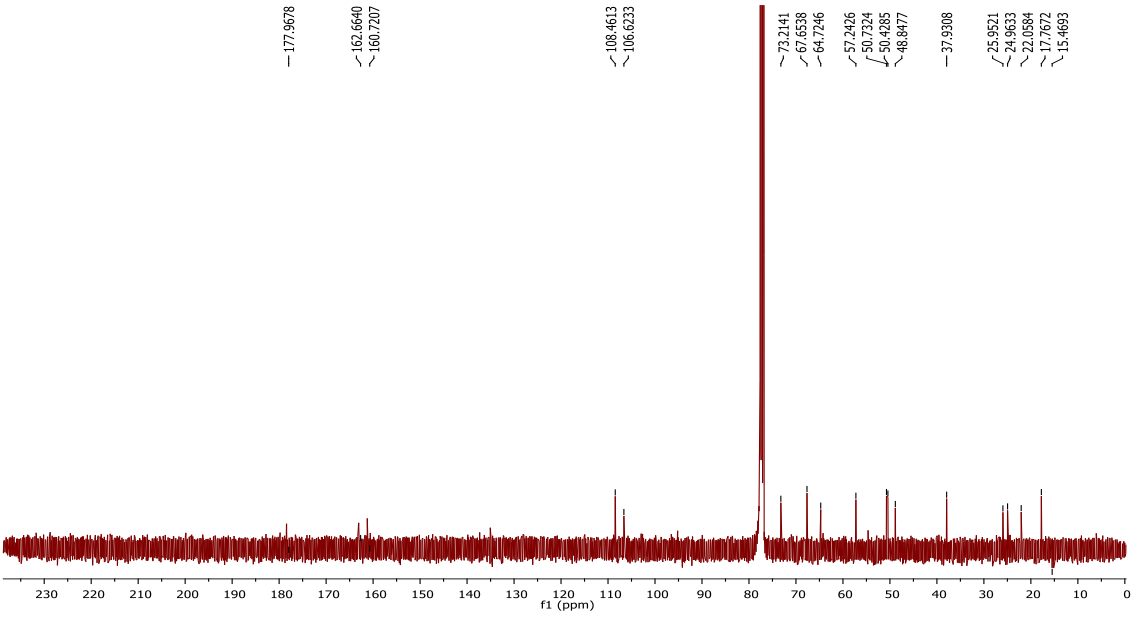

Figure 62. ^{13}C NMR spectrum of 15-hydroxynagilactone D (110) ($CDCl_3$, 100 MHz)

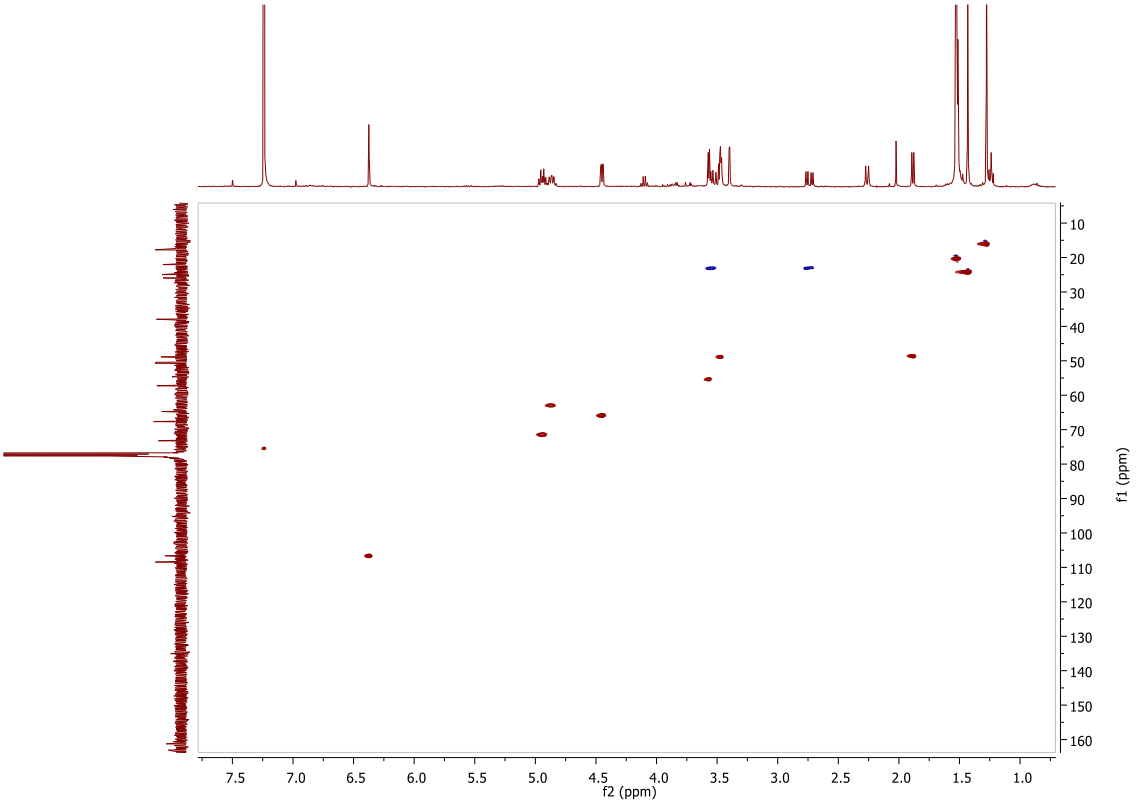

Figure 63. HSQC spectrum of 15-hydroxynagilactone D (110) ($CDCl_3$, 400 MHz)

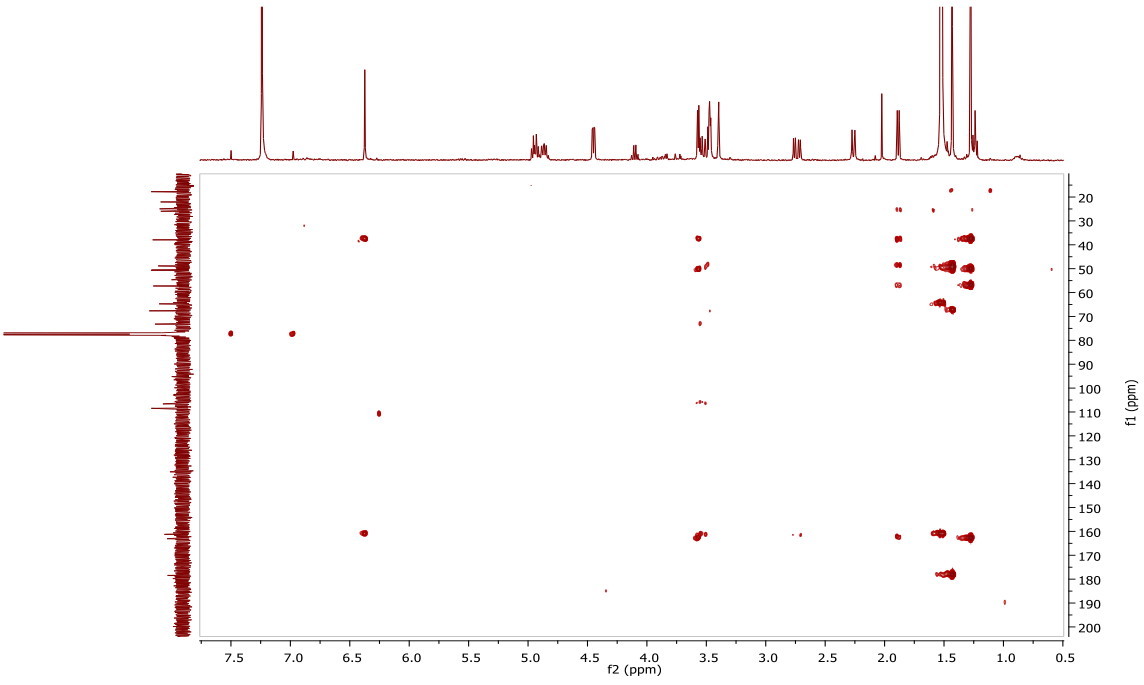

Figure 64. HMBC spectrum of 15-hydroxynagilactone D (110) ($CDCl_3$, 400 MHz)

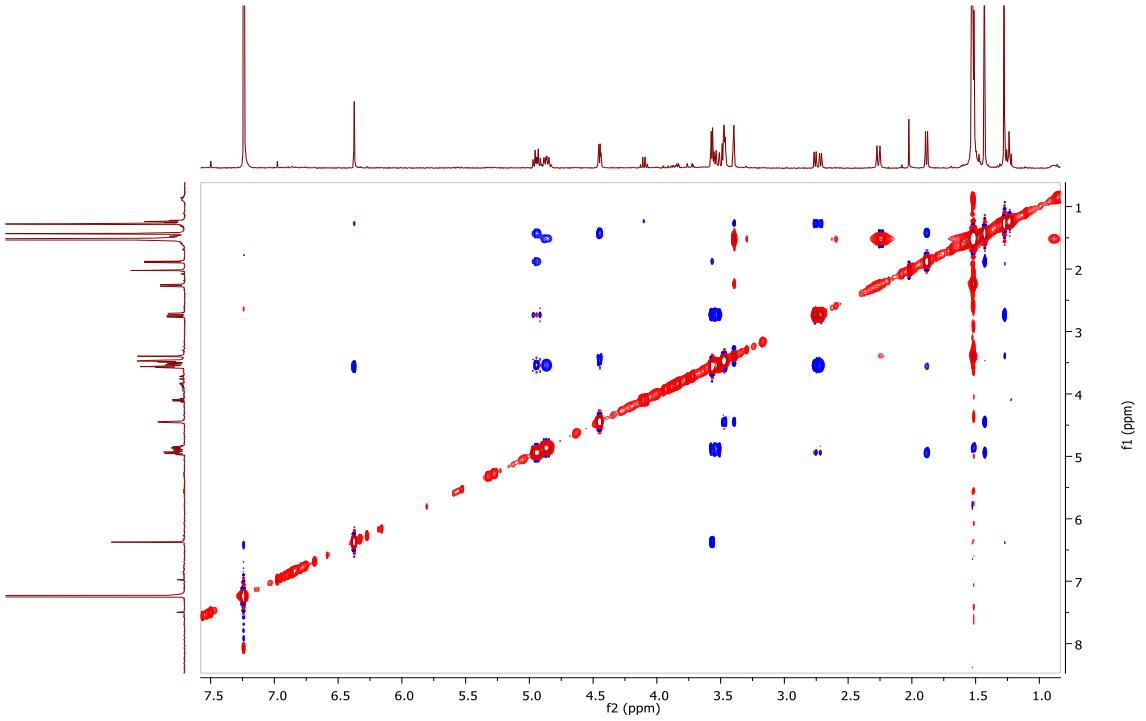

Figure 65. 2D-NOESY spectrum of 15-hydroxynagilactone D (110) ($CDCl_3$, 400 MHz)

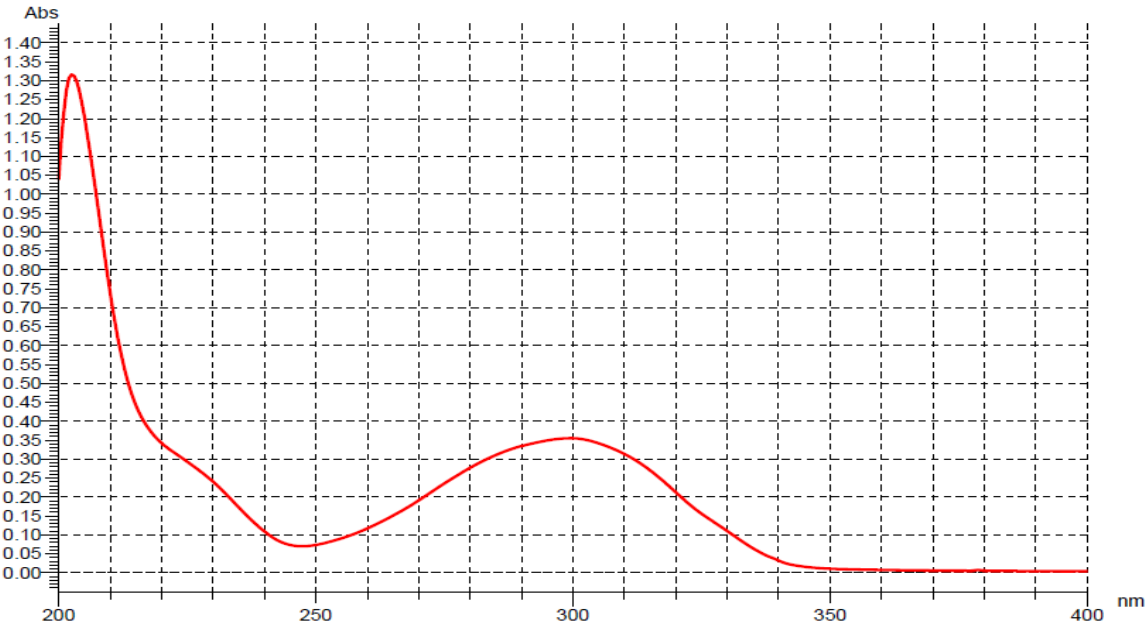

Figure 66. UV spectrum of 15-hydroxynagilactone D (110)

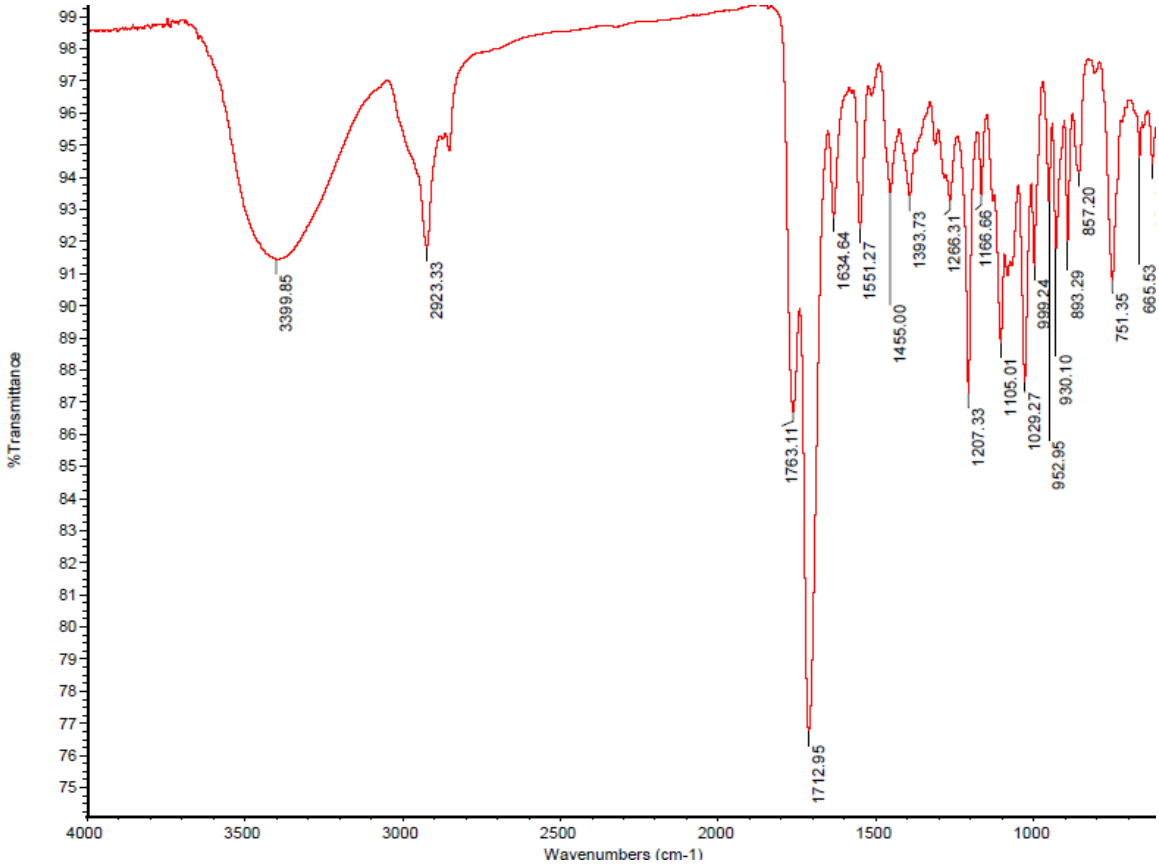

Figure 67. IR spectrum of 15-hydroxynagilactone D (110) (KBr)

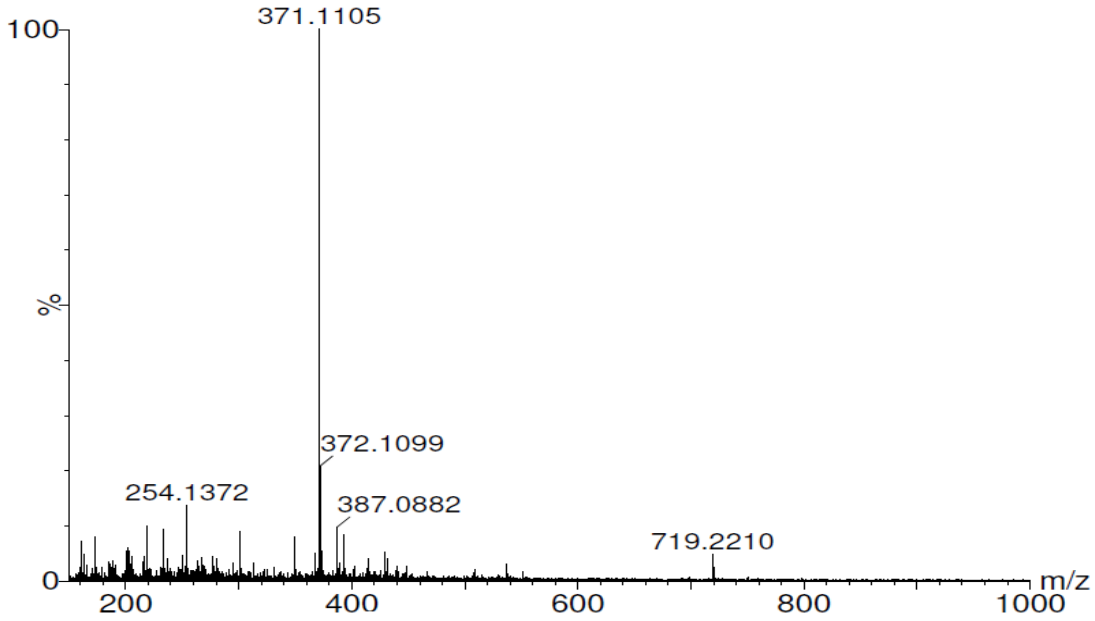

Figure 68. HRESIMS of 15-hydroxynagilactone D (110)

Appendix XII: X-ray crystallographic data of compounds 41, 108 and 109.

In each case a colorless crystal was mounted on the goniometer of an Agilent Nova diffractometer operating with Cu Kα radiation (λ = 1.541 84 Å). The data collection routine, unit cell refinement, and data processing were carried out with the program CrysAlisPro. The structure was solved using SHELXT-201442 and refined using SHELXL-2014 via OLEX.42 The final refinement model involved anisotropic displacement parameters for non-hydrogen atoms. A riding model was used for the aromatic and alkyl hydrogens. Hydrogen atom positions and isotropic displacement parameters were refined independently for the hydroxy and water hydrogens that are potentially involved in hydrogen bonding. The absolute configuration was established from anomalous dispersion effects for **41** [Flack x = -0.04(6); Hooft P2(true) = 1.000, P3(true) = 1.000, P3(rac-twin) = 0.000; P3(false) = 0.000, y = 0.01(7)], for **108** [Flack x = −0.07(13); Hooft P2(true) = 1.000, P3(true) = 1.000, P3(rac-twin) = 0.000; P3(false) = 0.000, y = −0.00(11)] and for **109** [Flack x = −0.13(8); Hooft P2(true) = 1.000, P3(true) = 1.000, P3(rac-twin) = 0.000; P3(false) = 0.000, y = −0.09(7)]. Olex2 was used for molecular graphics generation. The details of the structural analyses are described in the Tables 9–17 which, along with the CIF files, have also been deposited in the Cambridge Crystallographic Data Centre (CCDC Nos. 1038571, 1038573 and 1038572 for compounds **41**, **108** and **109**, respectively).

Crystal data of nagilactone D (41): $C_{18}H_{22}O_7$, M = 350.35, orthorhombic crystal system, crystal size 0.2002 × 0.1846 × 0.0543 mm^3, space group $P2_12_12_1$, a = 7.13350(10) Å α = 90°, b = 8.36010(10) Å β= 90°, c = 26.2049 Å γ = 90°, V = 1562.78(4) $Å^3$ reflections collected 18271, parameters 241.

Crystal data of 2β-hydroxynagilactone F (108): $C_{19}H_{24}O_5$, M = 332.38, orthorhombic crystal system, crystal size 0.44 × 0.13 × 0.23 mm^3, space group $P2_12_12_1$, a = 7.8220(2) Å α = 90°, b = 12.4501(4) β = 90°, c = 17.1803(6) Å γ = 90°, V = 1673.11(9) $Å^3$, reflections collected 10392, parameters 225.

Crystal data of nagilactone I (109): $C_{20}H_{24}O_7$, M = 376.39, orthorhombic crystal system, crystal size 0.14 × 0.19 × 0.28 mm^3, space group $P2_12_12_1$, a = 7.77930(10) Å α = 90°, b = 11.77260(10) Å β= 90°, c = 19.7352(3) Å γ = 90°, V = 1807.40(4) $Å^3$, reflections collected 11384, parameters 252.

Table 9. Crystal data and structure refinement for nagilactone D (41)

Identification code	cs2143	
Empirical formula	$C_{18}H_{22}O_7$	
Formula weight	350.35	
Temperature	99.90(14) K	
Wavelength	1.54184 Å	
Crystal system	Orthorhombic	
Space group	$P2_12_12_1$	
Unit cell dimensions	a = 7.13350(10) Å	α= 90°.
	b = 8.36010(10) Å	β= 90°.
	c = 26.2049(5) Å	γ = 90°.
Volume	1562.78(4) $Å^3$	
Z	4	
Density (calculated)	1.489 Mg/m^3	
Absorption coefficient	0.963 mm^{-1}	
F(000)	744	
Crystal size	0.2002 x 0.1846 x 0.0543 mm^3	
Theta range for data collection	3.373 to 74.877°.	
Index ranges	-8<=h<=5, -10<=k<=10, -32<=l<=32	
Reflections collected	18271	
Independent reflections	3207 [R(int) = 0.0483]	
Completeness to theta = 67.684°	100.0 %	
Absorption correction	Gaussian	
Max. and min. transmission	0.950 and 0.831	
Refinement method	Full-matrix least-squares on F^2	
Data / restraints / parameters	3207 / 0 / 241	
Goodness-of-fit on F^2	1.047	
Final R indices [I>2sigma(I)]	R1 = 0.0323, wR2 = 0.0818	
R indices (all data)	R1 = 0.0340, wR2 = 0.0834	
Absolute structure parameter	-0.04(6)	
Extinction coefficient	n/a	
Largest diff. peak and hole	0.255 and -0.204 $e.Å^{-3}$	

Table 10. Bond lengths [Å] and angles [°] for nagilactone D (41)

O(1)-C(1)	1.354(2)	C(12)-H(12B)	0.9900
O(1)-C(13)	1.464(2)	C(12)-C(13)	1.524(3)
O(2)-C(1)	1.204(3)	C(13)-H(13)	1.0000
O(3)-H(3)	0.78(4)	C(13)-C(14)	1.533(3)
O(3)-C(3)	1.424(2)	C(14)-H(14)	1.0000
O(4)-C(4)	1.446(3)	C(15)-H(15A)	0.9800
O(4)-C(5)	1.443(2)	C(15)-H(15B)	0.9800
O(5)-C(9)	1.217(3)	C(15)-H(15C)	0.9800
O(6)-C(9)	1.386(2)	C(16)-H(16A)	0.9800
O(6)-C(10)	1.371(2)	C(16)-H(16B)	0.9800
C(1)-C(2)	1.526(3)	C(16)-H(16C)	0.9800
C(2)-C(3)	1.558(3)	C(17)-H(17A)	0.9900
C(2)-C(14)	1.544(3)	C(17)-H(17B)	0.9900
C(2)-C(15)	1.546(3)	C(17)-C(18)	1.528(3)
C(3)-H(3A)	1.0000	C(18)-H(18A)	0.9800
C(3)-C(4)	1.532(3)	C(18)-H(18B)	0.9800
C(4)-H(4)	1.0000	C(18)-H(18C)	0.9800
C(4)-C(5)	1.473(3)	O(7)-H(7A)	0.90(5)
C(5)-H(5)	1.0000	O(7)-H(7B)	0.85(5)
C(5)-C(6)	1.536(3)	C(1)-O(1)-C(13)	110.30(15)
C(6)-C(7)	1.524(3)	C(3)-O(3)-H(3)	110(3)
C(6)-C(14)	1.554(3)	C(5)-O(4)-C(4)	61.31(12)
C(6)-C(16)	1.553(3)	C(10)-O(6)-C(9)	122.72(16)
C(7)-C(8)	1.354(3)	O(1)-C(1)-C(2)	110.92(16)
C(7)-C(11)	1.453(3)	O(2)-C(1)-O(1)	120.83(19)
C(8)-H(8)	0.9500	O(2)-C(1)-C(2)	128.11(18)
C(8)-C(9)	1.435(3)	C(1)-C(2)-C(3)	113.83(16)
C(10)-C(11)	1.354(3)	C(1)-C(2)-C(14)	103.13(15)
C(10)-C(17)	1.501(3)	C(1)-C(2)-C(15)	106.50(16)
C(11)-C(12)	1.510(3)	C(14)-C(2)-C(3)	115.40(17)
C(12)-H(12A)	0.9900	C(14)-C(2)-C(15)	109.55(16)

C(15)-C(2)-C(3)	108.03(16)	C(11)-C(10)-C(17)	126.67(19)
O(3)-C(3)-C(2)	111.92(16)	C(7)-C(11)-C(12)	119.28(18)
O(3)-C(3)-H(3A)	107.6	C(10)-C(11)-C(7)	118.34(19)
O(3)-C(3)-C(4)	113.22(17)	C(10)-C(11)-C(12)	122.30(18)
C(2)-C(3)-H(3A)	107.6	C(11)-C(12)-H(12A)	109.5
C(4)-C(3)-C(2)	108.59(16)	C(11)-C(12)-H(12B)	109.5
C(4)-C(3)-H(3A)	107.6	C(11)-C(12)-C(13)	110.73(17)
O(4)-C(4)-C(3)	116.41(17)	H(12A)-C(12)-H(12B)	108.1
O(4)-C(4)-H(4)	116.5	C(13)-C(12)-H(12A)	109.5
O(4)-C(4)-C(5)	59.23(12)	C(13)-C(12)-H(12B)	109.5
C(3)-C(4)-H(4)	116.5	O(1)-C(13)-C(12)	109.72(16)
C(5)-C(4)-C(3)	119.22(17)	O(1)-C(13)-H(13)	108.9
C(5)-C(4)-H(4)	116.5	O(1)-C(13)-C(14)	105.33(15)
O(4)-C(5)-C(4)	59.46(12)	C(12)-C(13)-H(13)	108.9
O(4)-C(5)-H(5)	116.3	C(12)-C(13)-C(14)	114.83(17)
O(4)-C(5)-C(6)	118.92(16)	C(14)-C(13)-H(13)	108.9
C(4)-C(5)-H(5)	116.3	C(2)-C(14)-C(6)	115.63(16)
C(4)-C(5)-C(6)	117.45(18)	C(2)-C(14)-H(14)	107.9
C(6)-C(5)-H(5)	116.3	C(6)-C(14)-H(14)	107.9
C(5)-C(6)-C(14)	103.14(16)	C(13)-C(14)-C(2)	103.42(16)
C(5)-C(6)-C(16)	112.44(16)	C(13)-C(14)-C(6)	113.64(16)
C(7)-C(6)-C(5)	113.68(16)	C(13)-C(14)-H(14)	107.9
C(7)-C(6)-C(14)	104.80(15)	C(2)-C(15)-H(15A)	109.5
C(7)-C(6)-C(16)	107.82(16)	C(2)-C(15)-H(15B)	109.5
C(16)-C(6)-C(14)	114.83(16)	C(2)-C(15)-H(15C)	109.5
C(8)-C(7)-C(6)	124.87(18)	H(15A)-C(15)-H(15B)	109.5
C(8)-C(7)-C(11)	119.90(18)	H(15A)-C(15)-H(15C)	109.5
C(11)-C(7)-C(6)	115.22(17)	H(15B)-C(15)-H(15C)	109.5
C(7)-C(8)-H(8)	119.4	C(6)-C(16)-H(16A)	109.5
C(7)-C(8)-C(9)	121.25(18)	C(6)-C(16)-H(16B)	109.5
C(9)-C(8)-H(8)	119.4	C(6)-C(16)-H(16C)	109.5
O(5)-C(9)-O(6)	116.04(17)	H(16A)-C(16)-H(16B)	109.5
O(5)-C(9)-C(8)	127.44(19)	H(16A)-C(16)-H(16C)	109.5
O(6)-C(9)-C(8)	116.51(17)	H(16B)-C(16)-H(16C)	109.5
O(6)-C(10)-C(17)	112.00(17)	C(10)-C(17)-H(17A)	108.2
C(11)-C(10)-O(6)	121.26(18)	C(10)-C(17)-H(17B)	108.2

C(10)-C(17)-C(18)	116.17(18)	C(17)-C(18)-H(18C)	109.5
H(17A)-C(17)-H(17B)	107.4	H(18A)-C(18)-H(18B)	109.5
C(18)-C(17)-H(17A)	108.2	H(18A)-C(18)-H(18C)	109.5
C(18)-C(17)-H(17B)	108.2	H(18B)-C(18)-H(18C)	109.5
C(17)-C(18)-H(18A)	109.5	H(7A)-O(7)-H(7B)	107(4)
C(17)-C(18)-H(18B)	109.5		

Table 11. Hydrogen bonds for nagilactone D (41) [Å and °]

D-H...A	d(D-H)	d(H...A)	d(D...A)	<(DHA)
O(3)-H(3)...O(4)	0.78(4)	2.28(4)	2.750(2)	120(3)
C(12)-H(12B)...O(5)#1	0.99	2.46	3.180(3)	128.9

Symmetry transformations used to generate equivalent atoms:

#1 x,y-1,z

Table 12. Crystal data and structure refinement for 2β-hydroxynagilactone F (108)

Identification code	ERXR-3	
Empirical formula	$C_{19}H_{24}O_5$	
Formula weight	332.38	
Temperature	100.00(10) K	
Wavelength	1.54184 Å	
Crystal system	Orthorhombic	
Space group	$P2_12_12_1$	
Unit cell dimensions	a = 7.8220(2) Å	α= 90°.
	b = 12.4501(4) Å	β= 90°.
	c = 17.1803(6) Å	γ = 90°.
Volume	1673.11(9) Å^3	
Z	4	
Density (calculated)	1.320 Mg/m^3	
Absorption coefficient	0.776 mm^{-1}	
F(000)	712	
Crystal size	0.2293 x 0.1311 x 0.0395 mm^3	
Theta range for data collection	4.386 to 74.732°.	
Index ranges	-9<=h<=7, -15<=k<=13, -21<=l<=21	
Reflections collected	10392	
Independent reflections	3407 [R(int) = 0.0476]	
Completeness to theta = 67.684°	99.9 %	
Absorption correction	Gaussian	
Max. and min. transmission	0.971 and 0.879	
Refinement method	Full-matrix least-squares on F^2	
Data / restraints / parameters	3407 / 0 / 225	
Goodness-of-fit on F^2	1.042	
Final R indices [I>2sigma(I)]	R1 = 0.0408, wR2 = 0.1041	
R indices (all data)	R1 = 0.0444, wR2 = 0.1074	
Absolute structure parameter	-0.07(13)	
Extinction coefficient	n/a	
Largest diff. peak and hole	0.616 and -0.176 e.Å^{-3}	

Table 13. Bond lengths [Å] and angles [°] for 2β-hydroxynagilactone F (108)

O(1)-C(1)	1.351(3)
O(1)-C(13)	1.475(3)
O(2)-C(1)	1.206(3)
O(3)-C(4)	1.424(3)
O(4)-C(9)	1.208(3)
O(5)-C(9)	1.353(3)
O(5)-C(10)	1.472(3)
C(1)-C(2)	1.519(4)
C(2)-C(3)	1.534(4)
C(2)-C(14)	1.538(3)
C(2)-C(15)	1.544(3)
C(3)-C(4)	1.512(3)
C(4)-C(5)	1.536(3)
C(5)-C(6)	1.546(3)
C(6)-C(7)	1.517(3)
C(6)-C(14)	1.548(3)
C(6)-C(16)	1.550(3)
C(7)-C(8)	1.338(3)
C(7)-C(11)	1.479(3)
C(8)-C(9)	1.474(3)
C(10)-C(11)	1.509(3)
C(10)-C(17)	1.520(3)
C(11)-C(12)	1.339(3)
C(12)-C(13)	1.501(3)
C(13)-C(14)	1.522(3)
C(17)-C(18)	1.530(3)
C(17)-C(19)	1.533(4)

C(1)-O(1)-C(13)	109.29(18)
C(9)-O(5)-C(10)	119.39(18)
O(1)-C(1)-C(2)	111.2(2)
O(2)-C(1)-O(1)	121.6(2)
O(2)-C(1)-C(2)	127.2(2)
O(1)-C(13)-C(14)	104.76(18)
C(12)-C(13)-C(14)	114.96(19)
C(2)-C(14)-C(6)	113.12(19)
C(13)-C(14)-C(2)	102.62(18)
C(1)-C(2)-C(3)	113.1(2)
C(1)-C(2)-C(14)	101.6(2)
C(1)-C(2)-C(15)	107.0(2)
C(3)-C(2)-C(14)	113.6(2)
C(3)-C(2)-C(15)	110.6(2)
C(14)-C(2)-C(15)	110.5(2)
C(4)-C(3)-C(2)	110.1(2)
O(3)-C(4)-C(3)	107.7(2)
O(3)-C(4)-C(5)	111.8(2)
C(3)-C(4)-C(5)	114.6(2)
C(4)-C(5)-C(6)	113.60(19)
C(5)-C(6)-C(14)	108.01(18)
C(5)-C(6)-C(16)	109.02(19)
C(7)-C(6)-C(5)	114.36(19)
C(7)-C(6)-C(14)	104.80(18)
C(7)-C(6)-C(16)	105.99(19)
C(14)-C(6)-C(16)	114.78(19)
C(8)-C(7)-C(6)	125.8(2)
C(8)-C(7)-C(11)	119.2(2)
C(11)-C(7)-C(6)	114.8(2)
C(7)-C(8)-C(9)	121.1(2)
O(4)-C(9)-O(5)	118.2(2)
O(4)-C(9)-C(8)	123.8(2)
O(5)-C(9)-C(8)	117.9(2)
O(5)-C(10)-C(11)	109.84(17)
O(5)-C(10)-C(17)	106.59(18)
C(11)-C(10)-C(17)	117.95(19)
C(7)-C(11)-C(10)	113.0(2)
C(12)-C(11)-C(7)	121.9(2)
C(12)-C(11)-C(10)	124.8(2)
C(11)-C(12)-C(13)	120.9(2)
O(1)-C(13)-C(12)	111.9(2)

C(13)-C(14)-C(6)	113.00(19)
C(10)-C(17)-C(18)	110.4(2)
C(10)-C(17)-C(19)	113.0(2)
C(18)-C(17)-C(19)	110.3(2)

Table 14. Hydrogen bonds for 2*β*-hydroxynagilactone F (108) [Å and °].

Table 3. Hydrogen bonds for cs2147 [Å and °].

D-H...A	d(D-H)	d(H...A)	d(D...A)	<(DHA)
O(3)-H(3)...O(2)#1	1.05(5)	1.83(5)	2.878(3)	173(4)

Symmetry transformations used to generate equivalent atoms:

#1 x+1,y,z

Table 15. Crystal data and structure refinement nagilactone I (109)

Identification code	ERXR-2	
Empirical formula	$C_{20}H_{24}O_7$	
Formula weight	376.39	
Temperature	100.00(10) K	
Wavelength	1.54184 Å	
Crystal system	Orthorhombic	
Space group	$P2_12_12_1$	
Unit cell dimensions	a = 7.77930(10) Å	α= 90°.
	b = 11.77260(10) Å	β= 90°.
	c = 19.7352(3) Å	γ = 90°.
Volume	1807.40(4) $Å^3$	
Z	4	
Density (calculated)	1.383 Mg/m^3	
Absorption coefficient	0.872 mm^{-1}	
F(000)	800	
Crystal size	0.2794 x 0.1872 x 0.1428 mm^3	
Theta range for data collection	4.373 to 74.703°.	
Index ranges	-9<=h<=9, -14<=k<=14, -24<=l<=21	
Reflections collected	11384	
Independent reflections	3688 [R(int) = 0.0356]	
Completeness to theta = 67.684°	99.8 %	
Absorption correction	Gaussian	
Max. and min. transmission	0.906 and 0.843	
Refinement method	Full-matrix least-squares on F^2	
Data / restraints / parameters	3688 / 0 / 252	
Goodness-of-fit on F^2	1.043	
Final R indices [I>2sigma(I)]	R1 = 0.0344, wR2 = 0.0920	
R indices (all data)	R1 = 0.0356, wR2 = 0.0931	
Absolute structure parameter	-0.13(8)	
Extinction coefficient	n/a	
Largest diff. peak and hole	0.230 and -0.191 e.$Å^{-3}$	

Table 16. Bond lengths [Å] and angles [°] for nagilactone I (109)

O(1)-C(1)	1.342(3)	O(1)-C(1)-C(2)	111.73(17)
O(1)-C(13)	1.471(2)	O(2)-C(1)-O(1)	121.37(19)
O(2)-C(1)	1.211(3)	O(2)-C(1)-C(2)	126.90(19)
O(3)-C(4)	1.430(2)	C(1)-C(2)-C(3)	111.11(17)
O(4)-C(9)	1.208(3)	C(1)-C(2)-C(14)	101.44(15)
O(5)-C(9)	1.351(2)	C(1)-C(2)-C(15)	107.67(16)
O(5)-C(10)	1.464(2)	C(14)-C(2)-C(3)	114.19(16)
O(6)-C(18)	1.198(3)	C(14)-C(2)-C(15)	110.22(18)
O(7)-C(18)	1.324(3)	C(15)-C(2)-C(3)	111.61(17)
O(7)-C(19)	1.443(3)	C(4)-C(3)-C(2)	114.22(17)
C(1)-C(2)	1.522(3)	O(3)-C(4)-C(3)	104.90(15)
C(2)-C(3)	1.542(3)	O(3)-C(4)-C(5)	111.10(16)
C(2)-C(14)	1.535(3)	C(3)-C(4)-C(5)	116.06(16)
C(2)-C(15)	1.538(3)	C(6)-C(5)-C(4)	114.51(15)
C(3)-C(4)	1.533(3)	C(5)-C(6)-C(14)	106.65(15)
C(4)-C(5)	1.556(3)	C(5)-C(6)-C(16)	109.95(16)
C(5)-C(6)	1.530(3)	C(7)-C(6)-C(5)	113.70(15)
C(6)-C(7)	1.514(3)	C(7)-C(6)-C(14)	105.12(15)
C(6)-C(14)	1.543(3)	C(7)-C(6)-C(16)	106.71(15)
C(6)-C(16)	1.547(3)	C(14)-C(6)-C(16)	114.79(16)
C(7)-C(8)	1.340(3)	C(8)-C(7)-C(6)	124.95(17)
C(7)-C(11)	1.470(3)	C(8)-C(7)-C(11)	119.03(17)
C(8)-C(9)	1.470(3)	C(11)-C(7)-C(6)	115.98(16)
C(10)-C(11)	1.508(3)	C(7)-C(8)-C(9)	122.15(18)
C(10)-C(17)	1.526(3)	O(4)-C(9)-O(5)	118.58(18)
C(11)-C(12)	1.340(3)	O(4)-C(9)-C(8)	123.52(19)
C(12)-C(13)	1.493(3)	O(5)-C(9)-C(8)	117.86(17)
C(13)-C(14)	1.525(3)	O(5)-C(10)-C(11)	111.26(16)
C(17)-C(18)	1.524(3)	O(5)-C(10)-C(17)	105.43(16)
C(17)-C(20)	1.532(3)	C(11)-C(10)-C(17)	118.14(17)
C(1)-O(1)-C(13)	109.06(15)	C(7)-C(11)-C(10)	114.00(17)
C(9)-O(5)-C(10)	119.25(16)	C(12)-C(11)-C(7)	121.07(18)
C(18)-O(7)-C(19)	116.82(19)	C(12)-C(11)-C(10)	124.75(18)

C(11)-C(12)-C(13)	121.38(18)	C(10)-C(17)-C(20)	110.88(17)
O(1)-C(13)-C(12)	111.74(16)	C(18)-C(17)-C(10)	114.66(17)
O(1)-C(13)-C(14)	104.67(14)	C(18)-C(17)-C(20)	110.61(18)
C(12)-C(13)-C(14)	114.88(16)	O(6)-C(18)-O(7)	122.8(2)
C(2)-C(14)-C(6)	113.97(16)	O(6)-C(18)-C(17)	123.7(2)
C(13)-C(14)-C(2)	102.54(15)	O(7)-C(18)-C(17)	113.46(18)
C(13)-C(14)-C(6)	113.04(15)		

Table 17. Hydrogen bonds for nagilactone I (109) [Å and °].

D-H...A	d(D-H)	d(H...A)	d(D...A)	<(DHA)
O(3)-H(3)...O(2)#1	0.88(5)	1.93(5)	2.804(2)	173(4)

Symmetry transformations used to generate equivalent atoms:

#1 x-1,y,z